ABSTRACT

Title of Thesis:	TROPHIC ECOLOGY AND PHYSIOLOGICAL CONDITION OF BLACK SEA BASS *CENTROPRISTIS STRIATA* IN THE MIDDLE ATLANTIC BIGHT
	Ginni Alice La Rosa, Master of Science, 2018
Thesis Directed By:	Assistant Professor Ryan J. Woodland Marine Estuarine Environmental Sciences

Black sea bass *Centropristis striata* (Linnaeus, 1758) is a valuable Middle Atlantic Bight fisheries species, but spatial patterns in condition and diet during summer residence at inshore reefs remain largely unknown. I examined a suite of potential drivers of physiological condition and trophic niche of *C. striata* using morphometric, stomach contents, and stable isotope indicators. Regional differences in liver tissue lipid content and standard condition indices covaried with additional biotic and abiotic factors. I show that liver tissue must be corrected for lipid content prior to interpreting liver carbon stable isotope data and I provide a correction equation for this species. Both spatial and biological factors explained observed patterns in diet and trophic niche metrics. An understanding of the factors that underlie spatial and temporal patterns in condition and trophic ecology provides insights necessary to help inform ecologically-focused management decisions.

TROPHIC ECOLOGY AND PHYSIOLOGICAL CONDITION OF BLACK SEA BASS *CENTROPRISTIS STRIATA* IN THE MIDDLE ATLANTIC BIGHT

by

Ginni Alice La Rosa

Thesis submitted to the Faculty of the Graduate School of the
University of Maryland, College Park, in partial fulfillment
of the requirements for the degree of
Master of Science
2018

Advisory Committee:
Assistant Professor Ryan J. Woodland, UMCES CBL Chair
Research Professor Lee Cooper, UMCES CBL
Professor Bradley G. Stevens, UMES

Acknowledgements

I wish to thank my primary advisor Dr. Ryan Woodland for all of his guidance and support. My committee members Dr. Lee Cooper and Dr. Bradley Stevens also provided valuable insight throughout the project.

I am grateful for all of the part-time and full-time members of the Woodland Lab, particularly Dani Quill, Theresa Van Gorden, Joe Molina, and Gabriela Zabel for their help with sample preparation and data collection.

I also wish to thank additional Chesapeake Biological Laboratory (CBL) faculty for providing advice in addition to materials and sample processing help, in particular Dr. Christopher Rowe and Dr. Cédric Magen.

I also wish to thank for financial support the Exelon Corporation, the Graduate Education Committee of the Chesapeake Biological Laboratory, and the Cove Point Natural Heritage Trust. I also received support through the University of Maryland, College Park Dean's Fellowship.

I am thankful for my fellow students at the Chesapeake Biological Laboratory for their friendship and solidarity through the years of course work and laboratory/field research.

Finally, none of my accomplishments would have been possible without the love and encouragement from my family throughout my years of school to this day. I am incredibly thankful for my parents Jerome La Rosa and Kristi Riddle-LaRosa, my brother Brian La Rosa, and for my husband Matthew Ponsini for their loving support through the past few years and into the next chapter of our life.

Table of Contents

Acknowledgements iii
Table of Contents iv
List of Tables vi
List of Figures ix

Chapter 1: Introduction 1
Ecosystem-based fisheries management 1
Description of study site 1
Black sea bass biology overview 3
Diet analysis overview 5
Stable isotope analysis and food web ecology 6
Condition indices, lipid content and physiology overview 9
Trophic ecology and management implications 12
Statement of objectives and hypotheses 14
References 16
Figures 24

Chapter 2: Spatiotemporal variability of muscle and liver tissue lipid content in black sea bass, *Centropristis striata*, and development of a δ^{13}C lipid-correction model ... 25
Abstract 25
Introduction 26
Materials and methods 31
Sample collection and condition indices 31
Lipid extraction 32
Stable isotope analysis 34
Lipid correction equations 35
Lipid content, condition, and factors 37
Results 38
Muscle tissue: lipid content 38
Liver tissue: lipid content 39
Lipid correction equations 40
Condition and reproductive indices 41
Regional variation 42
Discussion 43
Lipid content and condition indices 45
Physiology and fisheries management 48
Conclusion 49
References 50
Tables 56
Figures 61

Chapter 3: Spatial patterns of black sea bass (*Centropristis striata*) diet and trophic ecology in the Middle Atlantic Bight 67

Abstract 67
Introduction 68
Materials and methods 71
Sample collection and sampling area 71
Stomach contents analysis and feeding strategy plots 73
Bulk stable isotope analysis 74
Trophic enrichment and mixing models 75
Trophic position 77
Niche width 78
Results 79
Stomach contents analysis and feeding strategy 79
Prey models 80
Benthic pelagic coupling and mixing models 81
Trophic position 82
SIBER and niche width 82
Discussion 83
Regional patterns in reef feeding 83
Trophic position and benthic-pelagic coupling 85
Prey isotope variation and ecological stoichiometry 87
Measuring niche area: direct and indirect methods 88
Mixing models and their limitations 89
Equilibration rates: muscle and liver tissue 90
Conclusion 91
References 92
Tables 98
Figures 109

Full Bibliography 122

List of Tables

Chapter 2

Table 2.1. Sample data by region for *Centropristis striata* muscle (M) and liver (L) tissue before and after Soxhlet lipid extraction. Regions are New Jersey (NJ), Maryland (MD), and North Carolina (NC). Superscript letters with liver data represent pairwise comparisons for each variable: different letters signify that the regions differ significantly for that measurement. n = sample size.

Table 2.2. Pearson correlation coefficient (*r*) for *Centropristis striata* muscle and liver tissue lipid content (%) as compared to reproductive (gonadosomatic index [GSI]) and condition (Fulton *K*, hepatosomatic index [HSI]) indices. Bolded *P*-values are significant at $\alpha = 0.05$. n = sample size.

Table 2.3. Black sea bass (*Centropristis striata*) muscle (M) and liver (L) sample data by region before and after lipid correction using a nonlinear fitted model adapted from McConnaughey and McRoy (1979) and Kiljunen et al. (2006). Regions are Southern New England (SNE), New Jersey (NJ), Maryland (MD), and North Carolina (NC). Lipid-corrected carbon isotope ($\delta^{13}C'$) values for liver tissue include measurements for the subset of samples that underwent lipid extraction in addition to predicted values, based upon a model. Liver samples modeled to have negative lipid content (n = 3) were removed from analysis. Superscript letters with muscle and liver data ($\delta^{13}C$, $\delta^{13}C'$, Lipid %, $\Delta\delta^{13}C$) represent pairwise comparisons among regions for each variable: different letters signify significant differences between values. n = sample size.

Table 2.4. Summary table of regional *Centropristis striata* condition (hepatosomatic index [HSI], Fulton *K*) and reproductive (gonadosomatic index [GSI]) indices and liver tissue lipid content and density. Regions are Southern New England (SNE), New Jersey (NJ), Maryland (MD), and North Carolina (NC). Superscript letters represent pairwise comparisons for each variable: different letters signify that the regions differ significantly for that measurement. n = sample size for each comparison group.

Table 2.5. Generalized linear model (GLM) results for *Centropristis striata* condition (Fulton *K*, hepatosomatic index [HSI], liver lipid content [%] and reproductive [gonadosomatic index [GSI]) indices, where *df* = degrees of freedom, *F* = *F*-statistic, and *P* = *P*-value. Bolded *P*-values are significant at $\alpha = 0.05$. n = sample size for each analysis.

Chapter 3

Table 3.1. Sampling site depth data for *Centropristis striata* collected from inshore reefs in summer 2016 and offshore trawling (National Marine Fisheries Service) in

spring and autumn 2016. Regions are Southern New England (SNE), New Jersey (NJ), Maryland (MD), and North Carolina (NC). Depth data presented as mean ± standard deviation. n = number of sites.

Table 3.2. Biological data for *Centropristis striata* collected in 2016. Regions are Southern New England (SNE), New Jersey (NJ), Maryland (MD), and North Carolina (NC). n = counts of female (F), indeterminate (I), male (M), young of the year (YOY), small (S, with YOY included in count), and large (L) individuals. Total Length is mean ± standard deviation.

Table 3.3. Summary table of measurements and calculations for *Centropristis striata* muscle (M) and (L) tissue samples. Regions are Southern New England (SNE), New Jersey (NJ), Maryland (MD), and North Carolina (NC). Liver δ^{13}C values have been corrected for lipid content (see Chapter 2). BP = benthic proportion of diet, TP = relative trophic position, Total SEA_c = Standard Ellipse Area corrected for small sample size for the total regional group, Large SEA_c/Small SEA_c = SEA_c for large and small size classes for each region, respectively. Muscle tissue SEA_c values were calculated for areas in niche space (BP vs. TP), and liver tissue SEA_c values were calculated for areas in isotope space (δ^{13}C vs. δ^{15}N). n = sample size.

Table 3.4. Stomach contents of *Centropristis striata* from North Carolina (NC) and New Jersey (NJ) reefs separated into large (L) and small (S) size classes. Measurements presented as sums of dry weight in grams.

Table 3.5. Comparison of lengths and weights of *Centropristis striata* sampled from hook and line (Hook) and un-baited trap (Trap) offshore of Point Pleasant, New Jersey in June 2016. TL = total length, BW = body weight (total weight minus stomach weight), SW = stomach weight, SBR = stomach weight to body weight ratio. n = sample size.

Table 3.6. Prey summary table separated by region. Anchovy group combines *Anchoa hepsetus* and *Anchoa mitchilli* data, and Rock crab group is entirely comprised of *Cancer irroratus*. Regions are Southern New England (SNE), New Jersey (NJ), Maryland (MD), and North Carolina (NC). Length was measured as total length for anchovies and carapace width for *C. irroratus*. Values presented as mean ± standard deviation. The "δ^{13}C whole" and "δ^{15}N whole" values represent whole-body corrections for muscle tissue sample measurements. The "GAM δ^{15}N" values represent predictions from generalized additive models for *Centropristis striata* sample sites. n = sample size.

Table 3.7. Prey generalized additive model (GAM) results for Anchovy (*Anchoa mitchilli* + *Anchoa hepsetus*) and Atlantic rock crab (*Cancer irroratus*) for predicting δ^{15}N values at *Centropristis striata* sampling sites. Parameters with s( ) are non-parametric smoothed terms. Parameters joined with an asterisk "*" are interaction terms. Model *df* = degrees of freedom. Raw Akaike information criterion (AIC) score for each model was compared to the best model (lowest AIC) to compute ΔAIC, and

transformed to compute Akaike weights (wAIC) as described in Wagenmakers et al. (2004). Best-fitting (most parsimonious) model for each prey group is marked in bold.

Table 3.8. Generalized linear model (GLM) results for *Centropristis striata* benthic proportion (BP) of diet and relative trophic position (TP) based on muscle tissue stable isotope values, where *df* = degrees of freedom, *F* = *F*-statistic, and *P* = *P*-value. Bolded *P*-values are significant at $\alpha = 0.05$. n = sample size.

Table 3.9. Pairwise comparisons for *Centropristis striata* a) muscle tissue: large size class in isospace, b) muscle tissue: small size class in isospace, c) muscle tissue: large size class in niche space, d) muscle tissue: small size class in niche space, e) liver tissue: large size class in isospace, and f) liver tissue: small size class in isospace. Values represent probability (on a scale from 0 to 1) that Bayesian standard Ellipse B area is larger than the area of Bayesian standard Ellipse A. Comparison method rationale is explained by Jackson (2016).

List of Figures

Chapter 1

Figure 1.1. Map of the Middle Atlantic Bight (MAB). Arrows indicate the northern boundary of the MAB at Cape Cod, Massachusetts (MA) and the southern boundary at Cape Hatteras, North Carolina (NC).

Chapter 2

Figure 2.1. Map of sampling sites of *Centropristis striata* (black sea bass, BSB) along the Middle Atlantic Bight in 2016. Hook and line reef-sampled sites were located at Point Pleasant, New Jersey (NJ), Ocean City, Maryland (MD), and Cape Hatteras, North Carolina (NC).

Figure 2.2. Initial carbon to nitrogen (C:N) ratio versus empirical lipid content (%) for lipid-extracted *Centropristis striata* liver tissue (Soxhlet extraction method). Regions are Maryland (MD), North Carolina (NC), and New Jersey (NJ). Blue line is the regression line of best fit, and the grey shaded area represents the standard error range/confidence interval. Adjusted $r^2 = 0.85$.

Figure 2.3. Nonlinear model fitting for lipid-extracted *Centropristis striata* liver tissue. Observed values were derived from measurements of lipid extracted using the Soxhlet method. Model parameters were modified as needed from the model proposed by McConnaughey and McRoy (1979) and Kiljunen et al. (2006). Adjusted $r^2 = 0.85$.

Figure 2.4. Comparison by region of the difference in $\delta^{13}C$ before and after lipid extraction ($\Delta\delta^{13}C$) in *Centropristis striata* liver tissue. Regions are Southern New England (SNE), New Jersey (NJ), Maryland, (MD), and North Carolina (NC). Error bars represent the standard deviation.

Figure 2.5. Generalized linear model (GLM) results for liver lipid content (%), liver lipid density, hepatosomatic index (HSI) and gonadosomatic index (GSI) derived from isotope analysis of *Centropristis striata* liver and/or muscle tissue. Significant variable for liver lipid content was a) Depth; significant variable for HSI was b) Sex (female [F], Indeterminate [I], Male [M]); and significant variables for GSI were c) Depth, d) Sex, and e) Length. For regional pairwise comparisons of each condition index, see Table 2.4. For significance of each variable, see Table 2.5.

Chapter 3

Figure 3.1. Map of sampling sites of *Centropristis striata* (black sea bass, BSB), *Anchoa mitchilli* (Bay Anchovy), *A. hepsetus* (Striped Anchovy), and *Cancer irroratus* (Crab) along the Middle Atlantic Bight in 2016 and 2017.

Figure 3.2. Feeding strategy plots for *Centropristis striata* at reefs of the Middle Atlantic Bight in summer (June-August) 2016. Data are presented from a subset of stomachs examined for a) New Jersey (n = 40) and b) North Carolina (n = 30) reef sites. Images from the Integration and Application Network, University of Maryland Center for Environmental Science (ian.umces.edu/imagelibrary/).

Figure 3.3. Stable isotope mixing model plots by region: a) Southern New England (SNE), b) New Jersey (NJ), c) Maryland (MD), and d) North Carolina (NC). Open circles are individual *Centropristis striata* (black sea bass, BSB) muscle tissue samples (mixtures) sampled in 2016. Shapes with error bars represent regional prey sample means increased by one level of a trophic enrichment factor [(TEF), 0.5‰ for δ^{13}C and 2.3‰ for δ^{15}N, from McCutchan et al. (2003)]. Error bars represent one standard deviation of the TEF [±1.3‰ for δ^{13}C and ±1.5‰ for δ^{15}N, from McCutchan et al. (2003)]. Combined pelagic anchovy samples are *Anchoa hepsetus* and *A. mitchilli*, and benthic rock crab samples are *Cancer irroratus* sampled in 2016 and 2017.

Figure 3.4. Generalized linear model results for benthic proportion of diet (BP) and trophic position (TP) derived from isotope analysis of *Centropristis striata* muscle tissue. Significant variables for BP were a) Sex [female (F), Indeterminate (I), Male (M)] and b) Length. Significant variables for TP were d) Sex, d) Length, and e) Depth. For regional pairwise comparisons, see Table 3.1. For significance of each variable, see Table 3.6.

Figure 3.5. SIBER ellipses for *Centropristis striata* in isotope space (i.e., isospace, δ^{13}C vs. δ^{15}N) and in actual niche space [benthic proportion of diet (BP) vs. trophic position (TP)]. Plots are in the following order: a) muscle tissue: large size class (≥ 250 mm TL) in isospace, b) muscle tissue: small size class (< 250 mm TL) in isospace, c) muscle tissue: large size class in niche space, and d) muscle tissue: small size class in niche space, e) liver tissue: large size classes in isospace, and f) liver tissue: small size class in isospace.

Figure 3.6. SIBER Bayesian Standard Ellipse Area density plots for *Centropristis striata*: a) muscle tissue: large size class in isospace, b) muscle tissue: small size class in isospace, c) muscle tissue: large size class in niche space, d) muscle tissue: small size class in niche space, e) liver tissue: large size class in isospace, and f) liver tissue: small size class in isospace. Boxes represent 50%, 75%, and 95% credible intervals. Red x's represent the Standard Ellipse Area corrected for small sample size (SEA_c) point estimates.

Chapter 1: Introduction

Ecosystem-based fisheries management

Ecosystem-based fisheries management (EBFM) continues to gain prominence as a potentially powerful tool for maintaining viable fisheries stocks (Pikitch et al. 2004). An understanding of ecological interactions such as predation and competition among harvested and unharvested species is needed to inform EBFM models that predict biomass and energy transfer within an ecosystem. Therefore, understanding the niche of a fish species within a food web is crucial for effectively integrating that species into an ecosystem-based management framework (Link 2002, Malek et al. 2016). The ability to assess spatiotemporal variability in the fish's foraging needs allows for spatially-explicit and temporally-dynamic prediction of population-level responses and appropriate management adjustments (Byron & Link 2010). My research focuses on filling an existing knowledge gap in this trophic niche information for black sea bass *Centropristis striata*, an important fisheries species in the Middle Atlantic Bight.

Description of study site

The Middle Atlantic Bight (MAB) is the temperate region of the east coast of the United States bounded to the north by Nantucket Shoals (south of Cape Cod, Massachusetts) and by Cape Hatteras, North Carolina (NC) to the south (Fig. 1.1). To

the south, the South Atlantic Bight (SAB) extends from Cape Hatteras to the southern edge of the Florida peninsula (Able & Fahay 2010). The MAB is highly variable in its seasonal currents, temperature gradients, and weather conditions, particularly at smaller spatial scales (Cowen et al. 1993). The nearshore band of water varies greatly in salinity due to several major freshwater inputs including the Connecticut and Hudson Rivers, and the Delaware and Chesapeake Bays (Able & Fahay 2010). A coastal current originating from Greenland flows through the Scotian Shelf and into the MAB shelf water, moving in a predominantly southwestern direction (Lentz 2008). Near Cape Hatteras, the Gulf Stream moves in a northeastern direction, leading to shelf water entrainment and recirculation northwards along the slope (Chapman & Beardsley 1989, Cowen et al. 1993). The edge of the continental shelf has a sharp gradient where the lower-density shelf water meets the denser, more saline seawater along the slope. This frontal system at the shelf break encourages continuous suspension of dissolved nutrients and particulate material, generating high productivity in this region that supports many economically important commercial and recreational fisheries (Flagg et al. 2006, Able & Fahay 2010).

The surface area of the MAB floor is largely comprised of flat sedimentary bottom habitat, with a patchy distribution of natural rock or shell substrate reefs. Over the past two centuries however, artificial reef-like structures have increased in availability in the Bight due to intentional and unintentional placement in the form of shipwrecks and other large man-made substrates. These novel habitats have become the subject of recent increased ecological and fisheries research interest because of their ability to attract structure-associated fisheries species, and their potential to

support in situ secondary production in addition to becoming valuable fishing sites (Steimle & Zetlin 2000).

Black sea bass biology overview

C. striata is a popular recreational and commercial fish along the MAB, SAB and the eastern Gulf of Mexico. It is a demersal predator of crustaceans and fishes that are often associated with hard substrate habitat, including both natural and artificial reefs (Musick & Mercer 1977, Steimle & Zetlin 2000). They are protogynous hermaphrodites: most individuals begin life as females, but may transition into males in response to age or size thresholds interacting with visual or social cues (Benton & Berlinsky 2006). This has prompted concerns of skewed sex ratios resulting from heavy fishing pressure in past stock assessments (Musick & Mercer 1977). However, surveys have reported catching significant numbers of small, young males, suggesting that some individuals may mature directly as males rather than maturing as females before transitioning. The presence of small males may be a population-level response to fishing pressure (Wuenschel et al. 2011, Provost et al. 2017).

Populations of *C. striata* from the MAB migrate seasonally to overwinter on the outer continental shelf, returning in the spring and summer to spawn along the inner continental shelf (Musick & Mercer 1977, Moser & Shepherd 2009, Miller et al. 2016). Juveniles also migrate to the outer continental shelf or to deeper estuarine waters to remain at temperatures above 6°C (Drohan et al. 2007). In contrast, populations in the SAB are thought to remain over their residential reefs year-round

(Sedberry 1988, Drohan et al. 2007) or move shorter distances directly offshore (Moser & Shepherd 2009).

The coastal Atlantic *C. striata* population is managed as two separate stocks north and south of Cape Hatteras, NC. The northern stock is jointly managed by the Mid-Atlantic Fishery Management Council and the Atlantic States Marine Fisheries Commission, while the southern stock is managed by the South Atlantic Fishery Management Council (Roy et al. 2012). Reports have suggested that Cape Hatteras serves as a biogeographical barrier limiting gene flow between northern and southern *C. striata* populations; measurable genetic differences exist between populations on either side of this barrier. The population residing in the Gulf of Mexico has been classified as a subspecies, *C. striata melana* (Roy et al. 2012, McCartney et al. 2013).

The MAB stock is not overfished and is not currently at risk of being overfished based on 2016 harvest data (Northeast Fisheries Science Center 2017). In the SAB, the stock was determined to be overfished and undergoing overfishing in the 2010 assessment. As of the most recent report using 2016 data, however, the stock is no longer considered to be overfished (SEDAR 2018). Commercial trawl harvests of *C. striata* occur offshore during the winter, while inshore trap and recreational hook and line fishing takes place from spring through autumn. *C. striata* frequently co-occur with scup *Stenotomus chrysops* and summer flounder *Paralichthys dentatus*, and these three species are hypothesized to have similar trophic niches due to high dietary overlap of benthic organisms and small fishes (Shepherd & Terceiro 1994).

Diet analysis overview

Crustaceans, in particular decapods such as Atlantic rock crab *Cancer irroratus*, feature prominently in *C. striata* stomach contents as a major diet component across all size classes, along with smaller crustaceans including shrimps, amphipods and isopods that are frequently consumed by juveniles (Steimle & Figley 1996, Drohan et al. 2007). Piscivory also occurs among *C. striata*, and prior evidence suggests that the prominence of piscivory differs across biological and spatial gradients. Previous reports observe that piscivory becomes more prevalent in *C. striata* with increasing size (Sedberry 1988, Drohan et al. 2007). In addition, studies report that the overall diet of SAB *C. striata* is composed of greater proportions of fish prey than the diet of MAB individuals (Byron & Link 2010). Fisheries-independent trawl survey data indicate a trend toward piscivory with increased age of *C. striata*, as well as a potential latitudinal gradient of increased piscivory in southern groups (Bowman et al. 2000).

One of the most common and well-established methods for determining the diet of fishes is stomach content analysis, which provides an instantaneous 'snapshot' of the most recent meal. Prey items and materials within the food bolus of the stomach are identified to the lowest possible taxonomic group, and group proportions are calculated on the basis of occurrence, volume, or mass relative to the entire stomach contents. This type of analysis can be time-consuming, requiring a sound methodology and skill base to be able to identify fragments of prey at various stages of digestion (Hyslop 1980). Remains of previous feedings are seldom present for extended periods of time, and there can be biases due to the relative digestibility of

certain prey components. For example, hard structures such as bivalve or crustacean shells have a longer residence time in the stomach, leading to a risk of over-representation in diet estimates (Hyslop 1980).

Stable isotope analysis and food web ecology

The measurement of stable isotope composition of plants and animals, particularly ratios of carbon and nitrogen isotopes, has become a valuable alternative tool for trophic ecological applications. The heavier isotopes ^{13}C and ^{15}N can be used as tracers to examine energy and matter flows through a trophic network (Cabana & Rasmussen 1994, Vander Zanden et al. 1997) and to differentiate the feeding ecology of coexisting species within a shared area (Thomas & Cahoon 1993). Stable isotope analysis enables determination of the assimilated diet over a longer temporal scale than stomach content analysis alone. Nitrogen isotopic ratios ($^{15}N/^{14}N$) enable determination of a species' trophic position, and carbon ratios ($^{13}C/^{12}C$) can indicate the source or sources of primary production supporting consumers in both terrestrial and aquatic food webs (Fry 2006).

Ratios (R) of ^{13}C to ^{12}C and of ^{15}N to ^{14}N in tissue samples (R_{sample}) are reported in delta notation as $\delta^{13}C$ and $\delta^{15}N$ values, denoted in units of per mille (‰) relative to international standards ($R_{standard}$): Vienna Pee Dee Belemnite for carbon, and atmospheric N_2 gas for nitrogen (Fry 2006):

$$\delta = 1000 * [(R_{sample} / R_{standard}) - 1] \quad \text{(Eq. 1.1)}$$

Enrichment of ^{13}C across trophic transfers is small but variable, with muscle tissue increasing by an average of 0.5 ± 1.3‰ (standard deviation, SD) with each trophic level in a wide range of animal taxa (McCutchan et al. 2003). Thus examination of consumer $\delta^{13}C$ values provides information on ultimate carbon sources (e.g., different primary producers) and can provide spatial information on foraging locations. In aquatic ecosystems, carbon isotope ratios typically differ between pelagic and benthic sources of primary production: benthic producers tend to be more enriched in ^{13}C than pelagic producers (Post 2002, Malek et al. 2016).

The tissues of organisms higher in trophic position become enriched in ^{15}N through fractionation during protein synthesis (Minagawa & Wada 1984). Previous research has demonstrated the magnitude of $\delta^{15}N$ enrichment between a consumer and its prey, termed the trophic enrichment factor (TEF), to be approximately (± SD) 2.3 ± 1.5‰ across a wide range of animals and tissues (McCutchan et al. 2003). However, the magnitude of enrichment of carbon or nitrogen can vary substantially with diet, among species and among tissue types within a species (Sweeting et al. 2007a, Sweeting et al. 2007b).

For bulk (i.e., homogenized tissue) stable isotope analysis, a baseline organism (typically a primary consumer) is selected and analyzed for comparison to the organism of interest. Primary consumers are used to determine a baseline rather than primary producers because aquatic primary producers can have very dynamic, often cyclic, $\delta^{13}C$ and $\delta^{15}N$ values (Post 2002, Woodland et al. 2012). Baseline primary consumers have larger unit biomass, reducing the rate at which their tissues respond to short-term changes in dietary isotope values. This reduces the isotopic

variability of their tissues and yields a more stable reference value. For instance, primary consumers such as planktivorous Atlantic menhaden (*Brevoortia tyrannus*) contain muscle tissue that have assimilated primary production over time and thus have an integrated value that averages out the fine-scale variability in pelagic primary production. Despite this, isotopic values of primary consumers can also be subject to spatial and temporal fluctuations, which may result in complexities for interpreting baseline data in some circumstances for higher-level consumers. (Post 2002, Woodland et al. 2012).

In addition to possible baseline changes, the types of tissue samples analyzed from an individual consumer may differ in isotope composition due to variability in tissue metabolic turnover rates, the relative proportions of tissue components such as lipids and amino acids, and in proportion to the consumer's size and growth rate (Pinnegar & Polunin 1999, Herzka 2005, Perga & Gerdeaux 2005). For instance, liver tissue and blood plasma experience substantially higher relative turnover rates and are thus more likely to reflect recent dietary composition than tissues such as cartilage in elasmobranchs and bone collagen in teleosts, which have slower turnover rates. Isotopic studies of marine fishes have primarily analyzed white muscle tissue, in which turnover rates range from days to weeks in rapidly growing fishes (e.g., early life stages) to over a year in slower growing fishes. Thus, research intending to observe changes over shorter time frames may benefit from comparisons with liver or blood samples that have rapid metabolic uptake (MacNeil et al. 2006). This has been demonstrated in the case of temperate fishes, where muscle tissue may not at all reflect the assimilation of an isotopically different diet if those prey were consumed

outside of the main growing season (Perga & Gerdeaux 2005). Therefore, tissues with different isotopic fractionation and turnover rates can be analyzed within the same individual to provide information on diet assimilation over several temporal intervals (Herzka 2005, Sweeting et al. 2007a, Sweeting et al. 2007b).

Caution must be exercised when assessing C or N isotopic values from liver tissue or other tissues with high lipid content, as lipids tend to be ^{13}C depleted compared to carbohydrates and proteins due to isotopic fractionation during lipid synthesis (DeNiro & Epstein 1977). In order to account for this complexity, lipids may be directly extracted using standardized methods to enable a lipid-free $\delta^{13}C$ measurement (Dobush et al. 1985, Honeycutt et al. 1995, Manirakiza et al. 2001), or alternatively, the isotopic values may be numerically corrected using quantitative relationships between lipid content and correlated changes in $\delta^{13}C$ ($\Delta\delta^{13}C$) (McConnaughey & McRoy 1979, Kiljunen et al. 2006, Post et al. 2007).

Condition indices, lipid content and physiology overview

Studies of fish physiological condition often use traditional morphometric indices to assess individual condition. Length-weight relationships such as Fulton's condition factor (*K*) convey information on the physiological state of a fish (Nash et al. 2006).

$$K = (W / L^3) * 100 \qquad \text{(Eq. 1.2)}$$

where *W* is the total weight of the fish, and *L* is the total length.

Prior work has shown a positive correlation between Fulton condition factor and tissue energy content in the form of proteins and lipids (Lambert & Dutil 1997).

The gonadosomatic index (GSI) provides insight on the reproductive state of an individual by dividing the mass of the gonadal tissue relative to the gonad-free body weight (Zudaire et al. 2014). In this technique, body weight excludes the weight of the stomach and its contents to reduce bias as a result of variation in stomach fullness across individuals.

The hepatosomatic index (HSI) is calculated as the mass of the liver divided by the liver-free body weight. Liver condition is primarily of interest due to the organ's role as a lipid storage site in many fish taxa. This index can relay information on the growth, feeding history, and overall health of the fish (Lambert & Dutil 1997).

In addition to morphometric analyses, additional methods enable insight into the chemical composition of tissues as indicators of health and condition, particularly in terms of energy storage such as lipids. Two of the most widely-cited lipid estimation and carbon-isotope correction equations are derived from analysis of a wide array of taxa in the Bering Sea food web (McConnaughey & McRoy 1979). In this correction procedure, the lipid content (%) of a sample is estimated based on the ratio of carbon to nitrogen (C:N) in the tissues of each taxon as measured with an elemental analyzer:

$$L = 93 / [1 + (0.246 * C{:}N - 0.775)^{-1}] \quad \text{(Eq. 1.3)}$$

where L is the lipid content (%) and $C:N$ is the measured ratio of elemental carbon to nitrogen in the sample. This equation is based on the assumption that the combined percentages of lipid and protein within a sample of animal tissue will equal 93%, with the remaining 7% being comprised of carbohydrates and other components (McConnaughey 1978). The estimated lipid is then used to correct the measured $\delta^{13}C$ value by predicting what the carbon isotope value would be in the absence of lipid:

$$\delta^{13}C' = \delta^{13}C + D * [I + 3.9 / (1 + 287/L)] \quad \text{(Eq. 1.4)}$$

where D is the isotopic difference between protein and lipid, and I is a constant. In McConnaughey and McRoy (1979), D is defined as 6‰ and I is -0.2, whereas Kiljunen et al. (2006) re-estimated the parameters for their fish-only model as 7.0 ± 0.3 (mean ± SD) and 0.05 ± 0.01 for D and I, respectively.

Alternatively, three inter-related linear models were proposed by Post et al. (2007) for estimation of and correction for lipid content in aquatic animals:

$$\Delta\delta^{13}C = -0.47 + 0.13 * \%\ lipid \quad \text{(Eq. 1.5)}$$

$$\%\ lipid = -20.54 + 7.24 * C:N \quad \text{(Eq. 1.6)}$$

$$\Delta\delta^{13}C = -3.32 + 0.99 * C:N \quad \text{(Eq. 1.7)}$$

where $\Delta\delta^{13}C$ is the difference between initial and lipid-extracted carbon isotope values, and *C:N* is the carbon to nitrogen ratio. It should be noted that this linear relationship is effective only within a limited C:N range [approx. 3 - 6.9 in the case of Post et al. (2007)]. At higher C:N ratios, the relationship deviates from a straight line and curves toward an asymptote (McConnaughey & McRoy 1979, Kiljunen et al. 2006).

Many trophic studies have placed importance on white muscle tissue as an integrator of diet isotopic signatures over a period of months to years depending on the species (Pinnegar & Polunin 1999). However, there is growing interest in examining tissues with more rapid isotopic turnover rates to estimate the diet over shorter time-frames, using tissues such as blood and liver (MacNeil et al. 2006). Developing appropriate numerical lipid corrections enables the use of high-lipid tissues such as the liver for effective trophic analysis.

Trophic ecology and management implications

Debate continues as to whether artificial substrate reefs merely serve as resource 'sinks' by aggregating fishes from natural productive reefs, or whether they serve as their own 'sources' of secondary production. Earlier publications relying upon site surveys and stomach content analysis alone concluded that artificial reefs merely attracted structure-seeking fish such as *C. striata* (Steimle & Figley 1996). Moving beyond stomach contents analysis, stable isotope measurement techniques allow certain commonly occurring isotopes (e.g., ^{13}C and ^{15}N) to identify the flow of

matter and energy within food webs and communities and to identify overlaps in resource use among co-occurring species.

Contemporary studies using stable isotope techniques have found evidence suggesting that artificial reefs support their own secondary production. Artificial reefs may enhance organic matter retention by providing surfaces for filter feeders to collect pelagic phytoplankton and to transfer this organic material to the benthos. Additional structural surfaces also enable the growth of benthic algae, providing food to benthic grazers, which in turn feed benthic omnivores or carnivores. It has been argued that reefs could support small-scale local fisheries if properly managed (Cresson et al. 2014).

G. E. Hutchinson (1957) envisioned species occupying 'niches,' which he defined as a hyper-volume, or space, comprised of *n* dimensions, with each dimensional axis treated as an environmental variable. Unfortunately, this niche definition remained difficult to interpret quantitatively in the older ecological literature, leading to a gradual decline in the use of this terminology. However, Newsome et al. (2007) argue that the development of quantitative analysis methods in ecology, such as stable isotope food web analysis, enable new quantitative niche definitions and measurable axes. Hutchinson (1957) also described the ecological niche space as a combination of 'bionomic' (resource-related) and 'scenopoetic' (habitat-based) factors. In isotopic approaches, carbon isotope ratios can be used to estimate the primary source of production in the food web, which relates to habitat, while nitrogen isotope ratios enable quantitative measurement of the resources being consumed by a species. Measuring trophic position within the 'delta space,' i.e. $\delta^{13}C$

versus δ^{15}N, framework enables the ecological niche terminology to acquire a more quantitative meaning that can be used to compare across systems (Newsome et al. 2007). Using these quantitative approaches to group species into trophic guilds could allow functional groups to be managed together and supplement species-based fisheries management, leading to more effective ecosystem-based management (Malek et al. 2016).

Statement of objectives and hypotheses

Despite the commercial and recreational popularity of *C. striata*, much remains to be clarified regarding the species in terms of trophic ecology. The wide latitudinal distribution along the U.S. Atlantic coast has prompted genetic investigations of population substructure (Roy et al. 2012, McCartney et al. 2013) but it is unknown how much diet and foraging characteristics may also vary among subpopulations, particularly in the case of individuals sampled from distinct regional reef sites. In addition, the extent to which this species depends upon secondary production from reef structures, artificial or natural, in the MAB remains a point of uncertainty (Steimle and Zetlin 2000, Cresson et al. 2014).

The goal of this study was to investigate the trophic ecology and condition of *C. striata* across its latitudinal range in the MAB using stomach contents analysis, bulk carbon and nitrogen stable isotope analysis, lipid analysis and standard condition indices. The suitability of using carbon to nitrogen ratios as a proxy for lipid content of white muscle and liver tissue was assessed using empirical lipid extraction measurements and numerical models from the literature. Empirical studies have

revealed significant relationships between organism size, stomach contents, and trophic position (Akin & Winemiller 2008). I sought to verify whether trophic position changes with ontogeny/size class as has been suggested for *C. striata* based on stomach contents, and whether trophic position differs predictably across large latitudinal or depth gradients. The importance of *C. striata* in recreational and commercial fisheries is well recognized, but much remains to be fully understood regarding their ecology prior to considering ecosystem-based management practices.

Objective 1 – Lipid Content Analysis. *Objective 1 focuses on regional differences in* C. striata *physiological condition. Condition is measured via both standard condition metrics as well as measured and predicted lipid content using the isotopic ratios of white muscle and liver tissue.*

Objective 2 – Stomach Content Analysis. *Objective 2 assesses the trophic niche differences between* C. striata *from northern (New Jersey) and southern (North Carolina) areas of the Middle Atlantic Bight using graphical approaches for comparing the prevalence and frequency of occurrence of prey items.*

Objective 3 – Stable Isotope Analysis. *Objective 3 examines the carbon and nitrogen isotope ratios of* C. striata *white muscle and liver tissue relative to whole body prey tissue. These isotope ratios enable the regional comparison of trophic position, benthic-pelagic coupling, and trophic niche width in subsets of the Middle Atlantic Bight.*

References

Able KW, Fahay MP (2010) Ecology of estuarine fishes: temperate waters of the Western North Atlantic. The Johns Hopkins University Press, Baltimore, MD

Akin S, Winemiller KO (2008) Body size and trophic position in a temperature estuarine food web. Acta Oecologica-International Journal of Ecology 33:144-153

Benton CB, Berlinsky DL (2006) Induced sex change in black sea bass. Journal of Fish Biology 69:1491-1503

Bowman RE, Stillwell CE, Michaels WL, Grosslein MD (2000) Food of Northwest Atlantic Fishes and Two Common Species of Squid. NOAA Technical Memorandum NMFS-NE-155. National Oceanic and Atmospheric Administration: National Marine Fisheries Service, Woods Hole, Massachusetts

Byron CJ, Link JS (2010) Stability in the feeding ecology of four demersal fish predators in the US Northeast Shelf Large Marine Ecosystem. Marine Ecology Progress Series 406:239-250

Cabana G, Rasmussen JB (1994) Modelling food chain structure and contaminant bioaccumulation using stable nitrogen isotopes. Nature 372:255-257

Chapman DC, Beardsley RC (1989) On the origin of shelf water in the Middle Atlantic Bight. Journal of Physical Oceanography 19:384-391

Cowen RK, Hare JA, Fahay MP (1993) Beyond hydrography: can physical processes explain larval fish assemblages within the Middle Atlantic Bight? Bulletin of Marine Science 53:567-587

Cresson P, Ruitton S, Harmelin-Vivien M (2014) Artificial reefs do increase secondary biomass production: mechanisms evidenced by stable isotopes. Marine Ecology Progress Series 509:15-26

DeNiro MJ, Epstein S (1977) Mechanism of carbon isotope fractionation associated with lipid-synthesis. Science 197:261-263

Dobush GR, Ankney CD, Krementz DG (1985) The effect of apparatus, extraction time, and solvent type on lipid extractions of snow geese. Canadian Journal of Zoology-Revue Canadienne De Zoologie 63:1917-1920

Drohan AF, Manderson JP, Packer DB (2007) Essential fish habitat source document: black sea bass, Centropristis striata, life history and habitat characteristics. NOAA Technical Memorandum

Flagg CN, Dunn M, Wang D-P, Rossby HT, Benway RL (2006) A study of the currents of the outer shelf and upper slope from a decade of shipboard ADCP observations in the Middle Atlantic Bight. Journal of Geophysical Research 111:C06003. doi:10.1029/2005JC003116

Fry B (2006) Stable Isotope Ecology. Springer, New York, NY

Herzka SZ (2005) Assessing connectivity of estuarine fishes based on stable isotope ratio analysis. Estuarine, Coastal and Shelf Science 64:58-69

Honeycutt ME, McFarland VA, McCant DD (1995) Comparison of 3 lipid extraction methods for fish. Bulletin of Environmental Contamination and Toxicology 55:469-472

Hutchinson GE (1957) Concluding remarks: Cold Spring Harbor symposium. Quantitative Biology 22:415-427

Hyslop EJ (1980) Stomach contents analysis- a review of methods and their application. Journal of Fish Biology 17:411-429

Kiljunen M, Grey J, Sinisalo T, Harrod C, Immonen H, Jones RI (2006) A revised model for lipid-normalizing $\delta^{13}C$ values from aquatic organisms, with implications for isotope mixing models. Journal of Applied Ecology 43:1213-1222

Lambert Y, Dutil JD (1997) Can simple condition indices be used to monitor and quantify seasonal changes in the energy reserves of cod (*Gadus morhua*)? Canadian Journal of Fisheries and Aquatic Sciences 54:104-112

Lentz SJ (2008) Observations and a model of the mean circulation over the Middle Atlantic Bight continental shelf. Journal of Physical Oceanography 38:1203-1221

Link JS (2002) Ecological considerations in fisheries management: when does it matter? Fisheries 27:10-17

MacNeil MA, Drouillard KG, Fisk AT (2006) Variable uptake and elimination of stable nitrogen isotopes between tissues in fish. Canadian Journal of Fisheries and Aquatic Sciences 63:345-353

Malek AJ, Collie JS, Taylor DL (2016) Trophic structure of a coastal fish community determined with diet and stable isotope analyses. Journal of Fish Biology 89:1513-1536

Manirakiza P, Covaci A, Schepens P (2001) Comparative study on total lipid determination using Soxhlet, Roese-Gottlieb, Bligh & Dyer, and modified

Bligh & Dyer extraction methods. Journal of Food Composition and Analysis 14:93-100

McCartney MA, Burton ML, Lima TG (2013) Mitochondrial DNA differentiation between populations of black sea bass (*Centropristis striata*) across Cape Hatteras, North Carolina (USA). Journal of Biogeography 40:1386-1398

McConnaughey T (1978) Ecosystems naturally labeled with carbon-13: applications to the study of consumer food webs. M.S., University of Alaska, Fairbanks,

McConnaughey T, McRoy CP (1979) Food-web structure and the fractionation of carbon isotopes in the Bering Sea. Marine Biology 53:257-262

McCutchan JH, Lewis WM, Kendall C, McGrath CC (2003) Variation in trophic shift for stable isotope ratios of carbon, nitrogen, and sulfur. Oikos 102:378-390

Miller AS, Shepherd GR, Fratantoni (2016) Offshore habitat preference of overwintering juvenile and adult black sea bass, *Centropristis striata*, and the relationship to year-class success. PLoS ONE 11(1): e0147627. doi:10.1371/journal.pone.0147627

Minagawa M, Wada E (1984) Stepwise enrichment of N-15 along food-chains – further evidence and the relation between delta-N-15 and animal age. Geochimica Et Cosmochimica Acta 48:1135-1140

Moser J, Shepherd GR (2009) Seasonal distribution and movement of black sea bass (*Centropristis striata*) in the northwest atlantic as determined from a mark-recapture experiment. Journal of Northwest Atlantic Fishery Science 40:17-28

Musick JA, Mercer LP (1977) Seasonal distribution of black sea bass, *Centropristis striata*, in the Mid-Atlantic Bight with comments on the ecology and fisheries of the species. Transactions of the American Fisheries Society 106:12-25

Nash RDM, Valencia AH, Geffen AJ (2006) The origin of Fulton's condition factor - Setting the record straight. Fisheries 31:236-238

Newsome SD, Martinez del Rio C, Bearhop S, Phillips DL (2007) A niche for isotopic ecology. Frontiers in Ecology and the Environment 5:429-436

Northeast Fisheries Science Center (2017) 62nd Northeast Regional Stock Assessment Workshop (6nd SAW) Assessment Summary Report. US Department of Commerce, Woods Hole, Massachusetts

Perga ME, Gerdeaux D (2005) 'Are fish what they eat' all year round? Oecologia 144:598-606

Pikitch EK, Santora C, Babcock EA, Bakun A, Bonfil R, Conover DO, Dayton P, Doukakis P, Fluharty D, Heneman B, Houde ED, Link J, Livingston PA, Mangel M, McAllister MK, Pope J, Sainsbury KJ (2004) Ecosystem-based fishery management. Science 305:346-347

Pinnegar JK, Polunin NVC (1999) Differential fractionation of δ^{13}C and δ^{15}N among fish tissues: implications for the study of trophic interactions. Functional Ecology 13:225-231

Post DM (2002) Using stable isotopes to estimate trophic position: models, methods, and assumptions. Ecology 83:703-718

Post DM, Layman CA, Arrington DA, Takimoto G, Quattrochi J, Montaña CG (2007) Getting to the fat of the matter: models, methods and assumptions for dealing with lipids in stable isotope analyses. Oecologia 152:179-189

Provost MM, Jensen OP, Berlinsky DL (2017) Influence of size, age, and spawning season on sex change in black sea bass. Marine and Coastal Fisheries 9:126-138

Roy EM, Quattro JM, Greig TW (2012) Genetic management of black sea bass: influence of biogeographic barriers on population structure. Marine and Coastal Fisheries 4:391-402

SEDAR (2018) SEDAR 56 - South Atlantic black seabass assessment report. Book SEDAR, North Charleston SC

Sedberry GR (1988) Food and feeding of black sea bass, *Centropristis striata*, in live bottom habitats in the South Atlantic Bight. The Journal of the Elisha Mitchell Scientific Society 104:35-50

Shepherd GR, Terceiro M (1994) The Summer Flounder, Scup, and Black Sea Bass Fishery of the Middle Atlantic Bight and Southern New England Waters. NOAA Technical Report NMFS. U.S. Department of Commerce, Seattle, Washington

Steimle FW, Figley W (1996) The importance of artificial reef epifauna to black sea bass diets in the Middle Atlantic Bight. North American Journal of Fisheries Management 16:433-439

Steimle FW, Zetlin C (2000) Reef habitats in the Middle Atlantic Bight: abundance, distribution, associated biological communities, and fishery resource use. Marine Fisheries Review 62:24-42

Sweeting CJ, Barry J, Barnes C, Polunin NVC, Jennings S (2007a) Effects of body size and environment on diet-tissue delta N-15 fractionation in fishes. Journal of Experimental Marine Biology and Ecology 340:1-10

Sweeting CJ, Barry JT, Polunin NVC, Jennings S (2007b) Effects of body size and environment on diet-tissue delta C-13 fractionation in fishes. Journal of Experimental Marine Biology and Ecology 352:165-176

Thomas CJ, Cahoon LB (1993) Stable isotope analyses differentiate between different trophic pathways supporting rocky-reef fishes. Marine Ecology Progress Series 95:19-24

Vander Zanden MJ, Cabana G, Rasmussen JB (1997) Comparing trophic position of freshwater fish calculated using stable nitrogen isotope ratios (δ^{15}N) and literature dietary data. Canadian Journal of Fisheries and Aquatic Sciences 54:1142-1158

Woodland RJ, Rodriguez MA, Magnan P, Glemet H, Cabana G (2012) Incorporating temporally dynamic baselines in isotopic mixing models. Ecology 93:131-144

Wuenschel MJ, Shepherd GR, McBride RS, Jorgensen R, Oliveira K, Robillard E, Dayton J (2011) Sex and maturity of black sea bass collected in Massachusetts and Rhode Island waters; preliminary results based on macroscopic staging of gonads with a comparison to survey data. 53rd SAW Assessment Report.

National Oceanic and Atmospheric Administration, National Marine Fisheries Service, Northeast Fisheries Science Center, Woods Hole, Massachusetts

Zudaire I, Murua H, Grande M, Pernet F, Bodin N (2014) Accumulation and mobilization of lipids in relation to reproduction of yellowfin tuna (*Thunnus albacares*) in the Western Indian Ocean. Fisheries Research 160:50-59

Figures

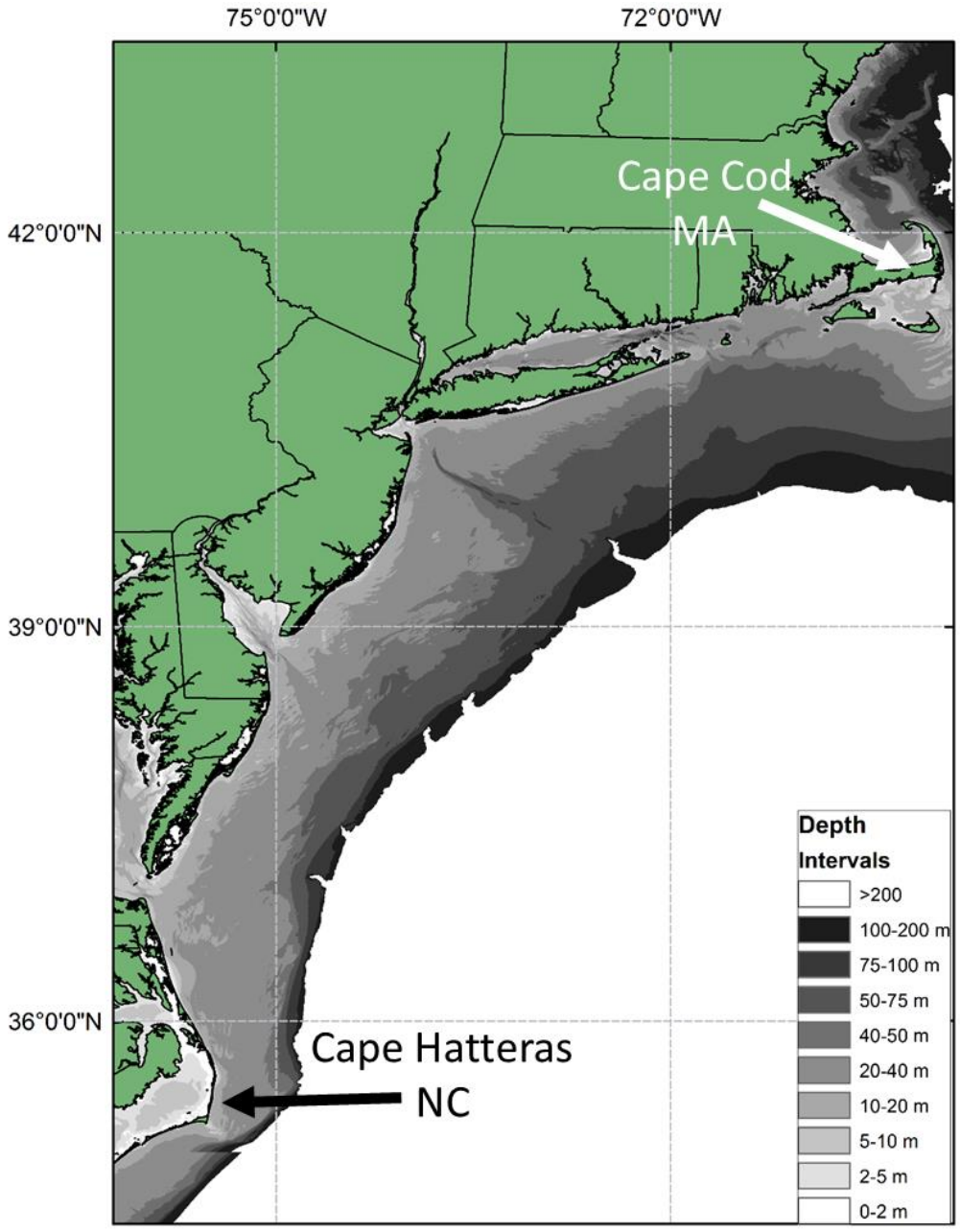

Figure 1.1. Map of the Middle Atlantic Bight (MAB). Arrows indicate the northern boundary of the MAB at Cape Cod, Massachusetts (MA) and the southern boundary at Cape Hatteras, North Carolina (NC).

Chapter 2: Spatiotemporal variability of muscle and liver tissue lipid content in black sea bass, *Centropristis striata*, and development of a δ^{13}C lipid-correction model

Abstract

Stable isotope analysis of multiple tissues from a consumer can provide insight into assimilated diet over different time-scales based on tissue-specific isotopic turnover rates. While tissue lipid content should be accounted for prior to comparing carbon isotope values (lipids are relatively depleted in ^{13}C), patterns in tissue lipid content across individuals can also yield valuable insight into the physiological condition of different consumer groups or populations, which may in turn indicate habitat quality. Extracting lipids directly or estimating a lipid-proxy for mathematical correction after sample analysis may yield information on consumer condition and facilitate stable isotope-based diet analysis. I hypothesized that the carbon to nitrogen (C:N) ratio of black sea bass (*Centropristis striata*) muscle and liver tissue would be a robust proxy for lipid content, that there would be clear relationships between lipid content and traditional indices, and that there would be spatial and biotic patterns of lipid content and condition. Significant differences were observed in tissue lipid content and condition indices between Middle Atlantic Bight regions. Changes to δ^{13}C via lipid extraction in *C. striata* liver displayed strong relationships to lipid content and C:N ratio. These relationships were used to construct a nonlinear lipid correction equation specific to *C. striata* liver. Muscle tissue was generally low in lipid content so it

requires no correction prior to use in dietary mixing models or other analyses. Differences in lipid content within an individual's tissues may be related to diet and reproductive timing as well as to habitat quality and connectivity.

Keywords: lipid extraction; lipid correction; condition index; black sea bass; stable isotope analysis; habitat quality

Introduction

Stable isotope analysis of nitrogen and carbon in metabolically active tissues has become a powerful and popular tool in trophic research. Studying the stable isotope composition of tissues enables investigation of a consumer's assimilated diet over periods of days to years, providing valuable trophic information unavailable from stomach content analysis alone. Nitrogen isotopic ratios ($^{15}N/^{14}N$; i.e., $\delta^{15}N$) enable determination of an individual's trophic position (Cabana & Rasmussen 1994), and carbon ratios ($^{13}C/^{12}C$; i.e., $\delta^{13}C$) can indicate the contribution of basal resources to the individual's diet (Post 2002). The different application of these elements is due to differences in isotope enrichment during trophic transfers. In contrast to the 2.5 – 5‰ enrichment in ^{15}N values typically observed between trophic levels (i.e., trophic enrichment factor, TEF), which is a function of protein synthesis, trophic shifts in ^{13}C are small and usually range between 0 and 2‰ for muscle and liver tissue (Pinnegar & Polunin 1999, McCutchan et al. 2003, Sweeting et al. 2007). The relative stability of $\delta^{13}C$ values across food chains facilitates reconstruction of trophic pathways by identifying primary producers that differ in their isotope values. For example, in

marine ecosystems, carbon isotope ratios typically differ between pelagic and benthic sources of primary production: benthic consumers are often more enriched in ^{13}C than pelagic consumers (Newsome et al. 2007, Malek et al. 2016).

White muscle and liver tissue are often used for stable isotope analysis of fish diet (Pinnegar & Polunin 1999, Post et al. 2007). These tissues provide intermediate (months to years – white muscle) to rapid (weeks to months – liver) indicators of diet (MacNeil et al. 2006). White muscle and liver also differ in their biochemical composition, particularly in regards to lipid content (Lambert & Dutil 1997, Alam et al. 2009). Lipid synthesis causes differential fractionation of ^{13}C isotopes; lipids are depleted in ^{13}C relative to synthesized proteins and carbohydrates. This isotopic fractionation results in lipid-rich tissues typically having lower $\delta^{13}C$ values relative to lipid-poor tissues (DeNiro & Epstein 1977). The variability in tissue lipid content within an organism can result in a wide range of reported $\delta^{13}C$ values for different tissue types and among individuals of the same species. Failure to account for lipid fractionation in comparative studies could lead to bias in estimates of relative prey contributions to diet and to incorrect estimates of trophic niche (Focken & Becker 1998, Pinnegar & Polunin 1999).

Two methods have been widely used to correct for the effect of differing lipid content on measured $\delta^{13}C$ values in fish tissues. First, lipids can be directly extracted from the tissue sample using standardized protocols and measured as a percentage of the total sample's mass (Dobush et al. 1985, Honeycutt et al. 1995, Manirakiza et al. 2001). Lipid-extracted samples can be measured for $\delta^{13}C$ to calculate the difference between untreated and lipid-free tissue ($\Delta\delta^{13}C$). Mechanical extraction methods

provide direct empirical measurements, yet they vary in their precision: those using only nonpolar solvents may underestimate total lipid content if there is a significant proportion of polar lipids that require separation from binding proteins and cell membranes (Manirakiza et al. 2001). In contrast, techniques using polar solvents can alter δ^{15}N values in samples after extraction (Pinnegar & Polunin 1999) as well as extract non-lipid materials, causing an overestimation of total lipid content (Dobush et al. 1985).

The second method is to construct numerical correction equations based on a subset of empirical data. In the majority of equations, the carbon to nitrogen (C:N) ratio of the tissue is assumed to be a direct predictor of lipid content. These equations can enable high numbers of samples to be corrected in a rapid, cost-effective manner. However, there is disagreement as to their applicability to a broad range of fish taxa and physiological states. Most equations are intended for white muscle tissue, while correction equations for other tissue types are less common (McConnaughey & McRoy 1979, Kiljunen et al. 2006, Post et al. 2007, Hoffman et al. 2015).

Fish condition indices have also been developed using length-weight relationships in order to identify stocks and to infer population-level dynamics (Jennings et al. 2001). One of the most commonly used morphometric indices is that of Fulton's condition (K) = $(W / L^3) * 100$, where W is the weight of the fish and L is the length of the fish (Nash et al. 2006). A positive relationship has been shown between the Fulton condition and the energy content of fish in the form of lipids and proteins (Lambert & Dutil 1997). Fishes typically store lipids within the liver, muscle, and mesentery. The proportions of storage in each depot site vary by species

and individual physiological factors (Sheridan 1988). Lipid characteristics and nutritional value varies by diet quality and quantity. These lipid stores can then be mobilized for energy allocations to metabolism, growth and reproduction (Tocher 2003, Alam et al. 2009, Bentley et al. 2009). The liver also plays a key role in reproductive development: it synthesizes and transfers lipids to the ovary for oocyte development (Zudaire et al. 2014). The hepatosomatic index (HSI) relays information on the physical health of a fish by identifying the relative mass of the liver. Similarly, the gonadosomatic index (GSI) provides information about the reproductive status of a fish as it varies by season by indicating the relative mass of the gonads (Wuenschel et al. 2013). In addition to traditional morphometric indices of fish condition, additional methods can identify the chemical composition of individuals to estimate the overall condition of the population. Of these composition indices, tissue energy content in the form of lipids or proteins can be closely linked to physiological condition, and can provide insight on foraging success and metabolic health. Changes to the lipid content of a population may reflect changes in food quality or availability, the introduction of novel stressors or disturbances, or behavioral shifts such as spawning or migration (Lambert & Dutil 1997, Alam et al. 2009, Schloesser & Fabrizio 2017).

The primary goals of this study were to 1) test the suitability of the tissue carbon to nitrogen (C:N) ratio as a predictor of lipid content in muscle and liver tissue of black sea bass (*Centropristis striata*) in order to derive a species-specific $\delta^{13}C$ correction model based on lipid content, 2) identify the relationship between tissue lipid content and three common condition indices (Fulton's *K*, HSI, GSI) of *C.*

striata, and 3) identify trends in lipid content relative to abiotic (depth, region, season) and biotic factors (length, sex). The studied fish, *C. striata*, is a demersal species commonly found on coastal reefs and structured bottom habitat along the Middle Atlantic Bight (MAB) of the United States. It resides near inshore reef structures during the summer, but northern fish migrate to overwinter in deeper offshore waters as temperatures decline in the autumn (Moser & Shepherd 2009). The stocks north and south of Cape Hatteras, North Carolina are managed as two separate fisheries. Genetic observations support this management system, having shown that the northern and southern stocks are two distinct groups with minimal gene flow (Roy et al. 2012, McCartney et al. 2013). While the general ecology of this species is fairly well known, there is much less information available on temporal patterns in diet, how diet differs across habitat types, and what effect these differences might have on individual condition.

I hypothesized that 1) the C:N ratio will have a strong relationship with muscle and liver lipid content across tissue types, 2) there will be significant relationships between tissue lipid content and the Fulton's *K*, GSI, and HSI indicators, and 3) there will be spatial, temporal, and physiological factors influencing the tissue lipid content.

Materials and methods

Sample collection and condition indices

Black sea bass samples were collected by hook and line from MAB reef sites offshore of Point Pleasant, New Jersey (June 2016), Ocean City, Maryland (August 2016), and Cape Hatteras, North Carolina (August 2016, Fig. 2.1). Fish were immediately frozen on dry ice when possible or kept on ice (0°C) in coolers for the duration of field sampling. Additional frozen specimens were acquired from the National Marine Fisheries Service (NMFS) spring and autumn bottom trawl surveys in 2016. For subsequent spatial analyses, sites were categorized into four regional groups from north to south: Southern New England (SNE), New Jersey (NJ), Maryland/Delmarva (MD), and North Carolina (NC).

Upon return to the Chesapeake Biological Laboratory (CBL) in Solomons, Maryland, USA, fish were stored in a -50°C freezer until thawed for dissection. Fish total length (TL, mm) and weight (g) were determined before dissection. Fish with TL < 170 mm were classified as young of the year (YOY), while those with TL ranging from 170 – 250 mm were categorized as juveniles/small adults, and fish ≥ 250 mm TL were classified as 'large adults' (Bowman et al. 2000, Able & Fahay 2010). Liver and gonads were weighed separately for condition and reproductive index calculations, respectively, and the sex of the fish was determined visually. Individuals were classified as being of indeterminate sex when the gonads could not be identified as male or female. The mass of the stomach and all contents was subtracted from the fish total mass to reduce bias in the masses of individual fish that

was due to variation in stomach fullness. These modified data were used in the calculation of condition indices described above.

Ten of the acquired NC individuals in the lipid analysis study had been previously filleted and could not be measured for whole weights, but were instead assigned estimated whole weights based on a length-weight relationship calculated for all fish with measured weights sampled from NC in this study (n = 25), enabling calculation of morphometric indices. The log-length –log-weight regression resulted in the following model parameterization: $Log_{10}\ Weight = -5.106 + 3.114 * Log_{10}\ Length$ ($r^2 = 0.997$, $P < 0.0001$) (Eq. 2.1).

For stable isotope analysis, approximately 1 cm^3 of white muscle tissue was cut from the anterior dorsal region of the fish. The sample was examined to ensure the sample was free from bone fragments, skin or scales, triple rinsed with deionized water, and dried in an oven at 60°C to a constant weight for 48-72 hrs. Liver tissue samples were similarly prepared. Dried tissue samples were homogenized to a fine powder using a mortar and pestle.

Lipid extraction

To avoid potential confounding effects of size and sex, an equal distribution of large and small fish and an equal number of females and males/indeterminate sex were selected from the NJ and NC reef muscle and liver tissue samples (no males were identified in the NC sample group, so an equal number of females and indeterminate individuals were analyzed instead). Due to limitations in sample availability, an equal number of each size class and sex was not practical for the MD

reef liver samples. Muscle tissue extractions were not conducted on MD reef fish, and no tissue lipid extractions were conducted on NMFS sampled fish.

Selected subsamples of powdered *C. striata* liver (n = 48) and muscle (n = 24) tissue, weighing approximately 50 mg each, were lipid extracted using the Soxhlet method with petroleum ether. Petroleum ether is a commonly used nonpolar solvent for the estimation of percent lipid content (Dobush et al. 1985, Wuenschel et al. 2006, Wuenschel et al. 2013). Muscle samples were packed into pre-weighed cellulose extraction thimbles (10 x 50 mm; Whatman plc [part of GE Healthcare Life Sciences], Buckinghamshire, UK) and liver samples were packed into glass fiber extraction thimbles (10 x 38 mm; Whatman plc) sealed overhead with cotton or quartz wool (Costech Analytical Technologies, Inc., Valencia, California, USA). Glass fiber thimbles and quartz wool were pre-combusted at 450°C for 90 minutes to remove any trace organic compounds prior to use. Samples were weighed prior to extraction after 24-48 hours at constant humidity. Sample thimbles (n =4) were nested in large cellulose thimbles (33 x 80 mm, Whatman plc), which were in turn topped with quartz wool and placed in a Soxhlet apparatus with a capacity to hold 6 large thimbles (total sample size = 24 per extraction run). Samples were fluxed in heated petroleum ether for approximately 4 hours and thoroughly dried prior to final weighing at the same constant humidity. Dobush et al. (1985) concluded that all nonpolar lipids were extracted from their 5g samples within 6 hours using Soxhlet with petroleum ether. The samples for my study were two orders of magnitude smaller, thus 4 hours of extraction time was likely more than sufficient. After air-

drying in the fume hood for 24 hours following extraction, samples were dried at 60°C for 24 hours then weighed at a constant humidity.

Lipid mass (nonpolar) was calculated as the *initial sample mass – final sample mass*, and percent lipid content was calculated as *(lipid mass/initial sample mass) * 100*. I assumed that the amount of polar lipids remaining in the tissue after extraction was negligible relative to the amount of nonpolar lipids.

Stable isotope analysis

For bulk analysis of *C. striata* tissues before and after extraction, 0.6-0.8 mg of dried, powdered sample was transferred to a pre-weighed tin foil capsule. Sample capsules were combusted using a Costech Elemental Analyzer (EA) (Costech Analytical Technologies, Inc., Valencia, California, USA) coupled to a ThermoScientific Delta V Plus (Thermo Fisher Scientific, Inc., Waltham, Massachusetts, USA) continuous flow Isotope Ratio Mass Spectrometer (IRMS) (at CBL, Solomons, Maryland, USA). Results are reported in the delta (δ) notation relative to international standards, Vienna Pee Dee Belemnite for carbon and atmospheric N_2 for nitrogen. Both $\delta^{15}N$ and $\delta^{13}C$ values were generated from the same samples. Data output from the IRMS also includes the relative masses of carbon and nitrogen in each sample, enabling calculation of the molar carbon to nitrogen (C:N) ratio. Internal standards were used to account for drift, and analytical precision of my duplicate *C. striata* samples (n = 42) was approximately 0.4 ± 0.9‰ for carbon and 0.2 ± 0.4‰ for nitrogen. Long-term IRMS precision using protein standards was

± 0.12‰ (SD) for carbon (n = 16) and ± 0.24‰ for nitrogen (n = 15) (C. Magen, personal communication).

Lipid correction equations

Relationships between tissue lipid content (%), C:N ratio, and $\Delta\delta^{13}C$ were assessed using a linear regression. One liver sample was identified as a statistical outlier (Bonferroni outlier test, $P = 0.01$) and was excluded from all analyses. Two duplicate liver samples were also excluded from statistical analyses. Comparison of lipid mass and lipid percentage differences suggested that the duplicate measurements were not substantially different from the original measurements.

Several lipid correction equations have been proposed in the literature for fish tissues, in particular for white muscle tissue. These equations quantify the relationships between lipid content (expressed as % of total tissue composition), C:N ratio, and difference in $\delta^{13}C$ before and after extraction ($\Delta\delta^{13}C$).

A linear regression approach was used in Post et al. (2007) for these relationships in aquatic animals:

$$\%\ lipid = -20.54 + 7.24 * C{:}N \quad \text{(Eq. 2.2)}$$

$$\Delta\delta^{13}C = -3.32 + 0.99 * C{:}N \quad \text{(Eq. 2.3)}$$

However, it must be noted that these parameters were developed using samples with C:N ratios that ranged from 3 to 6.9 and might not be appropriate for higher ratios (Post et al. 2007). The relationship becomes curvilinear at higher C:N ratios (Kiljunen et al. 2006, Hoffman et al. 2015), and one of the most frequently-used sets of equations is that of McConnaughey and McRoy (1979):

$$L = 93 / [1 + (0.246 * C{:}N - 0.775)^{-1}] \quad \text{(Eq. 2.4)}$$

where L is the percent lipid content and $C{:}N$ is the carbon to nitrogen ratio in the tissue. This equation assumes that the combined sum of protein and lipid in the tissue remains constant at 93 percent, with the remaining 7 percent comprising carbohydrates and other biological material. It is also assumed that protein is the sole source of nitrogen in the measured biomass (McConnaughey 1978). The calculated lipid content L is then used in the correction equation

$$\delta^{13}C' = \delta^{13}C + D * [I + 3.9 / (1 + 287 / L)] \quad \text{(Eq. 2.5)}$$

where D is the isotopic difference between protein and lipid material, and I is a constant. In McConnaughey and McRoy (1979), D was assigned a value of 6‰ and I was assigned a value of -0.2. Kiljunen et al. (2006) re-fitted the D and I parameters to their dataset, resulting in a value of 7.0 ± 0.3‰ (SD) for D and a value of 0.05 ± 0.01 for I.

For this study, a nonlinear model was fitted to the empirical lipid-extracted liver values by modifying two of the parameters (the values 0.246 and 0.775 in Eq. 2.4) in the McConnaughey and McRoy (1979) lipid equation. These parameters were optimized by minimizing the sum of squares of differences between observed and predicted lipid content. In turn, a second nonlinear model (Eq. 2.5) was also modified to predict $\Delta\delta^{13}$C (represented by the expression $D * [I + 3.9 / (1 + 287 / L)]$ within the equation) based on the sample lipid content. These fitted models were then used to calculate estimated lipid content and $\Delta\delta^{13}$C for a larger dataset of untreated liver samples.

An alternative metric, which was defined as lipid density, was computed using the empirical and predicted lipid content values. The estimated total lipid mass in the liver was determined by multiplying the percent lipid proportion by the mass of the liver for each individual. This lipid mass was in turn divided by each individual's body mass to assess the liver lipid density per unit body mass for each individual. This metric thus removes the confounding factors of body size when assessing lipid content in the liver.

Lipid content, condition, and factors

The isotope compositions of empirical lipid extraction samples were compared before and after extraction and compared among regions using two-sample *t* tests or ANOVA where applicable. The relationships among C:N ratio, lipid content, and $\Delta\delta^{13}C$ were examined using linear regression. Muscle and liver lipid content (both empirical and predicted values) were compared to condition and reproductive indices (Fulton's *K*, HSI, GSI) using Pearson correlation. Where appropriate, the model residuals were examined using QQ plotting and transformed using Box-Cox power transformation when necessary to satisfy the normality assumptions of the linear model.

In addition, generalized linear models (GLMs) were constructed to evaluate the factors responsible for the variability in liver lipid content, HSI, and GSI:

$$CI \sim Region + Sex + Length + Depth \quad \text{(Eq. 2.6)}$$

where *CI* is the condition (lipid content, HSI) or reproductive index (GSI), *Region* and *Sex* are class variables, and *Length* and *Depth* are continuous variables. Similarly,

a GLM was constructed to evaluate factors responsible for variability in Fulton condition. The length factor was removed due to autocorrelation from the index formula:

$$K \sim Region + Sex + Depth \quad \text{(Eq. 2.7)}$$

Statistical analyses were performed in R versions 3.3.1 (R Core Team 2016) and 3.5.1 (R Core Team 2018).

Results

Muscle tissue: lipid content

Muscle tissue lipid content in NJ and NC ranged from 1.7% to 5.3%, with a mean (± SD) of 2.7 ± 1.0 %. Fish muscle from the two regions differed in C:N ratio (Two sample *t*-test, $df = 16.04$, $t = -2.25$, $P = 0.04$) and in $\delta^{13}C$ (Two sample *t*-test, $df = 17.188$, $t = -3.60$, $P = 0.002$). The two regions also differed in muscle tissue lipid content (Two sample *t*-test, $df = 17.188$, $t = -3.60$, $P = 0.002$), with higher proportions in NJ samples. The $\delta^{15}N$ values also differed significantly between NJ and NC muscle tissue samples (Two sample *t*-test, $df = 20.662$, $t = -11.68$, $P < 0.0001$), with higher values from NJ samples (Table 2.1). It was not possible to obtain valid $\delta^{13}C'$ or $\Delta\delta^{13}C$ values for muscle tissue after extraction due to sample contamination in the cellulose thimbles.

Liver tissue: lipid content

The Soxhlet extraction method returned reproducible results, with a mean difference in lipid mass for duplicate liver samples of 0.45 mg and a mean difference in lipid content of 0.76%. Liver tissue lipid content in NJ, MD, and NC ranged widely from 5.6% to 54.9%, with a mean of 25.1 ± 16.2%. Untreated mean δ^{13}C values for liver were -19.5 ± 1.1‰ and treated (lipid-extracted) values (δ^{13}C′) were -18.1 ± 0.7‰. Lipid extraction reduced C:N ratios of liver samples from an initial mean of 8.5 ± 3.1 to a post-extraction mean of 5.2 ± 0.7 (Table 2.1). Lipid extraction had a significant effect on C:N ratios (Wilcoxon signed-ranks test, $V = 1035$, $P < 0.0001$) and measured δ^{13}C values (Paired *t*-test, $df = 44$, $t = 7.55$, $P < 0.0001$). Livers from NC underwent the greatest change in δ^{13}C after extraction ($\Delta\delta^{13}$C), with a mean 2.3 ± 1.1‰ difference compared to differences of 0.5 ± 0.4‰ for MD and 0.8 ± 0.9‰ for NJ. The average difference in δ^{15}N before and after extraction for all liver samples was 0.1 ± 0.2‰, which is below the analytical precision of the IRMS, indicating that the δ^{15}N values did not differ significantly before and after the Soxhlet procedure. Regional groups differed substantially in δ^{15}N (ANOVA, $F_{2,42} = 146.1$, $P < 0.0001$), with all three regions differing from one another (Tukey HSD test, $P < 0.05$). Rank order of δ^{15}N values from more heavy isotope-enriched to depleted was NJ, MD and NC (Table 2.1).

Prior to extraction, there were significant differences in liver δ^{13}C values among regions (ANOVA, $F_{2,42} = 8.50$, $P = 0.0008$) (Table 2.1), with significant differences between NJ and NC but not for the other pairwise comparisons. After extraction, the significant differences remained (ANOVA, $F_{2,42} = 17.27$, $P < 0.0001$),

but this time the NC – MD and NJ – MD pairs were significantly different (Table 2.1). Empirical liver lipid content differed significantly among regions (ANOVA, $F_{2,42} = 18.14$, $P < 0.0001$) with the NC group significantly different from both MD and NJ. Initial C:N ratio also differed significantly among regions (ANOVA, $F_{2,42} = 18.51$, $P < 0.0001$), with significant differences between NC – MD and NJ – NC pairs. In contrast to muscle tissue, *C. striata* from NC had the highest mean lipid content, followed by NJ and lowest in MD. This ranking is also evident in liver C:N ratios prior to extraction. After extraction, C:N ratios no longer differed significantly among regions (ANOVA, $F_{2,42} = 1.39$, $P = 0.26$) (Table 2.1).

Lipid correction equations

For muscle tissue (n = 24), there was no significant relationship between C:N ratio and lipid content ($P = 0.11$). However, removal of a statistical outlier (Bonferroni outlier test, $P = 0.002$), resulted in a positive and significant relationship (n = 23, $r^2 = 0.33$, $F_{1,21} = 11.63$, $P = 0.003$ [not shown]). Length of the individual was not a significant predictor of muscle lipid content ($P = 0.10$).

For liver tissue, however, there was a positive linear relationship between C:N ratios and lipid content (n = 45, $r^2 = 0.85$, $F_{1,43} = 251.1$, $P < 0.0001$) for C:N ratios ranging from 4.7 to 16.0, with a mean of 8.5 ± 3.1 SD (Fig. 2.2). Liver C:N ratios also had a similar linear relationship to $\Delta\delta^{13}C$ (Linear regression, $r^2 = 0.71$, $F_{1,43} = 111.1$, $P < 0.0001$ [not shown]). The linear regression equation, following the format of Post et al. (2007) (i.e., Eq. 2.2) was: *% lipid = -16.56 + 4.88 * C:N* (Eq. 2.8). Application of this linear equation to the larger bulk liver isotope dataset that was not empirically

measured for lipid content (n = 108), resulted in a predicted lipid content ranging from 5.6 to 79.9%, with a mean ± SD of 23.1 ± 15.8% when using the initial C:N ratio as a predictor. However, the C:N ratios of the untreated liver data extended beyond the range of the measured liver C:N ratios, with ratios as high as 19.8. Extrapolations of predicted lipid content for samples with higher C:N ratios based on the linear regression model yielded nonsensical values (e.g., % lipid content > 100). Thus a nonlinear model in the style of McConnaughey and McRoy (1979) and Kiljunen et al. (2006) (i.e., Eq. 2.4) was fitted to the empirical lipid extraction data to account for the asymptotic relationship between lipid content and C:N at higher ratios: $L = 93 / (1 + (0.110 * C{:}N - 0.505)^{-1})$ (Eq. 2.9). Predicted lipid content ranged from negligible (-0.4%, n = 3 predictions resulted in negative values) to 58.2%, with a mean ± SD of 22.6 ± 14.8% (Fig. 2.3).

The parameters in the model for determining the lipid-corrected δ^{13}C values (δ^{13}C′, Eq. 2.5) were adjusted to fit the lipid-extracted data as follows: $\delta^{13}C' = \delta^{13}C + 4.852 * (3.9 / [1 + (287 / L)])$ ($r^2 = 0.85$, $F_{1,43} = 244.9$, $P < 0.0001$) (Eq. 2.10). Initial (unextracted) δ^{13}C values ranged from -23.5‰ to -17.8‰ with a mean ± SD of -19.8 ± 1.2‰, and lipid-corrected δ^{13}C′ values ranged from -20.8‰ to -15.9‰, with a mean of -18.5 ± 1.0‰.

Condition and reproductive indices

Liver samples predicted to have a negative (negligible) lipid content (n = 3) were removed from all further analyses. In contrast to the initial hypotheses, there was no correlation between HSI and liver lipid content (measured or predicted), but

there was a correlation between HSI and measured muscle lipid content (Table 2.2). The relationship between Fulton's *K* condition index and liver lipid content was significant and positive, but was less significant for muscle lipid content (Table 2.2). In terms of reproductive condition, GSI was correlated positively with muscle lipid content but negatively correlated with liver lipid content (Table 2.2).

Regional variation

Regional differences in $\delta^{13}C'$ were significant (ANOVA, $F_{3,149} = 25.78$, $P < 0.0001$); all pairwise comparisons were significantly different except for NJ versus NC (Table 2.3). Spatial variation was evident in the $\Delta\delta^{13}C$ for both empirically- and numerically- corrected liver samples (ANOVA, $F_{3,149} = 16.01$, $P < 0.0001$) (Fig. 2.4), with all pairwise comparisons significant except for NJ vs. MD and SNE vs. NC (Table 2.3). In the case of muscle tissue, measured $\delta^{13}C$ values varied significantly by region (ANOVA, $F_{3,198} = 44.08$, $P < 0.0001$), with pairwise comparisons indicating similarities between NC vs. MD and between SNE vs. NJ (Table 2.3).

Generalized linear model results for liver lipid content indicated that region and depth were significant factors, while sex and length were not significant (Table 2.4). The relationship between depth and liver lipid content was positive (Fig. 2.5a), and there were significant pairwise differences among the regions (Table 2.4). Results from the HSI model indicated that region and sex were significant factors while length and depth were not significant (Table 2.5). Female individuals had the highest HSI values and differed significantly from males and indeterminate individuals (Fig. 2.5b). When confounding effects of body size were removed using the liver lipid

density metric, there were minor changes to the pairwise comparisons, but the pattern remained similar to liver lipid content (Table 2.4).

All factors measured were significant in the GSI model (Table 2.5). There was a positive relationship between GSI and length (Fig. 2.5e) and a negative relationship with depth (Fig. 2.5c). Female individuals had the highest GSI values and differed significantly from males and indeterminate individuals (Fig. 2.5d).

Finally, model results for Fulton's *K* indicated that only region was a significant factor while sex and depth were not significant (Tables 2.4 & 2.5).

Discussion

In contrast to dorsal muscle, there were consistently strong relationships among percent lipid content, C:N ratio, and $\Delta\delta^{13}C$ for *C. striata* liver tissue. These relationships were successfully applied to previously published numerical correction equations following adjustments. Previous studies of a similar serranid fish did not observe a relationship between lipid content and C:N ratios of liver tissue (Nelson et al. 2011), yet this was likely due to a small sample size of four individuals. I recommend that lipid content be accounted for when drawing conclusions from carbon isotope analyses in liver tissue in *C. striata*. The low range of lipid content and C:N ratios in white muscle tissue in this study is consistent with previous conclusions that tissues with low lipid content (below 15%) and low C:N ratios (3.5-4) do not require numerical lipid normalization (Hoffman et al. 2015, Skinner et al. 2016).

The similarities among regions for $\delta^{13}C$ values observed before and after lipid extraction varied substantially. These findings support hypotheses that high lipid content could obscure true regional differences in carbon isotopes. Accounting for lipid content via direct or indirect methods enables a better assessment of short-term prey assimilation for liver tissue because of its relatively rapid isotopic turnover rate (MacNeil et al. 2006). Lipid extraction using a standardized method is a useful way to remove distortions in carbon isotope signatures, yet it can be costly and time-consuming for large sample sizes. Developing an appropriate correction model can allow for rapid processing of high numbers of samples.

The differences in lipid content in dorsal muscle vs. liver is consistent with previous reports of *C. striata* lipid storage being primarily in liver and abdominal muscle. Dorsal muscle contains the highest amount of protein, while substantially less protein is found in the liver and abdominal muscle (Alam et al. 2009). While muscle tissue is not the primary energy storage site in *C. striata*, changes in muscle energy content reflect trends in overall energy storage within an individual (Wuenschel et al. 2013).

The highest liver lipid content was observed in NC fish and the lowest was found in MD, with SNE and NJ at intermediate levels. Liver lipid content and condition vary considerably among individual fishes due to a variety of factors, including diet (Alam et al. 2009), reproductive status (Bentley et al. 2009, Zudaire et al. 2014), health status and somatic growth status (Lambert & Dutil 1997, Wuenschel et al. 2006). In general, higher lipid content suggests more successful feeding and better environmental conditions than observed in individuals with lower lipid content.

The proportion of lipids present in individual fish tissues can serve as an indicator of habitat quality characteristics (Lloret & Planes 2003). However, the types of lipid play significant roles in the reproductive success of *C. striata*: a feeding study reported that fish fed a diet of silversides with higher levels of n-3 polyunsaturated fatty acids experienced higher spawning success and hatch rates than those fed a prepared diet with similar lipid amounts but lower proportions of these essential fatty acids (Bentley et al. 2009).

This study enabled comparisons of summer reef groups from NJ, MD, and NC, and I extrapolated some of these results to SNE fish tissue, assuming that lipid storage processes and seasonal dynamics would be equivalent to those from other regions. Seasonal sampling gaps also limit some of the conclusions that can be drawn. For example, there was a highly uneven distribution of samples for spring (n = 20) and autumn (n = 17) compared to summer samples (n = 116). The majority of samples were collected in summer when fish are residents on inshore reefs. Fewer samples were acquired from the spring and autumn bottom trawl surveys when fish are located offshore. Future studies should sample a more even distribution of latitudinal reef and offshore sites across seasons to assess spatial and temporal trends with greater statistical power and to assess seasonal patterns.

Lipid content and condition indices

The lack of a relationship between liver lipid content and HSI contrasted with observations of strong positive relationships between liver index and liver energy content in the form of lipids in Atlantic cod, *Gadus morhua* (Lambert & Dutil 1997). Liver size is typically associated with higher lipid content, suggesting that lipid

accumulation occurs in favorable environments (Lloret & Planes 2003). Nevertheless, the observed relationship between Fulton's *K* condition and liver lipid content has been supported by previous work (Lambert & Dutil 1997). A study of white seabream *Diplodus sargus* condition indices at different sites in the Mediterranean yielded similar results to my study: in both cases, fish length did not correlate with HSI or liver lipid content. However, GSI had significant relationships with fish length and sex, with females having higher GSI on average. In addition, females had the highest HSI values, which may relate to the liver's importance in storing and synthesizing lipids for egg development (Lloret & Planes 2003). The highest *C. striata* GSI values were observed in NJ and MD fish caught by hook and line from June-August, at the peak of the MAB population's spawning season. Gonads were typically large and easily identifiable without magnification. The spawning season of the northern MAB population peaks from May to August (Moser & Shepherd 2009), after which there is a significant drop in GSI from August through October prior to the onset of migration (Wuenschel et al. 2011).

In contrast, the NC fish in this study (the group with the lowest GSI values) were caught by hook and line in July and August, and the gonads were small and of indeterminate sex. This may have been in part due to some fish being immature [all reef-caught YOY (n = 6) were from this region] but it also may be due to the fact that the peak of the spawning season had already passed. In the case of the SAB stock, the spawning season extends from January to June, with peak spawning occurring from March to May. Additional spawning may also occasionally take place in September and October (Mercer 1989). Given their reproductive status at time of collection, it is

likely that the NC fish sampled here belong to the SAB population. Future analyses could categorize *C. striata* individuals by reproductive status and compare this variable to morphometric and body composition indices (Lloret & Planes 2003). It would also be of interest to compare the indices of fish sampled from MAB and SAB reefs during their respective peak spawning times.

The observed negative relationship between GSI and liver lipid content is similar to previous observations of an inverse relationship between gonad lipid content and liver lipid content in female yellowfin tuna. Pre-spawn female yellowfin tuna show increased lipids in gonads with a decrease in liver lipids, while the opposite is true for immature females (Zudaire et al. 2014). Future analysis could confirm these same seasonal reproductive shifts for *C. striata* gonad lipid content to and from liver and muscle lipid content, but it will require appropriate seasonal sampling that was not possible in this study.

I did not observe a directional relationship between length and liver lipid content; this may be due in part to the small number of young of the year examined (n = 11) compared to juveniles/adults (n = 139). Lipid storage in fishes tends to increase with length (Lloret & Planes 2003), as energy allocation strategies for adult fishes often differ from juveniles. Larvae and juveniles prioritize growth rather than storage in order to escape predation pressure at small sizes (Wuenschel et al. 2006, Drohan et al. 2007). Latitudinal patterns could also play a role: lower latitudes generally have more predictable resources and thus reduced chance of starvation compared to higher latitudes, reducing the need for energy storage (Wuenschel et al. 2006). Yet lower latitudes often contain a higher diversity of potential predators, causing growth to be

more important (Wuenschel et al. 2006). In the case of *C. striata*, lipids do not begin to accumulate until the individual reaches about 40 mm or more (Wuenschel et al. 2006, Drohan et al. 2007). Recent studies have examined juvenile fish lipid content and its implications for juvenile fitness, which can have significant cascading effects for population-level effects when successful individuals recruit to the spawning stock (Schloesser & Fabrizio 2017).

Physiology and fisheries management

When assessing the potential for recruitment, many stock-recruitment relationships overlook external environmental factors. Fish condition and energetic reserves, which can be directly influenced by environmental conditions such as temperature and salinity, play a critical role in migration and overwintering survival. The portion of the MAB *C. striata* population north of Hudson Canyon undergoes a more energetically demanding migration path as it travels longer distances southwards and offshore (Moser & Shepherd 2009, Miller et al. 2016), including stresses at the deeper areas at the continental slope that tend to be warmer by a few degrees compared to shallow shelf sites (Love & Chase 2007). Understanding their diet via stable isotope analysis and their physiological condition via liver lipid content by C:N proxy could provide insight into migration and overwintering survival as well as recruitment success.

Conclusion

Quickly and effectively monitoring patterns in fish condition can provide crucial insight into energy transfer in marine ecosystems and into the resource needs of important fisheries. By deriving targeted, species-specific models of tissue C:N stoichiometry to lipid content, future analyses using standardized IRMS and EA technology can simultaneously yield valuable information on individual feeding history as well as physiological condition. The ability to consistently determine lipid content and to numerically adjust isotopic fractionation in lipid-rich tissues can also expedite large-scale studies by removing the need for mechanical extraction of all isotope samples. I also showed that C:N modeled lipid content (%) can provide a complementary index of condition compared to traditional condition factors. I used these approaches to show that *C. striata* display broad spatial patterns in lipid content and physiological condition in the Middle Atlantic Bight.

References

Able KW, Fahay MP (2010) Ecology of estuarine fishes: temperate waters of the Western North Atlantic. The Johns Hopkins University Press, Baltimore, MD

Alam MS, Watanabe WO, Carroll PM, Rezek T (2009) Effects of dietary protein and lipid levels on growth performance and body composition of black sea bass *Centropristis striata* (Linnaeus 1758) during grow-out in a pilot-scale marine recirculating system. Aquaculture Research 40:442-449

Bentley CD, Watanabe WO, Rezek TC, Seaton PJ (2009) Preliminary investigations on the effects of dietary lipid on the spawning performance and egg quality of black sea bass *Centropristis striata* L. Aquaculture Research 40:1873-1883

Bowman RE, Stillwell CE, Michaels WL, Grosslein MD (2000) Food of Northwest Atlantic Fishes and Two Common Species of Squid. NOAA Technical Memorandum NMFS-NE-155. National Oceanic and Atmospheric Administration: National Marine Fisheries Service, Woods Hole, Massachusetts

Cabana G, Rasmussen JB (1994) Modelling food chain structure and contaminant bioaccumulation using stable nitrogen isotopes. Nature 372:255-257

DeNiro MJ, Epstein S (1977) Mechanism of carbon isotope fractionation associated with lipid-synthesis. Science 197:261-263

Dobush GR, Ankney CD, Krementz DG (1985) The effect of apparatus, extraction time, and solvent type on lipid extractions of snow geese. Canadian Journal of Zoology-Revue Canadienne De Zoologie 63:1917-1920

Drohan AF, Manderson JP, Packer DB (2007) Essential fish habitat source document: black sea bass, *Centropristis striata*, life history and habitat characteristics. NOAA Technical Memorandum

Focken U, Becker K (1998) Metabolic fractionation of stable carbon isotopes: implications of different proximate compositions for studies of the aquatic food webs using delta C-13 data. Oecologia 115:337-343

Hoffman JC, Sierszen ME, Cotter AM (2015) Fish tissue lipid-C:N relationships for correcting C-13 values and estimating lipid content in aquatic food-web studies. Rapid Communications in Mass Spectrometry 29:2069-2077

Honeycutt ME, McFarland VA, McCant DD (1995) Comparison of 3 lipid extraction methods for fish. Bulletin of Environmental Contamination and Toxicology 55:469-472

Jennings S, Kaiser MJ, Reynolds JD (2001) Marine Fisheries Ecology. Blackwell Science Ltd., Oxford, UK

Kiljunen M, Grey J, Sinisalo T, Harrod C, Immonen H, Jones RI (2006) A revised model for lipid-normalizing δ^{13}C values from aquatic organisms, with implications for isotope mixing models. Journal of Applied Ecology 43:1213-1222

Lambert Y, Dutil JD (1997) Can simple condition indices be used to monitor and quantify seasonal changes in the energy reserves of cod (*Gadus morhua*)? Canadian Journal of Fisheries and Aquatic Sciences 54:104-112

Lloret J, Planes S (2003) Condition, feeding and reproductive potential of white seabream *Diplodus sargus* as indicators of habitat quality and the effect of

reserve protection in the northwestern Mediterranean. Marine Ecology Progress Series 248:197-208

Love JW, Chase PD (2007) Marine fish diversity and composition in the Mid-Atlantic and South Atlantic Bights. Southeastern Naturalist 6:705-714

MacNeil MA, Drouillard KG, Fisk AT (2006) Variable uptake and elimination of stable nitrogen isotopes between tissues in fish. Canadian Journal of Fisheries and Aquatic Sciences 63:345-353

Malek AJ, Collie JS, Taylor DL (2016) Trophic structure of a coastal fish community determined with diet and stable isotope analyses. Journal of Fish Biology 89:1513-1536

Manirakiza P, Covaci A, Schepens P (2001) Comparative study on total lipid determination using Soxhlet, Roese-Gottlieb, Bligh & Dyer, and modified Bligh & Dyer extraction methods. Journal of Food Composition and Analysis 14:93-100

McCartney MA, Burton ML, Lima TG (2013) Mitochondrial DNA differentiation between populations of black sea bass (*Centropristis striata*) across Cape Hatteras, North Carolina (USA). Journal of Biogeography 40:1386-1398

McConnaughey T (1978) Ecosystems naturally labeled with carbon-13: applications to the study of consumer food webs. M.S., University of Alaska, Fairbanks

McConnaughey T, McRoy CP (1979) Food-web structure and the fractionation of carbon isotopes in the Bering Sea. Marine Biology 53:257-262

McCutchan JH, Lewis WM, Kendall C, McGrath CC (2003) Variation in trophic shift for stable isotope ratios of carbon, nitrogen, and sulfur. Oikos 102:378-390

Mercer LP (1989) Species profile: life histories and environmental requirements of coastal fishes and invertebrates (south Atlantic): black sea bass. Book 82(11). U.S. Fish and Wildlife Service Biological Report

Miller AS, Shepherd GR, Fratantoni (2016) Offshore habitat preference of overwintering juvenile and adult black sea bass, *Centropristis striata*, and the relationship to year-class success. PLoS ONE 11(1): e0147627. doi:10.1371/journal.pone.0147627

Moser J, Shepherd GR (2009) Seasonal distribution and movement of black sea bass (*Centropristis striata*) in the Northwest Atlantic as determined from a mark-recapture experiment. Journal of Northwest Atlantic Fishery Science 40:17-28

Nash RDM, Valencia AH, Geffen AJ (2006) The origin of Fulton's condition factor - Setting the record straight. Fisheries 31:236-238

Nelson J, Chanton J, Coleman F, Koenig C (2011) Patterns of stable carbon isotope turnover in gag, *Mycteroperca microlepis*, an economically important marine piscivore determined with a non-lethal surgical biopsy procedure. Environmental Biology of Fishes 90:243-252

Newsome SD, Martinez del Rio C, Bearhop S, Phillips DL (2007) A niche for isotopic ecology. Frontiers in Ecology and the Environment 5:429-436

Pinnegar JK, Polunin NVC (1999) Differential fractionation of δ^{13}C and δ^{15}N among fish tissues: implications for the study of trophic interactions. Functional Ecology 13:225-231

Post DM (2002) Using stable isotopes to estimate trophic position: models, methods, and assumptions. Ecology 83:703-718

Post DM, Layman CA, Arrington DA, Takimoto G, Quattrochi J, Montaña CG (2007) Getting to the fat of the matter: models, methods and assumptions for dealing with lipids in stable isotope analyses. Oecologia 152:179-189

R Core Team (2016) R: A language and environment for statistical computing. R Foundation for Statistical Computing, Vienna, Austria

R Core Team (2018) R: A language and environment for statistical computing. R Foundation for Statistical Computing, Vienna, Austria

Roy EM, Quattro JM, Greig TW (2012) Genetic management of black sea bass: influence of biogeographic barriers on population structure. Marine and Coastal Fisheries 4:391-402

Schloesser RW, Fabrizio MC (2017) Condition indices as surrogates of energy density and lipid content in juveniles of three fish species. Transactions of the American Fisheries Society 146:1058-1069

Sheridan MA (1988) Lipid dynamics in fish: aspects of absorption, transportation, deposition, and mobilization. Comparative Biochemistry and Physiology 90B:679-690

Skinner MM, Martin AA, Moore BC (2016) Is lipid correction necessary in the stable isotope analysis of fish tissues? Rapid Communications in Mass Spectrometry 30:881-889

Sweeting CJ, Barry JT, Polunin NVC, Jennings S (2007) Effects of body size and environment on diet-tissue delta C-13 fractionation in fishes. Journal of Experimental Marine Biology and Ecology 352:165-176

Tocher DR (2003) Metabolism and functions of lipids and fatty acids in teleost fish. Reviews in Fisheries Science 11:107-184

Wuenschel MJ, Jugovich AR, Hare JA (2006) Estimating the energy density of fish: the importance of ontogeny. Transactions of the American Fisheries Society 135:379-385

Wuenschel MJ, McBride RS, Fitzhugh GR (2013) Relations between total gonad energy and physiological measures of condition in the period leading up to spawning: Results of a laboratory experiment on black sea bass (*Centropristis striata*). Fisheries Research 138:110-119

Wuenschel MJ, Shepherd GR, McBride RS, Jorgensen R, Oliveira K, Robillard E, Dayton J (2011) Sex and maturity of black sea bass collected in Massachusetts and Rhode Island waters; preliminary results based on macroscopic staging of gonads with a comparison to survey data. 53rd SAW Assessment Report. National Oceanic and Atmospheric Administration, National Marine Fisheries Service, Northeast Fisheries Science Center, Woods Hole, Massachusetts

Zudaire I, Murua H, Grande M, Pernet F, Bodin N (2014) Accumulation and mobilization of lipids in relation to reproduction of yellowfin tuna (*Thunnus albacares*) in the Western Indian Ocean. Fisheries Research 160:50-59

Tables

Table 2.1. Sample data by region for *Centropristis striata* muscle (M) and liver (L) tissue before and after Soxhlet lipid extraction. Regions are New Jersey (NJ), Maryland (MD), and North Carolina (NC). Superscript letters with liver data represent pairwise comparisons for each variable: different letters signify that the regions differ significantly for that measurement. n = sample size.

			Before extraction		After extraction					
Region	Tissue	n	δ^{13}C ‰	C:N	δ^{15}N ‰	δ^{13}C′ ‰	C:N′	δ^{15}N′ ‰	Lipid %	$\Delta\delta^{13}$C
NJ	M	12	-17.1 ± 0.6	3.8 ± 0.1	15.0 ± 0.8	-	-	-	3.1 ± 1.2	-
NC	M	12	-17.8 ± 0.3	3.7 ± 0.1	11.7 ± 0.6	-	-	-	2.2 ± 0.3	-
NJ	L	17	-18.8 ± 1.0^{b}	7.3 ± 1.7^{a}	13.2 ± 0.7^{c}	-18.0 ± 0.4^{b}	5.1 ± 0.6^{a}	13.3 ± 0.6^{c}	20.0 ± 12.3^{a}	0.8 ± 0.9^{a}
MD	L	8	-19.6 ± 0.4^{ab}	5.6 ± 1.0^{a}	12.1 ± 0.9^{b}	-19.0 ± 0.5^{a}	5.1 ± 0.7^{a}	12.0 ± 0.8^{b}	7.9 ± 2.0^{a}	0.5 ± 0.4^{a}
NC	L	20	-20.1 ± 1.1^{a}	10.8 ± 3.0^{b}	9.6 ± 0.5^{a}	-17.8 ± 0.6^{b}	5.4 ± 0.8^{a}	9.8 ± 0.5^{a}	36.4 ± 14.1^{b}	2.3 ± 1.1^{b}

Table 2.2. Pearson correlation coefficient (*r*) for *Centropristis striata* muscle and liver tissue lipid content (%) as compared to reproductive (gonadosomatic index [GSI]) and condition (Fulton *K*, hepatosomatic index [HSI]) indices. Bolded *P*-values are significant at $\alpha = 0.05$. n = sample size.

	Muscle lipid %			Liver lipid %		
Index	n	*r*	*P*	n	*r*	*P*
GSI	19	0.74	**0.0003**	135	-0.28	**0.001**
HSI	23	0.82	< **0.0001**	150	0.08	0.35
Fulton *K*	23	0.41	0.05	135	0.42	< **0.0001**

Table 2.3. Black sea bass (*Centropristis striata*) muscle (M) and liver (L) sample data by region before and after lipid correction using a nonlinear fitted model adapted from McConnaughey and McRoy (1979) and Kiljunen et al. (2006). Regions are Southern New England (SNE), New Jersey (NJ), Maryland (MD), and North Carolina (NC). Lipid-corrected carbon isotope ($\delta^{13}C'$) values for liver tissue include measurements for the subset of samples that underwent lipid extraction in addition to predicted values, based upon a model. Liver samples modeled to have negative lipid content (n = 3) were removed from analysis. Superscript letters with muscle and liver data ($\delta^{13}C$, $\delta^{13}C'$, Lipid %, $\Delta\delta^{13}C$) represent pairwise comparisons among regions for each variable: different letters signify significant differences between values. n = sample size.

Region	Tissue	n	$\delta^{13}C$	C:N	$\delta^{15}N$	$\delta^{13}C'$	Lipid %	$\Delta\delta^{13}C$
SNE	M	16	-17.3 ± 0.6^{b}	3.9 ± 0.2	14.0 ± 0.9	-	-	-
NJ	M	98	-17.1 ± 0.5^{b}	3.9 ± 0.2	14.7 ± 0.8	-	-	-
MD	M	26	-17.9 ± 0.5^{a}	3.8 ± 0.1	14.0 ± 0.6	-	-	-
NC	M	62	-18.1 ± 0.6^{a}	3.8 ± 0.1	11.7 ± 0.6	-	-	-
SNE	L	14	-20.7 ± 0.9^{a}	9.4 ± 2.1	11.6 ± 0.9	-18.9 ± 0.6^{b}	31.1 ± 9.1^{bc}	1.8 ± 0.5^{b}
NJ	L	79	-19.2 ± 1.0^{b}	7.7 ± 3.0	12.8 ± 0.8	-18.1 ± 0.8^{c}	21.1 ± 13.3^{b}	1.2 ± 0.8^{a}
MD	L	21	-20.2 ± 1.1^{a}	6.2 ± 2.1	12.2 ± 0.6	-19.5 ± 0.7^{a}	11.5 ± 10.6^{a}	0.7 ± 0.7^{a}
NC	L	36	-20.2 ± 1.2^{a}	10.5 ± 3.2	9.7 ± 0.5	-18.1 ± 0.8^{c}	34.3 ± 14.9^{c}	2.1 ± 1.0^{b}

Table 2.4. Summary table of regional *Centropristis striata* condition (hepatosomatic index [HSI], Fulton *K*) and reproductive (gonadosomatic index [GSI]) indices and liver tissue lipid content and density. Regions are Southern New England (SNE), New Jersey (NJ), Maryland (MD), and North Carolina (NC). Superscript letters represent pairwise comparisons for each variable: different letters signify that the regions differ significantly for that measurement. n = sample size for each comparison group.

Region	n_{HSI}	HSI	$n_{Fulton\ K}$	Fulton *K*	$n_{Liver\ \%\ lipid}$	Liver % lipid	Lipid density	n_{GSI}	GSI
SNE	15	0.01 ± 0.003^{a}	16	0.001 ± 0.0002^{b}	14	31.1 ± 9.1^{bc}	0.003 ± 0.002^{ab}	14	0.02 ± 0.01^{ab}
NJ	98	0.01 ± 0.005^{c}	98	0.001 ± 0.0001^{a}	79	21.1 ± 13.3^{b}	0.003 ± 0.003^{b}	96	0.05 ± 0.02^{b}
MD	24	0.01 ± 0.005^{bc}	26	0.001 ± 0.0001^{ab}	21	11.5 ± 10.6^{a}	0.001 ± 0.002^{a}	22	0.04 ± 0.02^{a}
NC	60	0.01 ± 0.005^{ab}	62	0.001 ± 0.0001^{ab}	36	34.3 ± 14.9^{c}	0.004 ± 0.003^{b}	39	0.001 ± 0.0006^{b}

Table 2.5. Generalized linear model (GLM) results for *Centropristis striata* condition (Fulton *K*, hepatosomatic index [HSI], liver lipid content [%] and reproductive [gonadosomatic index [GSI]) indices, where *df* = degrees of freedom, *F* = *F*-statistic, and *P* = *P*-value. Bolded *P*-values are significant at $\alpha = 0.05$. n = sample size for each analysis.

Response	Variable	*df*	*F*	*P*
GSI	Region	3	45.20	< **0.0001**
n = 171	Sex	2	6.05	**0.003**
	Length	1	14.39	**0.0002**
	Depth	1	13.14	**0.0004**
HSI	Region	3	9.68	< **0.0001**
n = 197	Sex	2	16.86	< **0.0001**
	Length	1	1.31	0.25
	Depth	1	3.30	0.07
Fulton *K*	Region	3	4.38	**0.005**
n = 202	Sex	2	2.31	0.10
	Depth	1	0.07	0.79
Liver lipid %	Region	3	16.86	< **0.0001**
n = 150	Sex	2	1.28	0.28
	Length	1	0.63	0.43
	Depth	1	9.78	**0.002**

Figures

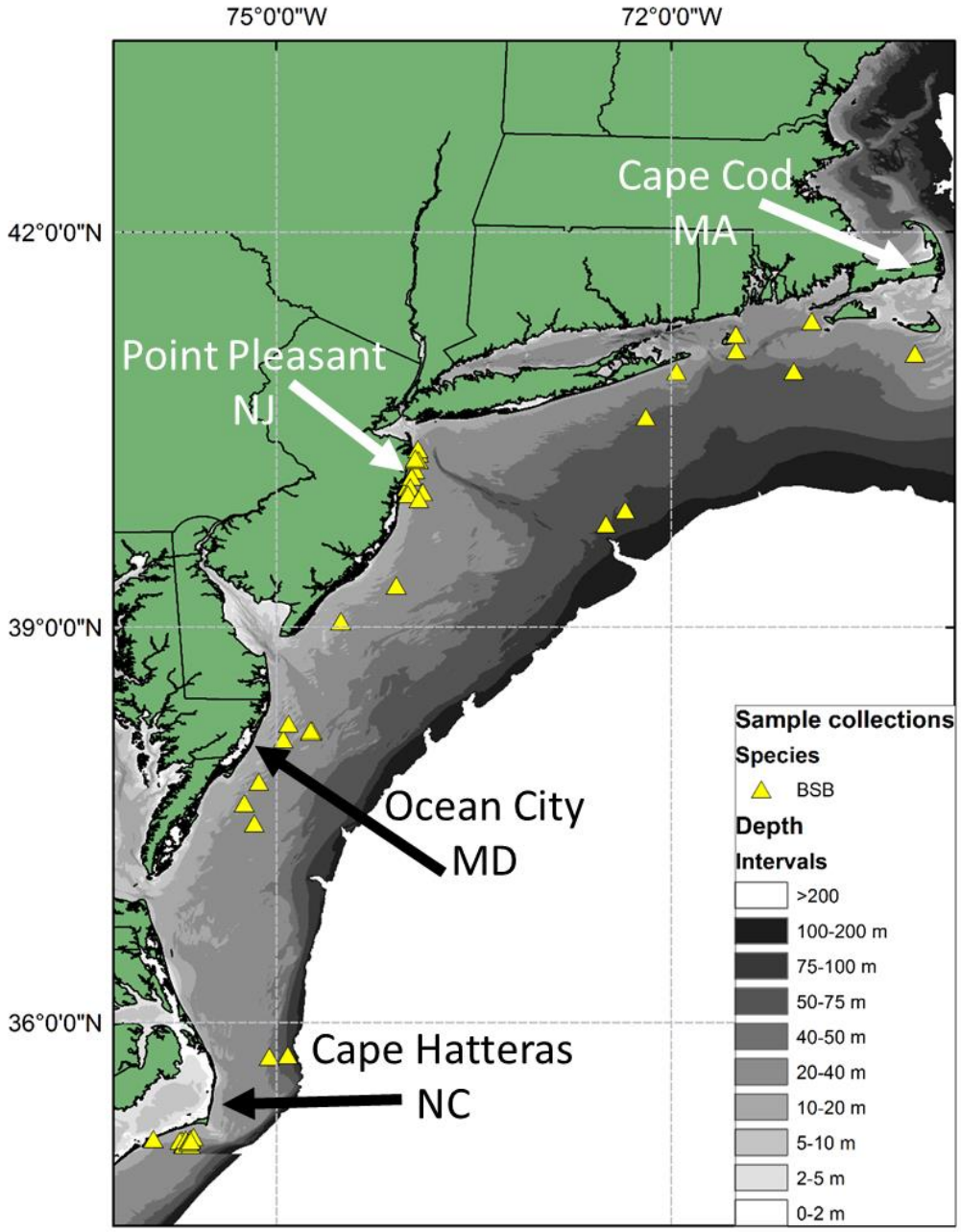

Figure 2.1. Map of sampling sites of *Centropristis striata* (black sea bass, BSB) along the Middle Atlantic Bight in 2016. Hook and line reef-sampled sites were located at Point Pleasant, New Jersey (NJ), Ocean City, Maryland (MD), and Cape Hatteras, North Carolina (NC).

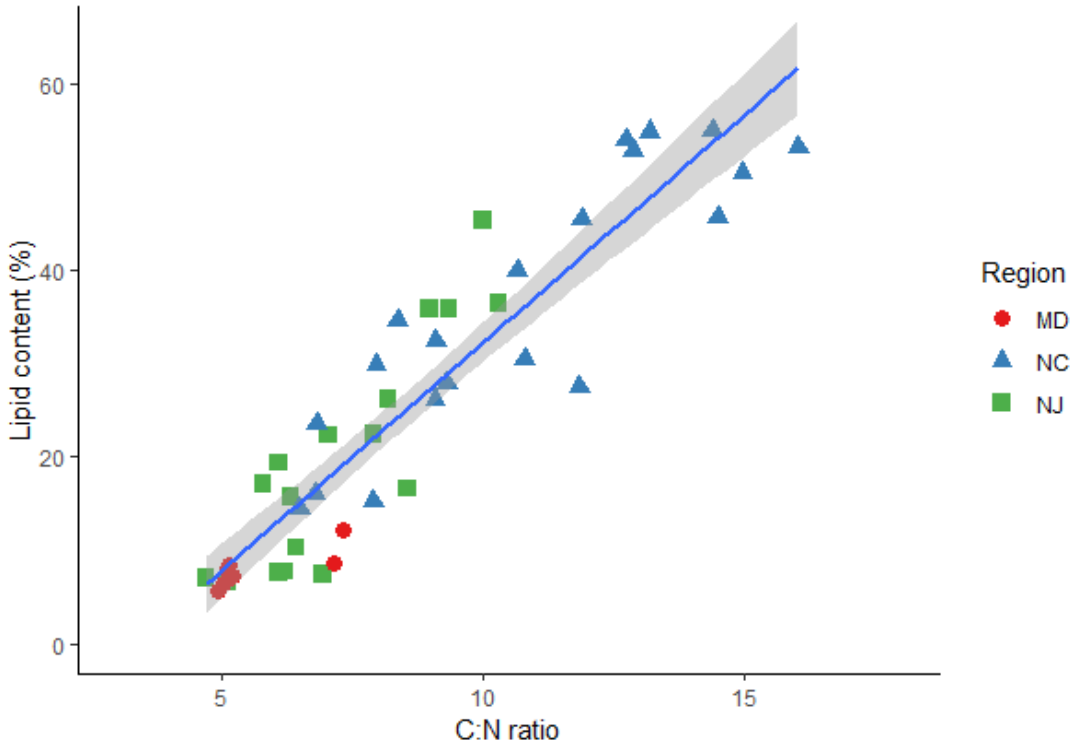

Figure 2.2. Initial carbon to nitrogen (C:N) ratio versus empirical lipid content (%) for lipid-extracted *Centropristis striata* liver tissue (Soxhlet extraction method). Regions are Maryland (MD), North Carolina (NC), and New Jersey (NJ). Blue line is the regression line of best fit, and the grey shaded area represents the standard error range/confidence interval. Adjusted $r^2 = 0.85$.

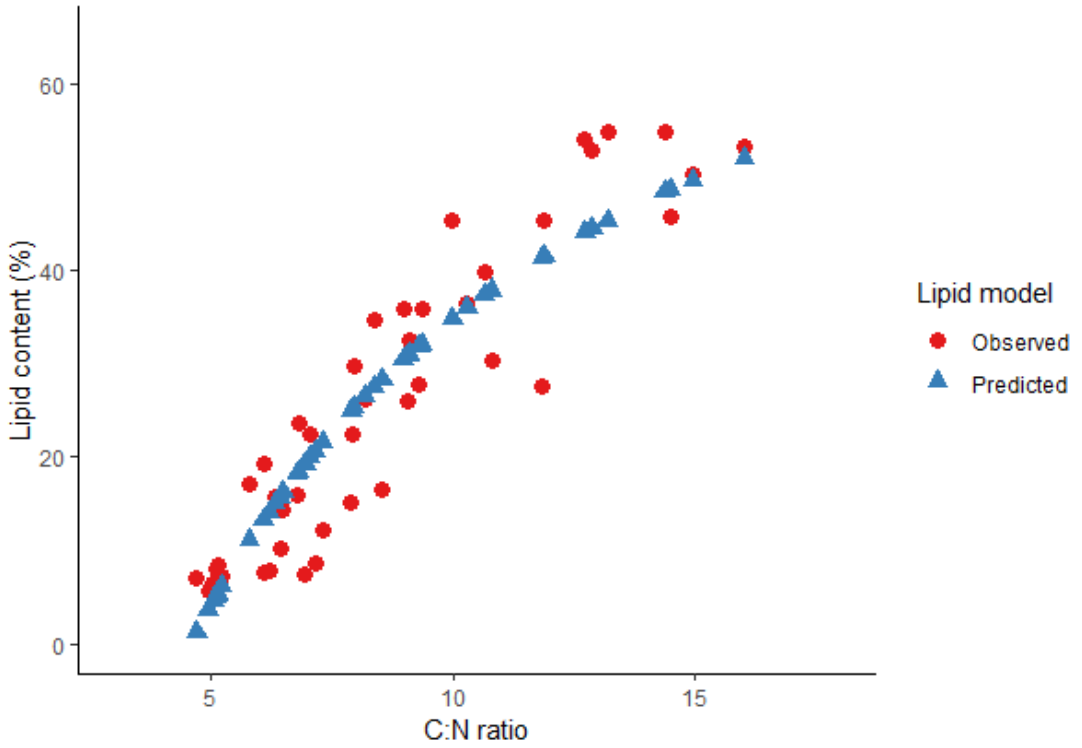

Figure 2.3. Nonlinear model fitting for lipid-extracted *Centropristis striata* liver tissue. Observed values were derived from measurements of lipid extracted using the Soxhlet method. Model parameters were modified as needed from the model proposed by McConnaughey and McRoy (1979) and Kiljunen et al. (2006). Adjusted $r^2 = 0.85$.

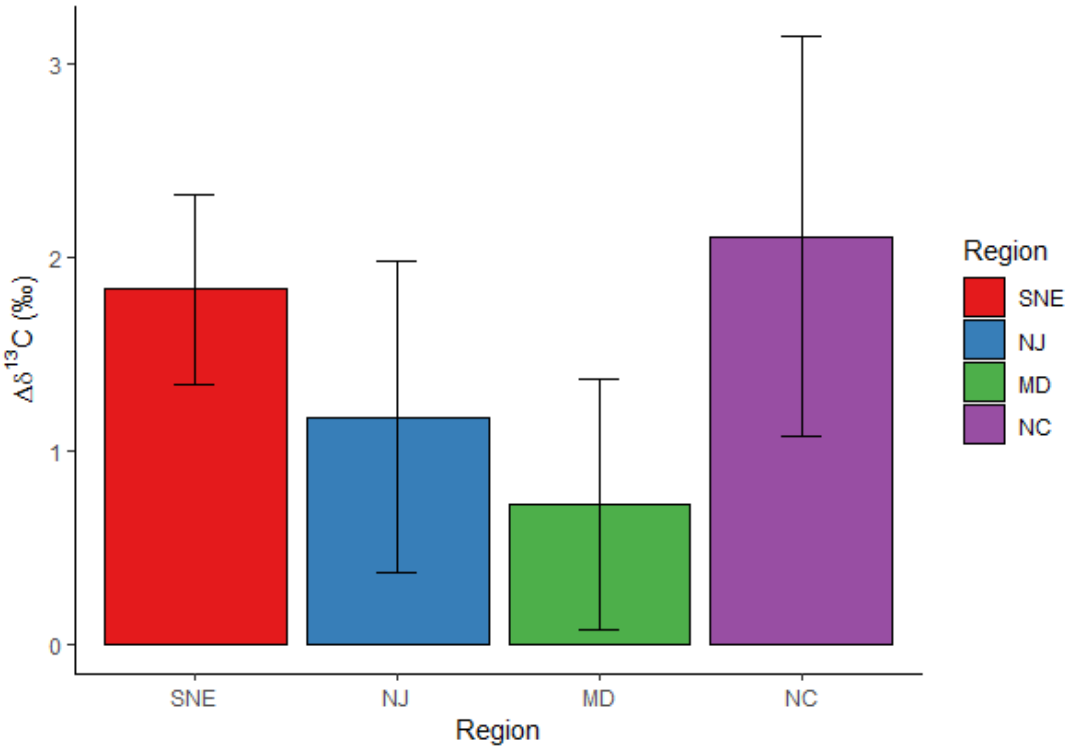

Figure 2.4. Comparison by region of the difference in δ^{13}C before and after lipid correction ($\Delta\delta^{13}$C) in *Centropristis striata* liver tissue. Regions are Southern New England (SNE), New Jersey (NJ), Maryland, (MD), and North Carolina (NC). Error bars represent the standard deviation.

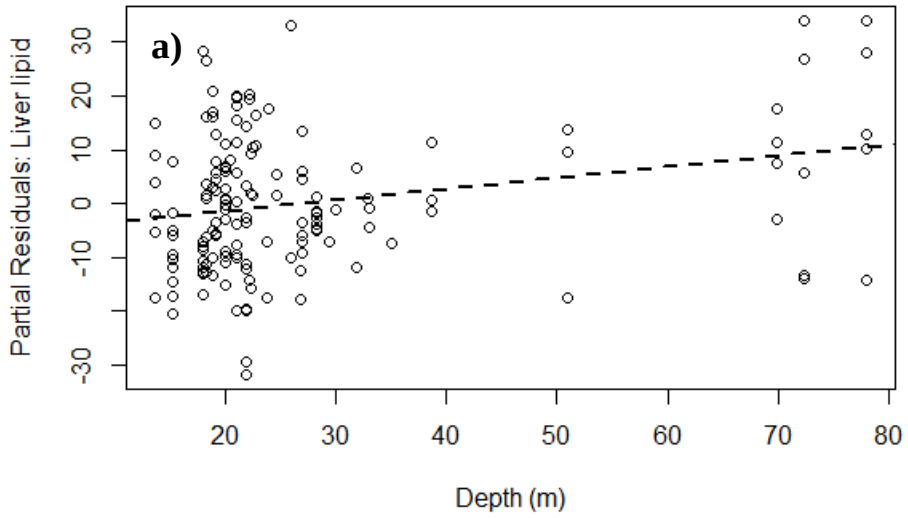
a)
Partial Residuals: Liver lipid
-30
-10
0
10
20
30
20
30
40
50
60
70
80
Depth (m)

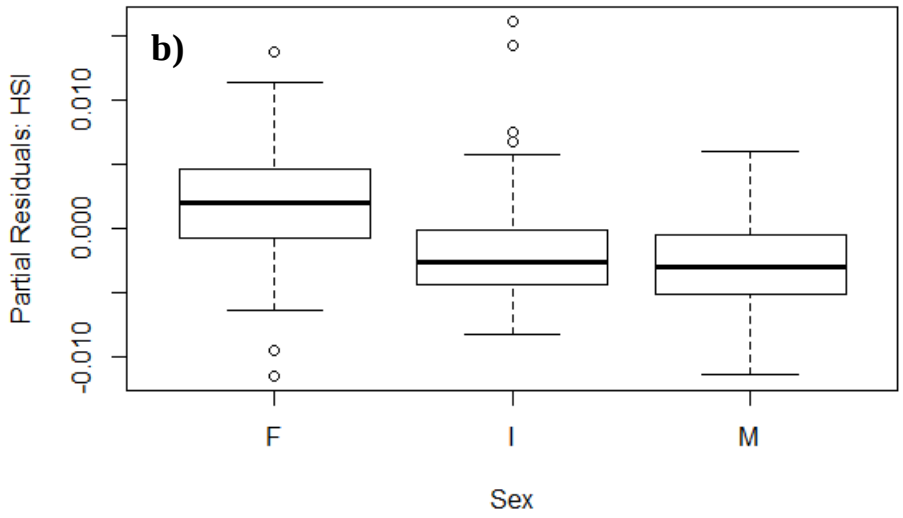
b)
Partial Residuals: HSI
-0.010
0.000
0.010
F
I
M
Sex

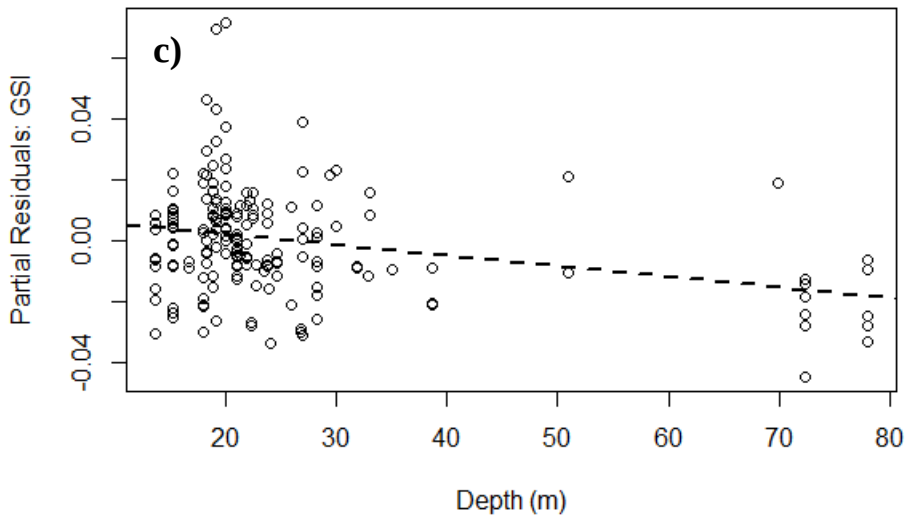
c)
Partial Residuals: GSI
-0.04
0.00
0.04
20
30
40
50
60
70
80
Depth (m)

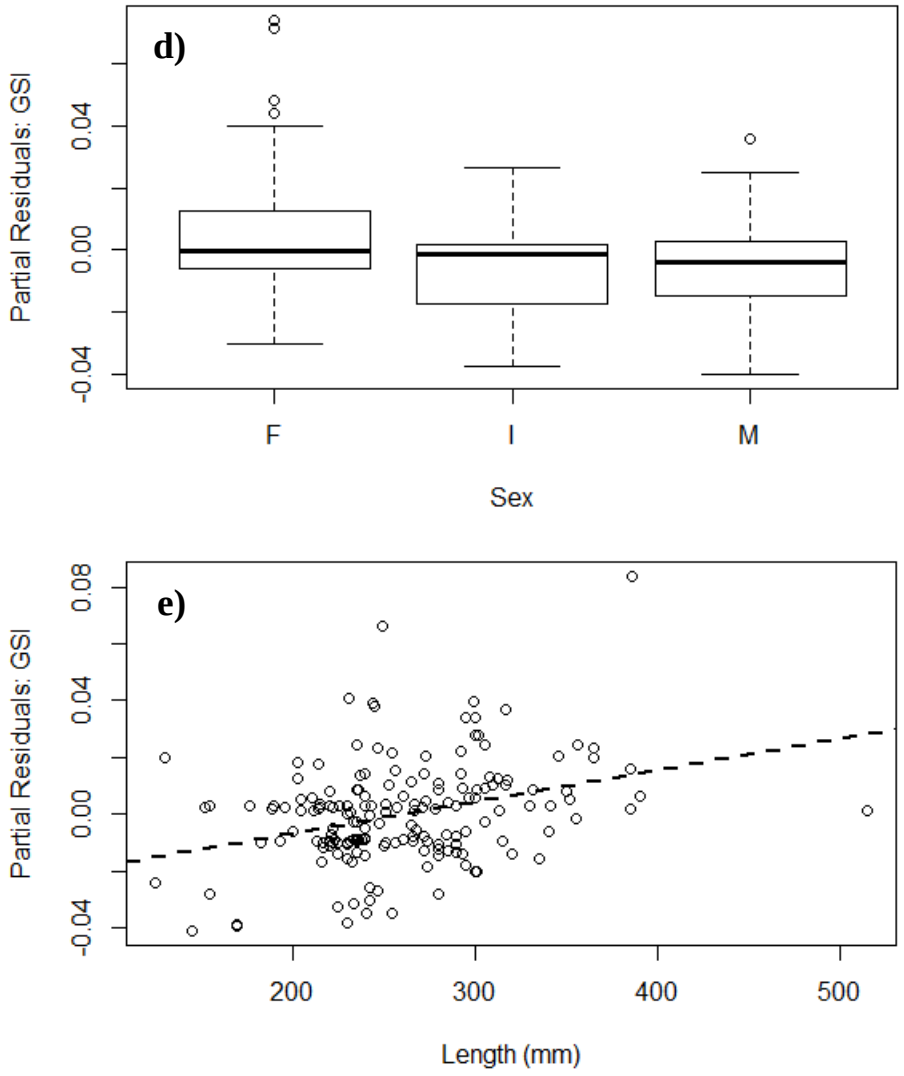

Figure 2.5. Generalized linear model (GLM) results for liver lipid content (%), liver lipid density, hepatosomatic index (HSI) and gonadosomatic index (GSI) derived from isotope analysis of *Centropristis striata* liver and/or muscle tissue. Significant variable for liver lipid content was a) Depth; significant variable for HSI was b) Sex (female [F], Indeterminate [I], Male [M]); and significant variables for GSI were c) Depth, d) Sex, and e) Length. For regional pairwise comparisons of each condition index, see Table 2.4. For significance of each variable, see Table 2.5.

Chapter 3: Spatial patterns of black sea bass (*Centropristis striata*) diet and trophic ecology in the Middle Atlantic Bight

Abstract

Ecosystem-based fisheries management is gaining prominence as a tool for sustaining fisheries stocks by taking ecological interactions into consideration. Ecosystem-based models rely on robust estimates of trophic relationships, yet much of the information required to develop explicit spatial or temporal estimates is often lacking, even for established, economically important fisheries species. Black sea bass (*Centropristis striata*) is a key demersal fishery species and predator in structured reef habitat of the Middle Atlantic Bight (MAB). The objective of this study was to assess spatial patterns in diet and trophic position across the entire range of the MAB *C. striata* stock, from Southern New England to Cape Hatteras, North Carolina. Stomach contents were analyzed from fish off northern (New Jersey, NJ) and southern (North Carolina, NC) reefs. Prey representing pelagic and benthic food webs were collected by seasonal trawl surveys at inshore and offshore sites. Muscle tissue samples of *C. striata* and prey were analyzed for δ^{13}C and δ^{15}N to provide information on trophic position, relative importance of pelagic and benthic trophic pathways, and niche dimensions. NJ stomachs indicated decapod crustaceans were a dominant prey item, while NC stomachs suggested individual specialization on decapods and bivalves. Both biotic and abiotic factors influenced benthic prey importance, trophic position, and isotopic niche. Understanding spatial patterns of *C. striata* isotope variability

along the MAB enables future analysis of seasonal patterns to assess the critical resources required by this species.

Key words: trophic ecology; stable isotopes; coastal ecosystem, black sea bass (*Centropristis striata*), benthic-pelagic coupling, stomach contents analysis

Introduction

Effective ecosystem-based fisheries management requires understanding niche positions of critical species within food webs (Pikitch et al. 2004). Another need is the ability to assess spatiotemporal variability in fish foraging needs to allow for region-specific management adjustments (Link 2002). In the Middle Atlantic Bight (MAB) and South Atlantic Bight (SAB), black sea bass (*Centropristis striata*) sustains an important inshore and offshore fishery. *C. striata* is a structure-associated species that resides on inshore reefs in the summer, and the northern population seasonally migrates southwards and offshore to overwinter in deeper shelf waters. The black sea bass stock is currently managed as two separate fisheries north and south of Cape Hatteras, North Carolina (Northeast Fisheries Science Center 2017).

In addition to their commercial value, *C. striata* occupy an ecologically important niche as demersal predators, and are present on natural and artificial reefs, integrating prey from both benthic and pelagic pathways (Malek et al. 2016). Although demersal fish predators typically feed within bottom-associated food webs, a significant proportion of their diet can nevertheless come from pelagic sources, due to diel migration, vertical mixing, and prey movements (Woodland & Secor 2013). Stomach content analysis can provide an instantaneous glimpse of the most recent

feeding of an individual (Hyslop 1980), but a more comprehensive view of diet and feeding ecology requires supplementation of direct stomach content analysis with examination of assimilated components in tissues via natural biomarkers such as stable isotope analysis. This allows for analysis of ingested and assimilated material over short-term and long-term scales, respectively (Giménez et al. 2017).

The isotopic signature of carbon ($\delta^{13}C$) provides insight into original primary production sources while nitrogen in consumer tissues becomes enriched in ^{15}N with each trophic transfer (Cabana & Rasmussen 1994). Stable isotope studies of fishes often use white muscle as the preferred tissue type, which typically undergoes isotopic turnover rates ranging from months to years (MacNeil et al. 2006) depending primarily on size and growth rate (Herzka 2005, Perga & Gerdeaux 2005). Alternatively, important insights can be gained by examining more metabolically active tissues with more rapid turnover rates such as the liver. Comparing tissues from the same groups of individuals may provide insight into feeding ecology at different time scales, with muscle representing long-term assimilation and liver representing more recent assimilation (Herzka 2005, MacNeil et al. 2006).

Previous assessments of *C. striata* feeding strategy have relied upon stomach contents analysis for insight on feeding patterns and the species has been described as having a generalized carnivorous diet comprised of motile epibenthic fishes and invertebrates (Sedberry 1988). Data from a long-term trawl survey suggest that piscivory is low in Southern New England, but the proportion of fish prey increases in inshore and offshore regions south of Cape Hatteras (Bowman et al. 2000). In contrast, the opposite general pattern is observed for crustacean consumption, with

high proportions in northern regions with a decline south of Cape Hatteras (Bowman et al. 2000). These observations suggest that *C. striata* at lower latitudes would occupy a relatively higher trophic position with increased piscivory. Despite the close association of *C. striata* with structural habitat during the summer, to the best of my knowledge, no large-scale studies of diet from reef habitat currently exist. Moreover, the variation in the feeding ecology and trophic position of *C. striata* at inshore reef sites over local or broad regional scales has not yet been tested using integrative approaches such as stable isotope analysis.

In addition to spatial differences, diet composition often varies with the size and thus the age of the fish. In the SAB, small *C. striata* consume more small crustaceans such as amphipods, while larger fishes more frequently consume larger crustaceans and fishes (Sedberry 1988). This is likely due to the increase in mouth size (gape) of the fish as body size increases with growth (Scharf et al. 2000). This pattern of increased piscivory with size is also observed in groups of *C. striata* pooled from multiple latitudinal regions (Bowman et al. 2000). Higher consumption of fish prey by a consumer implies that the trophic level and/or trophic position of the consumer will increase with size, and this positive relationship with body size, whether by length or by mass, has been confirmed by both stomach content and stable isotope analyses (Jennings et al. 2001, Akin & Winemiller 2008).

An alternative expectation is that the trophic position of a generalist such as *C. striata* would be lower in southern areas because food chain length tends to decrease at lower latitudes. This could be in part due to the greater year-round availability of primary production, enabling a greater proportion of lower-level consumers and

increased omnivory among higher-level consumers. However, ecosystem productivity alone may not be sufficient to fully explain the complex factors that influence food chain length (Post 2002a, Ward & McCann 2017).

The objective of this study was to examine spatial differences in the diet and trophic ecology of *C. striata* along a latitudinal gradient and to assess patterns in representative benthic and pelagic prey. I focus on the analysis of fish collected from reef sites in summer to identify summer foraging patterns during their main growth period. Based on previous observations, I hypothesized that increased piscivory and thus increased dependence on pelagic resources would be observed in fish from southern regions, and I also hypothesized that larger individuals would have a higher trophic position.

Materials and methods

Sample collection and sampling area

Fish were primarily collected by hook and line and un-baited trap June-August 2016 at or near reef sites offshore of Point Pleasant, New Jersey and by hook and line only from Ocean City, Maryland and Cape Hatteras, North Carolina reef sites (Table 3.1, Table 3.2). Samples were flash-frozen over dry ice in the field when possible or stored in ice water until brought to shore. A smaller number of *C. striata* were acquired from the National Marine Fisheries Service (NMFS) Spring and Autumn Bottom Trawl Surveys in 2016 from stations ranging from southern New England in the north to Cape Hatteras, North Carolina in the south. Representative

pelagic (striped anchovy *Anchoa hepsetus*, bay anchovy *Anchoa mitchilli*) and benthic (Atlantic rock crab *Cancer irroratus*) prey items were collected during the NMFS and NorthEast Area Monitoring and Assessment Program (NEAMAP) bottom trawl surveys in 2016 and 2017 across the same latitudinal range (Fig. 3.1). Sites were separated into four main regional areas ordered from north to south: Southern New England (SNE), New Jersey (NJ), Maryland (MD), and North Carolina (NC).

Fish and crabs were stored at -50°C upon arrival to the laboratory. Prior to dissection, specimens were thawed and measured for total length (TL, mm) or carapace width (CW [crabs only], mm) and weighed to the nearest 0.01 g. Those *C. striata* with TL < 250 mm were categorized as belonging to a 'Small' size class (individuals < 170 mm labeled as young of the year [YOY]), while *C. striata* ≥ 250 mm TL were classified as 'Large'. Size classifications were based on historical diet composition summaries of *C. striata* that suggest an increase in piscivory at roughly 250 mm TL (Bowman et al. 2000, Able & Fahay 2010). Upon dissection, *C. striata* stomachs were excised, weighed, and stored frozen for further content analysis. Gonads and liver were also excised, weighed separately, and the sex of each fish was determined when possible. Individuals of unknown sex (possessing immature or spent gonads) were classified as 'Indeterminate.' Approximately 1 cm^3 of dorsal white muscle tissue was cut from the anterior dorsal region of each individual, rinsed with deionized water, and dried at 60°C for 48-72 hours until completely dry. A section of liver tissue was similarly prepared. Muscle tissue and a subset of whole body samples were collected from *A. hepsetus*, *A. mitchilli* and *C. irroratus*. The two anchovy species are pelagic consumers and are representative of pelagic trophic pathways,

while *C. irroratus* is a demersal consumer and was selected to represent benthic trophic pathways. Dried tissue samples from both *C. striata* and prey were pulverized to a fine powder using a mortar and pestle.

Stomach contents analysis and feeding strategy plots

The ratio of stomach weight to body weight (SBR) was calculated as a proxy for stomach fullness. I compared the mean SBR between hook and line- and trap-sampled *C. striata* from NJ collected over two days in June 2016 to examine whether gear type was a source of potential bias in stomach contents analysis. Individuals caught by un-baited trap had a significantly lower SBR compared to hook and line sampled fish (Two sample *t*-test, $df = 211.63$, $t = -4.70$, $P < 0.0001$) (Table 3.5). This difference could be due to digestion of stomach contents during extended time in traps with no additional feeding. Thus only data from hook and line sampled fish were analyzed in this study.

A subset of *C. striata* stomachs from NJ and NC reef sites were preserved in 10% buffered formalin for stomach contents analysis, in which prey were identified to the lowest possible taxonomic level and dried prior to weighing. Stomachs were classified as empty when no identifiable material was present. Prey taxonomic groups and biomass were used for diet composition calculations and feeding strategy plots (Amundsen et al. 1996). Feeding strategy plots visualize the degree of generalization or specialization on certain prey types consumed by plotting the prey-specific abundance against the prey's frequency of occurrence in two-dimensional space. The

prey-specific abundance is the proportion of stomach mass made up by a particular prey item across only the subset of stomachs in which that prey item was found:

$$P_i = (\Sigma S / \Sigma S_t) * 100 \quad \text{(Eq. 3.1)}$$

Where P_i represents the prey-specific abundance of prey *i*, *Si* is the amount of stomach contents (dry weight in this case) composed of prey *i*, and S_t is the total stomach content of the predators in which prey *i* was present (Amundsen et al. 1996).

Prey items located on the lower left of the feeding strategy plot are relatively rare components of the diet, being low in prey-specific abundance and with low occurrence. In contrast, prey items at the upper right of the plot are dominant components of the diet for the observed predator population, being both high in occurrence and in prey-specific abundance. Placement in the upper left corner suggests that this prey item is a target of specialization by individual predators, while the lower right suggests that it is a frequent yet minor component by biomass of the generalized diet of the full population (Amundsen et al. 1996).

Bulk stable isotope analysis

Powdered samples of *C. striata* muscle and liver tissue, as well as prey muscle and whole body tissue (0.6-0.8 mg) were packed in pre-weighed tin capsules, and analyzed for carbon (δ^{13}C) and nitrogen (δ^{15}N) stable isotope values. Samples were analyzed with a ThermoScientific Delta V Plus (Thermo Fisher Scientific, Inc., Waltham, Massachusetts, USA) continuous flow Isotope Ratio Mass Spectrometer (IRMS) with Costech Elemental Analyzer (Costech Analytical Technologies, Inc., Valencia, California, USA) at the Stable Isotopes Lab (Chesapeake Biological

Laboratory, Solomons, MD, USA). Measurements are reported in the traditional delta (δ) notation relative to international standards Vienna Pee Dee Belemnite (C) and atmospheric air (N). Both δ^{15}N and δ^{13}C values were simultaneously measured and recorded for each sample. The relative masses of carbon and nitrogen in each sample were measured by the elemental analyzer, enabling calculation of the molar carbon to nitrogen (C:N) ratio. Internal standards were used to compensate for drift during runs, and analytical precision using duplicate *C. striata* and prey samples (n = 46) was 0.4 ± 0.9‰ (difference between duplicate samples ± SD) for carbon and 0.2 ± 0.4‰ for nitrogen. Machinery longer-term precision using protein standards was ± 0.1‰ (SD) in the case of carbon (n = 16) and ± 0.2‰ in the case of nitrogen (n = 15) (C. Magen, personal communication).

Liver δ^{13}C values were corrected for lipid content. A lipid correction model was developed by fitting the nonlinear models reported in McConnaughey & McRoy (1979) and Kiljunen et al. (2006) (see Chapter 2) to measured *C. striata* liver lipid data (n = 45). Lipid extractions were carried out using a Soxhlet apparatus with petroleum ether as a solvent. Tissue-specific model results for *C. striata* indicated that muscle tissues did not require correction due to low lipid content (< 15%, see Chapter 2).

Trophic enrichment and mixing models

I produced a spatial model to predict the δ^{13}C and δ^{15}N values of the pelagic and benthic baselines for the observed consumer sampling sites. There were no significant differences in muscle tissue δ^{13}C or δ^{15}N values between *A. hepsetus* and

A. mitchilli (ANOVA, $P > 0.05$), so the isotope measurements from the two taxa were pooled as a single pelagic prey group. Anchovy and *C. irroratus* isotope baseline δ^{15}N values were predicted for *C. striata* sampling sites using generalized additive models (GAMs). Previous studies (e.g., Bacheler et al. 2009) have implemented GAMs for modeling the effects of multiple environmental variables in a nonlinear fashion using non-parametric smoothed curves. Latitude, longitude, depth and prey size (TL or CW) were included as potential continuous explanatory variables. Models were developed and compared using the 'mgcv' package (Wood 2006) within the R statistical software framework (R Core Team 2016). A subset of all model permutations were fitted and the most parsimonious models were selected using Akaike's Information Criterion weights (AIC_w) (Wagenmakers & Farrell 2004) for comparison, and summarized based on explained deviance, degrees of freedom (*df*) and adjusted r-squared (r^2 adj.) values. The best model (highest AIC_w) was then used to predict baseline δ^{15}N at sites where *C. striata* were sampled. The mean length of sampled anchovies or crabs was used as a predictor when the selected model included prey length as an explanatory variable. Predicted baseline δ^{15}N values were used to calculate spatially-explicit means and standard deviations for stable isotope mixing models. Attempts to model δ^{13}C using GAMs resulted in models with low predictive power (r^2 adj. < 0.6), thus arithmetic regional means were calculated instead for prey δ^{13}C inputs to mixing models.

The extent of benthic-pelagic (BP) coupling by *C. striata* was measured as the proportion of diet from benthic sources based on output from a Bayesian mixing model using the R package 'simmr' (Parnell et al. 2010, Parnell et al. 2013). A carbon

trophic enrichment factor (TEF) of 0.5 ± 1.3‰ (mean ± SD) and nitrogen TEF of 2.3 ± 1.5‰ per trophic transfer was assumed (McCutchan et al. 2003). Preliminary testing of model behavior with alternative C and N TEFs (Sweeting et al. 2007a, Sweeting et al. 2007b) resulted in intractable prey polygons in isotope space and were not considered further. Bayesian posterior distributions were estimated using a Markov chain Monte Carlo (MCMC) simulation (Parnell et al. 2013).

Trophic position

Estimates of trophic position (TP) from bulk stable isotope values were calculated as deviations from a trophic baseline, as provided by analyzed prey taxa (Post 2002b). The trophic position estimates used the two-source baseline equation:

$$TP = \lambda + (\delta^{15}N_C - [\delta^{15}N_{base1} * \alpha + \delta^{15}N_{base2} * (1 - \alpha)]) / \Delta_n \quad \text{(Eq. 3.2)}$$

where TP is the relative trophic position, λ is a common trophic level shared by all consumers being examined, $\delta^{15}N_C$ is the nitrogen value of the consumer of interest (*C. striata*), $\delta^{15}N_{base1}$ is the nitrogen value of the first baseline (*C. irroratus*), $\delta^{15}N_{base2}$ is the nitrogen value of the second baseline (anchovies), α is the proportion of nitrogen derived from the first baseline (benthic proportion in this case), and Δ_n is the TEF for nitrogen [= 2.3‰; McCutchan et al. (2003)].

Patterns in BP and TP calculations were analyzed using generalized linear models (GLMs):

$$BP \text{ or } TP \sim Region + Sex + Length + Depth \quad \text{(Eq. 3.3)}$$

where region and sex were treated as class variables, and depth and length were treated as continuous variables. All GLMs were performed in R 3.5.1 (R Core Team 2018) using the 'lm' function.

Niche width

The R package 'SIBER' (Stable Isotope Bayesian Ellipses in R) was used to fit ellipses to regional groups of *C. striata* muscle and liver tissue in order to compare isotopic niche width in an "isospace" (δ^{13}C vs. δ^{15}N) and in niche space (BP vs. TP) based on standard ellipse area (SEA) corrected for small sample size (SEA_c). In addition to the SEA_c point estimate, a Bayesian posterior distribution for each regional SEA (Bayesian SEA) was also calculated using SIBER. Bayesian techniques enable the use of prior information as well as measurement uncertainty to produce posterior distribution estimates (Jackson et al. 2011, Parnell et al. 2010). Ellipse areas calculated in isotope space (i.e., isospace, δ^{13}C vs. δ^{15}N) can be considered a proxy for niche space, whereas ellipse areas calculated using BP and TP estimates represent actual niche space (Woodland & Secor 2011). Convex hull area is of limited usefulness due to its high sensitivity to sample size, therefore the SEA methods provide more robust comparison among groups differing in sample size (Jackson et al. 2011). However, it is not possible to directly compare the means or medians of Bayesian distributions with common statistical methods. An alternative way to compare posterior distributions among groups is to calculate the probability that one group's posterior distribution is larger or smaller than another (Jackson 2016). I used

this approach to conduct pairwise comparisons among regional groups and rank each regional group by its probable Bayesian SEA.

All statistical analyses were performed in R versions 3.3.1 (R Core Team 2016) and 3.5.1 (R Core Team 2018). Whenever necessary, data transformations in statistical tests such as *t* tests, ANOVA, and linear regressions were conducted to adjust residuals to normal distributions.

Results

Stomach contents analysis and feeding strategy

A total of 94 stomachs from hook and line caught fish were analyzed for contents. Stomachs from NJ reef fish (n = 56) were collected in June 2016 and NC reef fish (n = 38 total) were collected in the months of July (n = 15) and August (n = 23) 2016. Of these stomachs, 20 were empty (Table 3.4). Soft tissue components were also often at an advanced stage of digestion, and fish prey material could not be reliably identified to a lower taxonomic level. Prey items with shells and exoskeletons such as crustaceans and bivalves were more easily identifiable taxonomically. Decapod fragments were identified when possible, or otherwise categorized as unidentified decapods.

The feeding strategy plots constructed using measures of prey-specific abundance and frequency of occurrence indicated differences in the feeding strategies of NJ and NC reef *C. striata* groups (Fig. 3.2). In the case of NJ stomachs with

contents present (n = 40), decapod crustaceans functioned as a dominant component of the *C. striata* diet, followed by moderately high proportions of bivalves such as clams. In contrast, polychaetes and small crustaceans such as amphipods were relatively rare components of the diet, with a low importance of fish prey as well (Fig. 3.2a). In the case of NC stomach contents (n = 30), the relative importance of fish, polychaete and small crustacean prey were similarly low. However, there was a relatively high importance of both bivalve and decapod crustacean prey, with both categories at an equal level of occurrence (Fig. 3.2b).

Prey models

A total of 64 *A. mitchilli/A. hepsetus* and 42 *C. irroratus* specimens were sampled over 2016 and 2017 (Table 3.6). Mean lengths of prey were 96 ± 23 mm (SD) for anchovies (n = 64) and 60 ± 17 mm for *C. irroratus* (n = 42). For anchovies, mean muscle δ^{13}C value was -18.4 ± 0.6‰; for *C. irroratus* it was -17.4 ± 0.8‰. In the case of muscle δ^{15}N, anchovies were 14.3 ± 1.1‰ and crabs were 12.2 ± 1.5‰ (Table 3.6).

Significant pairwise differences between muscle tissue and whole body samples were observed for nitrogen and carbon isotope ratios of anchovy relative to matching muscle tissue alone (n = 8). Anchovy isotope values were adjusted to whole body values by subtracting 0.9‰ from muscle δ^{13}C and subtracting 1.1‰ from muscle δ^{15}N values. Likewise, crab muscle δ^{15}N values were adjusted by subtracting 2.3‰. The new whole body corrected values for δ^{15}N for anchovies and *C. irroratus*

were 13.2 ± 1.1‰ and 10.0 ± 1.5‰, respectively, and anchovy δ^{13}C were adjusted to -19.3 ± 0.6‰ (Table 3.6). Adjusting for whole body values provided more realistic isotope values for prey and enabled a better fit for *C. striata* within observed prey polygons for stable isotope mixing model estimates (Fig 3.3).

Based on AIC values, the best GAM variant for anchovy δ^{15}N included depth, length, latitude, and longitude smoothing terms. The final model explained 73% of residual deviance, with r^2 adj. = 0.65 (Table 3.7). The predicted values ranged from 9.9 to 14.2‰, with a mean ± SD of 12.4 ± 1.2‰ (Table 3.6).

The best GAM variant for rock crab δ^{15}N included length, latitude, and longitude smoothing terms. The final model explained 81.8% of residual deviance, with r^2 adj. = 0.78 (Table 3.7). The predicted values ranged from 8.0 to 11.5‰, with a mean ± SD of 10.2 ± 1.1‰ (Table 3.6).

Benthic pelagic coupling and mixing models

A total of 202 *C. striata* muscle samples and 153 liver samples were measured for stable isotopes from fish collected in 2016 (Table 3.3). All muscle tissue isotope mixing models converged successfully. Across all regions, BP ranged from 0.31 to 0.81, with a mean of 0.53 ± 0.08 (SD) (Table 3.3). Results from the GLM indicated that BP varied significantly by region, length, and sex ($P < 0.05$), and that there was a negative relationship between BP and length (Table 3.8, Fig. 3.4a, b). Pairwise comparisons revealed that the MD region differed significantly from the others with a

lower BP, indicating that a higher proportion of the diet was derived from pelagic sources (Tukey, $P < 0.05$) (Table 3.3).

Trophic position

Relative TP of *C. striata* across all regions ranged from 3.6 to 6.1, with a mean ± SD of 4.3 ± 0.4 (Table 3.3). It is important to note that these calculated values are relative to the baseline indicator organisms used and thus cannot be compared to absolute TP values across other studies. Generalized linear model results reported all four variables contributed significantly to TP ($P < 0.05$) (Table 3.8). Trophic position varied positively with both length and depth (Fig. 3.4c, d, e). Pairwise comparisons revealed that the TP for the NC region was significantly lower than the other regions (Tukey, $P < 0.05$) (Table 3.3).

SIBER and niche width

There were consistent differences in SEA for large and small size classes within the same region for muscle in both isospace and in niche space, so the regional comparisons were separated by size class for further analyses (Fig. 3.5). There was no consistent pattern between the sexes in terms of their SEA (results not shown). Differences were observed in isotopic width between regional groups by size class. For muscle tissue from the large size class, there was significant overlap in the ellipses for SNE, NJ, and MD, but not for NC (Fig. 3.5a). Bayesian SEA order from largest to smallest area was NJ > NC > MD > SNE based on the pairwise comparison

probabilities (Table 3.9a, Fig. 3.6a). For muscle tissue from the small size class, there was considerably more overlap among regional ellipses, with the NC group still having the lowest δ^{15}N values (Fig. 3.5b). Bayesian SEA order from largest to smallest was SNE > NJ > NC > MD (Table 3.9b, Fig. 3.6b). For muscle tissue from the large size class using niche (BP vs. TP) ellipses, all regions overlapped substantially (Fig. 3.5c). Bayesian SEA order from largest to smallest was NJ > SNE > MD > NC (Table 3.9c, Fig. 3.6c). For muscle tissue from the small size class using niche ellipses, there was also considerably more overlap among regional ellipses (Fig. 3.5d). Bayesian SEA order from largest to smallest was NJ > SNE > NC > MD (Table 3.9d, Fig. 3.6d). For liver tissue from the large size class, the NC ellipse also experienced the least amount of overlap (Fig 3.5e). Bayesian SEA order from largest to smallest was NJ > MD > NC > SNE (Table 3.9e, Fig 3.6e). For liver tissue from the small size class, there was also considerably more overlap among regional ellipses (Fig 3.5f). Bayesian SEA order from largest to smallest was SNE > NJ > MD > NC (Table 3.9f, Fig 3.6f).

Discussion

Regional patterns in reef feeding

My research explored the stomach contents of *C. striata* sampled from reef sites from two distinct regions during the summer residential period. Previous studies that analyzed diet across broad spatial scales (Bowman et al. 2000, Garrison & Link 2000) have compared trawl-sampled fish by region in the spring and autumn, whereas

those that have examined reef-caught fish were much more spatially constrained (Sedberry 1988, Malek et al. 2016). In this study, reef sample observations are consistent with previous observations of high abundances of crustacean prey in stomachs from both reef (Malek et al. 2016) and trawl collections (Bowman et al. 2000, Garrison & Link 2000). The dominance of decapod crustaceans in the NJ reef *C. striata* diet suggests that the population in this region may specialize on these prey, occupying a narrower niche width. On the other hand, the similar importance of bivalve and decapod prey in NC reef *C. striata* stomachs suggests a trend towards specialization for both of these prey items, but it is uncertain whether this preliminary evidence of specialization reflects the observed subsample or broader patterns within the regional population. Not all available stomachs in this study were examined for contents, and a conclusive proportion of empty stomachs over total stomachs sampled was not possible to obtain. There is likely an inherent bias in the identifiable contents, which may over-represent prey with hard exoskeletons that take a longer time to digest (Hyslop 1980). There is also the possibility for identification error when fish have previously ingested bait from earlier fishing attempts and the bait biomass is included in stomach content data. Prey with softer tissues were digested more rapidly, creating difficulty in reliable identification. This has likely caused under-representation of observable fish consumption in this study, thus it was not possible to test the hypothesis of increased piscivory by *C. striata* in southern regions. For example, several observations of piscivory were linked to the presence of scales, eyes, or other hard structures. Future studies of *C. striata* reef prey consumption across regions could collect samples and assess prey species richness using species

accumulation curve techniques (e.g., Gotelli & Colwell 2001) in order to gather data with a strong statistical foundation for more quantitative analyses such as niche breadth and dietary guild (Malek et al. 2016) to complement stable isotope niche estimates. In addition, additional stomach data from locations I was unable to analyze (e.g., SNE and MD reefs) will contribute substantially to determining regional feeding ecology patterns in summer residence habitats.

Trophic position and benthic-pelagic coupling

The estimated TP of the NC regional group was distinctly lower than the other northern groups. Although this does not align with my initial hypothesis based on previous diet analyses of from trawl-caught fish, it is in agreement with the general macroecological prediction of reduced trophic position at lower latitudes, where primary production and ecosystem stability were previously assumed to be the main determining factors for food chain length. However, more recent meta-analyses have determined that food chain length is more likely a result of interacting characteristics that include ecosystem size, energy flux, and interactions between predators and prey. In addition, simplified models of ecosystems with linear trophic interactions often underestimate the extent of omnivory, intraguild predation, and microbial transfers that increase the complexity of natural food webs (Post 2002a, Ward & McCann 2017).

There was a positive relationship observed between body length and trophic position, which supports my hypothesis of increasing trophic position with increasing size. However, the relationship between size and trophic position or level becomes

substantially more relevant when examined beyond the scale of individual species and within the framework of a community of interacting taxa (Jennings et al. 2001). Comparing these trophic estimates with similarly derived predictions for sympatric community members in the MAB and SAB would allow for a more robust exploration of body size patterns.

The Maryland region differed significantly in benthic proportion, suggesting that this regional group consumed a higher proportion of pelagic prey. Due to the nature of the samples available, I was unable to clearly determine the definitive factors responsible for this pattern. The pattern could be in part due to nutrient inputs from the coastline, such as the Chesapeake and Delaware Bays, which contribute plumes of organic matter and nutrients to the shelf system, supporting highly productive pelagic food webs (Filippino et al. 2011). There is also the seasonal variability of carbon export from the MAB waters that may play a role: off-shelf water movement is at its strongest in fall, winter, and spring, but is reduced in the summer, enabling relatively high primary productivity (Savidge & Savidge 2014). Increased physical contact between pelagic primary production and reef consumers, whether due to strong vertical mixing or shallow reef habitats, could also contribute to higher pelagic contributions to reef consumers. Unexpectedly, the MD reef sites were deeper on average than the other regional reef sites considered here (Table 3.1). Future studies that include water quality data collection may be able to identify environmental covariates that correlate with food web characteristics along the MAB. These data would also be useful for identifying conditions under which benthic-pelagic coupling could be impaired (e.g., water column stratification). My results

reinforce the general assumption that benthic resources are highly important to *C. striata* diet, but there is also a notable contribution from pelagic resources as well. Future studies could include more data for prey captured in these regions, particularly bivalves that have a low trophic position and a pelagic δ^{13}C signature.

Prey isotope variation and ecological stoichiometry

Ecological stoichiometry studies in aquatic systems have observed that the elemental ratios at the base of the food web (particularly C, N, and P as nutrient components) have profound effects on the body composition and food quality of consumers at all trophic levels (Glibert et al. 2011). The carbon to nitrogen ratio is often used as a proxy for lipid content (Fagan et al. 2011). Higher lipid content typically suggests better condition and can be an indicator of higher quality food or habitat conditions (Lloret & Planes 2003, see Chapter 2). Here, a comparison of northern and southern *C. striata* and baseline prey C:N ratios did not indicate clear spatial patterns or correlations. For example, northern (SNE, NJ, MD) and southern (NC) *C. striata* muscle tissue C:N ratio was invariant (3.9 ± 0.2 and 3.8 ± 0.1, respectively). Baseline prey C:N ratios showed similarly stable values (northern anchovies = 3.9 ± 0.1, southern anchovies = 3.9 ± 0.1; northern *C. irroratus* = 4.2 ± 0.2, southern *C. irroratus* = 4.1 ± 0.2). The relationship between actual prey (rather than baseline taxa) and *C. striata* stoichiometry could not be examined in detail due to the fact that the prey examined were not collected from reef sites, and the NMFS and NEAMAP sampling sites do not necessarily correspond with sites where *C.*

striata were sampled. Future studies could examine prey spatial variation in $\delta^{13}C$, $\delta^{15}N$ values, and the C:N ratio at a finer spatial and temporal resolution by collection from the same reefs as *C. striata* samples and at similar times.

Measuring niche area: direct and indirect methods

The NC ellipses for muscle tissue in isotope space (Fig. 3.5a, b) overlap less with the ellipses of other regions (particularly within the large muscle group), suggesting that their trophic niche may be distinct from the other regions. However, when the muscle isotope data is translated into niche space (BP vs. TP) (Fig. 3.5c, d), there is considerably more overlap. This suggests that despite locally distinct isotope values, NC fish may occupy more similar niches to their northern counterparts than what would be predicted from isotope ratios alone. It is important to note that isotopic niche and trophic niche are distinct measurements and should not be confused, despite the fact that they are often correlated to one another (Jackson et al. 2011). A study by Woodland and Secor (2011) observed similar discrepancies between isotopic niche and realized niche in two fish species in the Chesapeake Bay and offshore of MD. Future studies could collect more prey and food web base samples in NC to compare the system's isotopic signature compared to more northern regions.

For muscle tissue, small individuals appeared to have a greater SEA compared to large individuals from the same region. The range of available prey generally increases as individuals increase in total length and gape size (Scharf et al. 2000), which would be consistent with a broadening of niche width. However, the body tissues of smaller individuals may respond more quickly (i.e. equilibrate) to localized

changes in food, thus the patterns observed here may simply be a signal of local feeding. The tissues of larger-bodied individuals require longer equilibration time after a change in diet due to either prey switching or movement to a new feeding location (Herzka 2005).

There are also differences in the relative sizes and positions of the regional ellipses for liver tissue for both size groups (Fig. 3.5e, f) compared to the muscle tissue groups in isospace. This may indicate that the liver tissue represents a narrower time frame of food assimilation due to tissue-based differences in isotope turnover rates (Herzka 2005, MacNeil et al. 2006).

Mixing models and their limitations

Stable isotope mixing models enable the examination of mixtures (consumers) to determine the relative proportions of sources (prey) with distinct isotopic signatures (Moore & Semmens 2008). However, there are several precautions and assumptions that must be taken into account when developing plausible mixing models (Phillips et al. 2014). Of primary concern is the high level of uncertainty when estimating the diet of a consumer; Bayesian statistical frameworks function exceptionally well in this case due to their ability to factor in previous information *a priori* to inform predictive output (Parnell et al. 2010). One of the most important requirements of an appropriately set up mixing model is that the mixtures fit within the prey polygon in order to estimate relative proportions (Phillips et al. 2014). My prey muscle isotope data required transformation to estimated whole-body prey values as well as model prediction to the *C. striata* sampling sites in order to more

closely meet the polygon fit requirement. Prey samples that are collected from the same sampling areas as the consumers in future studies may be more likely to meet the criteria for mixing model analysis.

Equilibration rates: muscle and liver tissue

In order to produce estimates of regional niche metrics, I assumed that the isotope ratios of the individuals were equilibrated to the prey of that region. Given *C. striata* seasonal migrations to overwinter offshore from reefs, the assimilated isotope composition in reef fish muscle tissue soon after return in the spring may not yet reflect the local prey signatures, particularly in the case of larger-bodied fish (Herzka 2005). The majority of the fish examined in this study were collected at reefs in mid- to late summer (June-August), which I assumed would allow for more time to equilibrate to the local food sources. I also relied on the assumption that the selected δ^{13}C and δ^{15}N TEFs from McCutchan et al. (2003) were valid for *C. striata* muscle tissue, but this may not necessarily be the case. It was not possible to calculate BP or TP based on liver tissue due to the lack of knowledge of an appropriate TEF representative of *C. striata* liver tissue; liver estimates compiled from experiments in the literature are highly variable due to the variety of fish taxa studied, the variability in feed type and experimental setup, and whether or not the lipid was removed (Sweeting et al. 2007a, Sweeting et al. 2007b). Future research that experimentally validates the TEF and isotopic turnover rate of *C. striata* tissues through controlled feeding studies would enable estimates of BP and TP using tissues with a more rapid equilibration time.

Conclusion

Black sea bass *C. striata* in the MAB is a key demersal predator on natural and artificial reefs, and the fishery's high commercial and recreational value warrants ongoing monitoring and management from both ecological and economic perspectives. My study is one of the first to directly compare *C. striata* diet and trophic ecology among regions during the summer residential period. My stable isotope analysis has enabled insight into the assimilated diet within muscle tissue, and to determine the trophic ecology of the species at different sites along the MAB. The NC group of *C. striata* examined here appears to have a distinct isotopic signature compared to the northern groups, but whether its actual trophic niche differs substantially from the others remains to be investigated. With appropriate TEF data, liver tissue could be used for trophic niche analysis over shorter time frames, enabling higher-resolution insight into *C. striata* trophic niche changes between their residential and migratory periods. Combining this spatial information with seasonal studies of *C. striata* feeding patterns during migratory movement and including further analysis of rapidly-equilibrating tissues will provide a clearer view of the extent of resources essential to the fishery and will promote better understanding of broader-scale trophic dynamics in the MAB.

References

Able KW, Fahay MP (2010) Ecology of estuarine fishes: temperate waters of the Western North Atlantic. The Johns Hopkins University Press, Baltimore, MD

Akin S, Winemiller KO (2008) Body size and trophic position in a temperature estuarine food web. Acta Oecologica-International Journal of Ecology 33:144-153

Amundsen PA, Gabler HM, Staldvik FJ (1996) A new approach to graphical analysis of feeding strategy from stomach contents data - Modification of the Costello (1990) method. Journal of Fish Biology 48:607-614

Bacheler NM, Paramore LM, Buckel JA, Hightower JE (2009) Abiotic and biotic factors influence the habitat use of an estuarine fish. Marine Ecology Progress Series 377:263-277

Bowman RE, Stillwell CE, Michaels WL, Grosslein MD (2000) Food of Northwest Atlantic Fishes and Two Common Species of Squid. NOAA Technical Memorandum NMFS-NE-155. National Oceanic and Atmospheric Administration: National Marine Fisheries Service, Woods Hole, Massachusetts

Cabana G, Rasmussen JB (1994) Modelling food chain structure and contaminant bioaccumulation using stable nitrogen isotopes. Nature 372:255-257

Fagan K, Koops MA, Arts MT, Power M (2011) Assessing the utility of C:N ratios for predicting lipid content in fishes. Canadian Journal of Fisheries and Aquatic Sciences 68:374-385

Filippino KC, Mulholland MR, Bernhardt PW (2011) Nitrogen uptake and primary productivity rates in the Mid-Atlantic Bight (MAB). Estuarine, Coastal and Shelf Science 91:13-23

Garrison LP, Link JS (2000) Dietary guild of the fish community in the Northeast United States continental shelf ecosystem. Marine Ecology Progress Series 202:231-240

Giménez J, Marçalo A, Ramírez F, Verborgh P, Gauffier P, Esteban R, Nicolau L, González-Ortegón E, Baldó F, Vilas C, Vingada J, Forero MG, de Stephanis R (2017) Diet of bottlenose dolphins (*Tursiops truncatus*) from the Gulf of Cadiz: Insights from stomach content and stable isotope analyses. PLoS ONE 12(9):e0184673. doi:10.1371/journal.pone.0184673

Glibert PM, Fullerton D, Burkholder JM, Cornwell JC, Kana TM (2011) Ecological stoichiometry, biogeochemical cycling, invasive species, and aquatic food webs: San Francisco estuary and comparative systems. Reviews in Fisheries Science 19:358-417

Gotelli NJ, Colwell RK (2001) Quantifying biodiversity: procedures and pitfalls in the measurement and comparison of species richness. Ecology Letters 4:379-391

Herzka SZ (2005) Assessing connectivity of estuarine fishes based on stable isotope ratio analysis. Estuarine, Coastal and Shelf Science 64:58-69

Hyslop EJ (1980) Stomach contents analysis- a review of methods and their application. Journal of Fish Biology 17:411-429

Jackson AL (2016) SIAR-examples-and-queries/learning-resources/siber-comparing-populations.Rmd. Accessed August 31 2018. https://github.com/AndrewLJackson/SIAR-examples-and-queries/blob/master/learning-resources/siber-comparing-populations.Rmd

Jackson AL, Inger R, Parnell AC, Bearhop S (2011) Comparing isotopic niche widths among and within communities: SIBER - Stable Isotope Bayesian Ellipses in R. Journal of Animal Ecology 80:595-602

Jennings S, Pinnegar JK, Polunin NVC, Boon TW (2001) Weak cross-species relationships between body size and trophic level belie powerful size-based trophic structuring in fish communities. Journal of Animal Ecology 70:934-944

Kiljunen M, Grey J, Sinisalo T, Harrod C, Immonen H, Jones RI (2006) A revised model for lipid-normalizing $\delta^{13}C$ values from aquatic organisms, with implications for isotope mixing models. Journal of Applied Ecology 43:1213-1222

Link JS (2002) Ecological considerations in fisheries management: when does it matter? Fisheries 27:10-17

Lloret J, Planes S (2003) Condition, feeding and reproductive potential of white seabream *Diplodus sargus* as indicators of habitat quality and the effect of reserve protection in the northwestern Mediterranean. Marine Ecology Progress Series 248:197-208

MacNeil MA, Drouillard KG, Fisk AT (2006) Variable uptake and elimination of stable nitrogen isotopes between tissues in fish. Canadian Journal of Fisheries and Aquatic Sciences 63:345-353

Malek AJ, Collie JS, Taylor DL (2016) Trophic structure of a coastal fish community determined with diet and stable isotope analyses. Journal of Fish Biology 89:1513-1536

McConnaughey T, McRoy CP (1979) Food-web structure and the fractionation of carbon isotopes in the Bering Sea. Marine Biology 53:257-262

McCutchan JH, Lewis WM, Kendall C, McGrath CC (2003) Variation in trophic shift for stable isotope ratios of carbon, nitrogen, and sulfur. Oikos 102:378-390

Moore JW, Semmens BX (2008) Incorporating uncertainty and prior information into stable isotope mixing models. Ecology Letters 11:470-480

Northeast Fisheries Science Center (2017) 62nd Northeast Regional Stock Assessment Workshop (6nd SAW) Assessment Summary Report. US Department of Commerce, Woods Hole, Massachusetts

Parnell AC, Inger R, Bearhop S, Jackson AL (2010) Source partitioning using stable isotopes: coping with too much variation. PLoS ONE 5(3): e9672. doi:10.1371/journal.pone.0009672

Parnell AC, Phillips DL, Bearhop S, Semmens BX, Ward EJ, Moore JW, Jackson AL, Grey J, Kelly DJ, Inger R (2013) Bayesian stable isotope mixing models. Environmetrics 24:387-399

Perga ME, Gerdeaux D (2005) 'Are fish what they eat' all year round? Oecologia 144:598-606

Phillips DL, Inger R, Bearhop S, Jackson AL, Moore JW, Parnell AC, Semmens BX, Ward EJ (2014) Best practices for use of stable isotope mixing models in food-web studies. Canadian Journal of Zoology 92:823-835

Pikitch EK, Santora C, Babcock EA, Bakun A, Bonfil R, Conover DO, Dayton P, Doukakis P, Fluharty D, Heneman B, Houde ED, Link J, Livingston PA, Mangel M, McAllister MK, Pope J, Sainsbury KJ (2004) Ecosystem-based fishery management. Science 305:346-347

Post DM (2002a) The long and short of food-chain length. Trends in Ecology & Evolution 17:269-277

Post DM (2002b) Using stable isotopes to estimate trophic position: models, methods, and assumptions. Ecology 83:703-718

R Core Team (2016) R: A language and environment for statistical computing. R Foundation for Statistical Computing, Vienna, Austria

R Core Team (2018) R: A language and environment for statistical computing. R Foundation for Statistical Computing, Vienna, Austria

Savidge DK, Savidge WB (2014) Seasonal export of South Atlantic Bight and Mid-Atlantic Bight shelf waters at Cape Hatteras. Continental Shelf Research 74:50-59

Scharf FS, Juanes F, Rountree RA (2000) Predator size - prey size relationships of marine fish predators: interspecific variation and effects of ontogeny and body size on trophic-niche breadth. Marine Ecology Progress Series 208:229-248

Sedberry GR (1988) Food and feeding of black sea bass, *Centropristis striata*, in live bottom habitats in the South Atlantic Bight. The Journal of the Elisha Mitchell Scientific Society 104:35-50

Sweeting CJ, Barry J, Barnes C, Polunin NVC, Jennings S (2007a) Effects of body size and environment on diet-tissue delta N-15 fractionation in fishes. Journal of Experimental Marine Biology and Ecology 340:1-10

Sweeting CJ, Barry JT, Polunin NVC, Jennings S (2007b) Effects of body size and environment on diet-tissue delta C-13 fractionation in fishes. Journal of Experimental Marine Biology and Ecology 352:165-176

Wagenmakers EJ, Farrell S (2004) AIC model selection using Akaike weights. Psychonomic Bulletin & Review 11:192-196

Ward CL, McCann KS (2017) A mechanistic theory for aquatic food chain length. Nature Communications. doi: 10.1038/s41467-017-02157-0

Wood SN (2006) Generalized Additive Models: An Introduction with R. Chapman and Hall/CRC, Boca Raton, FL

Woodland RJ, Secor DH (2011) Differences in juvenile trophic niche for two coastal fish species that use marine and estuarine nursery habitats. Marine Ecology Progress Series 439:241-U290

Woodland RJ, Secor DH (2013) Benthic-pelagic coupling in a temperate inner continental shelf fish assemblage. Limnology and Oceanography 58:966-976

Tables

Table 3.1. Sampling site depth data for *Centropristis striata* collected from inshore reefs in summer 2016 and offshore trawling (National Marine Fisheries Service) in spring and autumn 2016. Regions are Southern New England (SNE), New Jersey (NJ), Maryland (MD), and North Carolina (NC). Depth data presented as mean ± standard deviation. n = number of sites.

	n	Depth (m)	min_{Depth}	max_{Depth}
Reef Total	30	20.5 ± 4.3	6.1	35.1
NJ	11	17.6 ± 2.2	13.7	20.1
MD	6	28.7 ± 2.4	26	35.1
NC	13	21.8 ± 2.3	6.1	23.8
Trawl Total	18	46.1 ± 21.4	20.5	78
SNE	7	35.4 ± 10.6	24.7	52
NJ	5	57.0 ± 25.2	22.3	78
MD	4	27.5 ± 6.0	20.5	33
NC	2	62.1 ± 12.0	46.5	69.8

Table 3.2. Biological data for *Centropristis striata* collected in 2016. Regions are Southern New England (SNE), New Jersey (NJ), Maryland (MD), and North Carolina (NC). n = counts of female (F), indeterminate (I), male (M), young of the year (YOY), small (S, with YOY included in count), and large (L) individuals. Total Length is mean ± standard deviation.

	n_F	n_I	n_M	Total Length (mm)	n_{YOY}	n_S	n_L
Reef Total	86	37	34	255.7 ± 50.4	6	81	76
NJ	51	2	28	272.5 ± 49.8	0	36	45
MD	14	0	6	267.8 ± 38.6	0	7	13
NC	21	35	0	227.0 ± 42.2	6	38	18
Trawl Total	17	19	9	217.5 ± 92.5	14	29	16
SNE	11	2	3	250.3 ± 72.3	1	8	8
NJ	6	5	6	259.4 ± 84.6	1	9	8
MD	0	6	0	122.5 ± 26.2	6	6	0
NC	0	6	0	106.7 ± 31.3	6	6	0

Table 3.3. Summary table of measurements and calculations for *Centropristis striata* muscle (M) and (L) tissue samples. Regions are Southern New England (SNE), New Jersey (NJ), Maryland (MD), and North Carolina (NC). Liver $\delta^{13}C$ values have been corrected for lipid content (see Chapter 2). BP = benthic proportion of diet, TP = relative trophic position, Total SEA_c = Standard Ellipse Area corrected for small sample size for the total regional group, Large SEA_c/Small SEA_c = SEA_c for large and small size classes for each region, respectively. Muscle tissue SEA_c values were calculated for areas in niche space (BP vs. TP), and liver tissue SEA_c values were calculated for areas in isotope space ($\delta^{13}C$ vs. $\delta^{15}N$). n = sample size.

Region	Tissue	n	$\delta^{13}C$	C:N	$\delta^{15}N$	BP	TP	Total SEA_c	Large SEA_c	Small SEA_c
SNE	M	16	-17.3 ± 0.6	3.9 ± 0.2	14.0 ± 0.9	0.58 ± 0.07[b]	4.48 ± 0.36[b]	0.08	0.05	0.09
NJ	M	98	-17.1 ± 0.5	3.9 ± 0.2	14.7 ± 0.8	0.53 ± 0.07[b]	4.48 ± 0.42[b]	0.09	0.08	0.10
MD	M	26	-17.9 ± 0.5	3.8 ± 0.1	14.0 ± 0.6	0.46 ± 0.06[a]	4.37 ± 0.27[b]	0.04	0.03	0.04
NC	M	62	-18.1 ± 0.6	3.8 ± 0.1	11.7 ± 0.6	0.56 ± 0.07[b]	4.08 ± 0.24[a]	0.04	0.03	0.05
SNE	L	14	-20.7 ± 0.9	9.4 ± 2.1	11.6 ± 0.9	-	-	1.85	0.42	2.16
NJ	L	80	-19.2 ± 1.0	7.7 ± 3.0	12.9 ± 0.8	-	-	1.86	2.22	1.46
MD	L	22	-20.2 ± 1.1	6.1 ± 2.1	12.2 ± 0.6	-	-	1.38	1.34	1.24
NC	L	37	-20.2 ± 1.2	10.3 ± 3.3	9.7 ± 0.5	-	-	1.26	1.06	1.10

Table 3.4. Stomach contents of *Centropristis striata* from North Carolina (NC) and New Jersey (NJ) reefs separated into large (L) and small (S) size classes. Measurements presented as sums of dry weight in grams.

Region	NC		NJ	
Size class	L	S	L	S
CRUSTACEA TOTAL	4.1594	0.9616	15.876	1.8055
Amphipoda	-	-	0.0106	0.0292
Avoridae	-	-	0.0047	-
Listriella sp.	-	-	-	0.0292
Amphipoda unid.	-	-	0.0059	-
Decapoda	4.1391	0.9616	15.8654	1.7763
Calappa flammea	-	0.2362	-	-
Callinectes sapidus	0.5889	-	-	-
Cancer eurypanopeus depressus	-	-	0.9898	-
Cancer irroratus	-	-	7.9396	1.5716
Cancer sp.	-	-	1.4795	-
Decapoda unid.	0.8902	0.1231	3.3874	0.2047
Emerita sp.	-	-	0.1166	-
Hepatus epheliticus	1.4899	-	-	-
Hippolyte sp.	-	0.1178	-	-
Libinia sp.	0.4949	0.035	-	-
Pagurus sp.	0.0871	-	0.2316	-
Panopeus herbstii	0.1556	-	1.7209	-
Portunus sayi	0.1841	-	-	-
Portunus sp.	0.246	-	-	-
Crustacea unid.	0.0024	-	-	-
Parthenope granulata	-	0.4495	-	-
Isopoda	0.0203	-	-	-
MISCELLANEOUS TOTAL	0.5193	0.3649	5.3075	1.1991
Inorganic	0.0914	-	1.8422	0.4676
Organic	0.4279	0.3649	3.4653	0.7315
MOLLUSCA TOTAL	5.9344	3.2559	3.5695	1.2001
Bivalvia	5.9344	3.2509	3.5695	1.2001
Bivalvia unid.	1.0485	1.5887	3.5695	1.2001
Laevicardium mortoni	4.8859	1.6622	-	-
Gastropoda	-	0.005	-	-
Terebra dislocata	-	0.005	-	-
OSTEICHTHYES TOTAL	0.3538	0.0479	0.0131	0.1782
POLYCHAETA TOTAL	0.2212	0.234	0.0786	0.0157
Polychaeta unid.	0.2212	-	0.0786	0.0157
Sthenelais boa	-	0.234	-	-

ECHINODERMATA TOTAL	-	0.0623	-	-
Asteroidea	-	0.0623	-	-
Number sampled	18	20	41	15
Number empty	4	1	12	3
Mean total dry stomach content (g)	0.622	0.246	0.578	0.293

Table 3.5. Comparison of lengths and weights of *Centropristis striata* sampled from hook and line (Hook) and un-baited trap (Trap) offshore of Point Pleasant, New Jersey in June 2016. TL = total length, BW = body weight (total weight minus stomach weight), SW = stomach weight, SBR = stomach weight to body weight ratio. n = sample size.

Gear	n	TL (mm)	BW (g)	SW (g)	SBR
Hook	120	270 ± 48.4	277 ± 139	5.58 ± 5.69	0.0195 ± 0.0154
Trap	106	258 ± 40.9	235 ± 102	3.82 ± 3.81	0.0165 ± 0.0148

Table 3.6. Prey summary table separated by region. Anchovy group combines *Anchoa hepsetus* and *Anchoa mitchilli* data, and Rock crab group is entirely comprised of *Cancer irroratus*. Regions are Southern New England (SNE), New Jersey (NJ), Maryland (MD), and North Carolina (NC). Length was measured as total length for anchovies and carapace width for *C. irroratus*. Values presented as mean ± standard deviation. The "δ^{13}C whole" and "δ^{15}N whole" values represent whole-body corrections for muscle tissue sample measurements. The "GAM δ^{15}N" values represent predictions from generalized additive models for *Centropristis striata* sample sites. n = sample size.

	n	δ^{13}C	C:N	δ^{15}N	Length (mm)	δ^{13}C whole	δ^{15}N whole	GAM δ^{15}N
Anchovy	64	-18.4 ± 0.6	3.9 ± 0.1	14.3 ± 1.1	96.2 ± 23.3	-19.3 ± 0.6	13.2 ± 1.1	12.4 ± 1.2
SNE	5	-18.9 ± 0.3	3.9 ± 0.0	15.4 ± 1.2	59.2 ± 6.8	-19.8 ± 0.3	14.3 ± 1.2	12.8 ± 1.2
NJ	23	-18.2 ± 0.6	3.9 ± 0.1	14.8 ± 1.2	92.8 ± 25.1	-19.1 ± 0.6	13.7 ± 1.2	13.1 ± 1.0
MD	6	-18.2 ± 0.4	3.9 ± 0.0	14.5 ± 0.6	98.2 ± 30.2	-19.1 ± 0.4	13.4 ± 0.6	12.5 ± 0.2
NC	30	-18.5 ± 0.5	3.9 ± 0.1	13.8 ± 0.8	104.0 ± 15.0	-19.4 ± 0.5	12.7 ± 0.8	11.0 ± 0.3
Rock crab	42	-17.4 ± 0.8	4.2 ± 0.2	12.3 ± 1.5	60.0 ± 16.7	-	10.0 ± 1.5	10.2 ± 1.1
SNE	9	-17.6 ± 0.7	4.2 ± 0.4	12.9 ± 1.6	67.2 ± 27.5	-	10.6 ± 1.6	10.2 ± 0.6
NJ	8	-17.2 ± 0.6	4.1 ± 0.1	12.9 ± 1.3	58.2 ± 13.5	-	10.6 ± 1.3	11.0 ± 0.9
MD	21	-17.3 ± 1.0	4.2 ± 0.2	12.1 ± 1.4	57.6 ± 12.2	-	9.8 ± 1.4	10.4 ± 0.2
NC	4	-17.9 ± 0.2	4.1 ± 0.2	10.7 ± 0.5	60.0 ± 13.5	-	8.4 ± 0.5	9.0 ± 0.3

Table 3.7. Prey generalized additive model (GAM) results for Anchovy (*Anchoa mitchilli* + *Anchoa hepsetus*) and Atlantic rock crab (*Cancer irroratus*) for predicting δ^{15}N values at *Centropristis striata* sampling sites. Parameters with s( ) are non-parametric smoothed terms. Parameters joined with an asterisk "*" are interaction terms. Model *df* = degrees of freedom. Raw Akaike information criterion (AIC) score for each model was compared to the best model (lowest AIC) to compute ΔAIC, and transformed to compute Akaike weights (wAIC) as described in Wagenmakers et al. (2004). Best-fitting (most parsimonious) model for each prey group is marked in bold.

Model Parameters	*df*	% Deviance explained	r^2 adj	AIC	ΔAIC	wAIC
Anchovy						
δ^{15}N ~ s(Depth)+s(Length)+s(Latitude)+s(Longitude)	**17.05**	**73**	**0.65**	**143.87**	**0**	**0.30**
δ^{15}N ~ s(Depth)+s(Length)+s(Latitude)+s(Longitude)+Latitude*Longitude	17.01	73	0.65	143.87	0.01	0.30
δ^{15}N ~ s(Depth)+s(Length)+s(Latitude)+s(Longitude)+Depth*Longitude	15.64	71.5	0.64	144.57	0.70	0.21
δ^{15}N ~ s(Depth)+s(Length)+s(Latitude)+s(Longitude)+Depth*Latitude	17.34	72.5	0.64	145.51	1.64	0.13
δ^{15}N ~ s(Depth)+s(Length)+s(Latitude)	15.31	69.3	0.61	148.57	4.70	0.03
δ^{15}N ~ s(Depth)+s(Latitude)	14.93	68.8	0.61	148.93	5.06	0.02
Atlantic rock crab						
δ^{15}N ~ s(Depth)+s(Length)+s(Latitude)+s(Longitude)	9.70	81.9	0.78	98.24	1.27	0.19
δ^{15}N ~ s(Depth)+s(Length)+s(Latitude)+s(Longitude)+Latitude*Longitude	8.86	80.3	0.76	100.16	3.19	0.07
δ^{15}N ~ s(Depth)+s(Length)+s(Latitude)+s(Longitude)+Depth*Longitude	10.45	82	0.77	99.51	2.54	0.10
δ^{15}N ~ s(Depth)+s(Length)+s(Latitude)+s(Longitude)+Depth*Latitude	10.87	82.5	0.78	99.20	2.22	0.12
δ^{15}N ~ s(Length)+s(Latitude)+s(Longitude)	**8.94**	**81.8**	**0.78**	**96.97**	**0**	**0.36**
δ^{15}N ~ s(Latitude)+s(Longitude)	9.74	81.9	0.78	98.49	1.52	0.17

Table 3.8. Generalized linear model (GLM) results for *Centropristis striata* benthic proportion (BP) of diet and relative trophic position (TP) based on muscle tissue stable isotope values, where *df* = degrees of freedom, *F* = *F*-statistic, and *P* = *P*-value. Bolded *P*-values are significant at $\alpha = 0.05$. n = sample size.

Response	Variable	*df*	*F*	*P*
BP	Region	3	16.81	< **0.0001**
n = 202	Sex	2	3.33	**0.04**
	Length	1	6.52	**0.01**
	Depth	1	0.08	0.77
TP	Region	3	13.12	< **0.0001**
n = 202	Sex	2	3.29	**0.04**
	Length	1	24.01	< **0.0001**
	Depth	1	117.86	< **0.0001**

Table 3.9. Pairwise comparisons for *Centropristis striata* a) muscle tissue: large size class in isospace, b) muscle tissue: small size class in isospace, c) muscle tissue: large size class in niche space, d) muscle tissue: small size class in niche space, e) liver tissue: large size class in isospace, and f) liver tissue: small size class in isospace. Values represent probability (on a scale from 0 to 1) that Bayesian standard Ellipse B area is larger than the area of Bayesian standard Ellipse A. Comparison method rationale is explained by Jackson (2016).

a)		Ellipse A			
		SNE	NJ	MD	NC
Ellipse B	SNE		0.23	0.46	0.41
	NJ	0.77		0.78	0.76
	MD	0.54	0.22		0.43
	NC	0.59	0.24	0.57	

b)		Ellipse A			
		SNE	NJ	MD	NC
Ellipse B	SNE		0.64	0.90	0.88
	NJ	0.36		0.90	0.92
	MD	0.10	0.10		0.35
	NC	0.12	0.08	0.65	

c)		Ellipse A			
		SNE	NJ	MD	NC
Ellipse B	SNE		0.10	0.77	0.85
	NJ	0.90		0.99	1.00
	MD	0.23	0.01		0.60
	NC	0.15	0.00	0.40	

d)		Ellipse A			
		SNE	NJ	MD	NC
Ellipse B	SNE		0.36	0.95	0.93
	NJ	0.64		0.99	1.00
	MD	0.05	0.01		0.26
	NC	0.07	0.00	0.74	

e)		Ellipse A			
		SNE	NJ	MD	NC
Ellipse B	SNE		0.00	0.01	0.02
	NJ	1.00		0.93	0.99
	MD	0.99	0.07		0.72
	NC	0.98	0.01	0.28	

f)		Ellipse A			
		SNE	NJ	MD	NC
Ellipse B	SNE		0.75	0.84	0.92
	NJ	0.25		0.73	0.87
	MD	0.16	0.27		0.60
	NC	0.08	0.13	0.40	

Figures

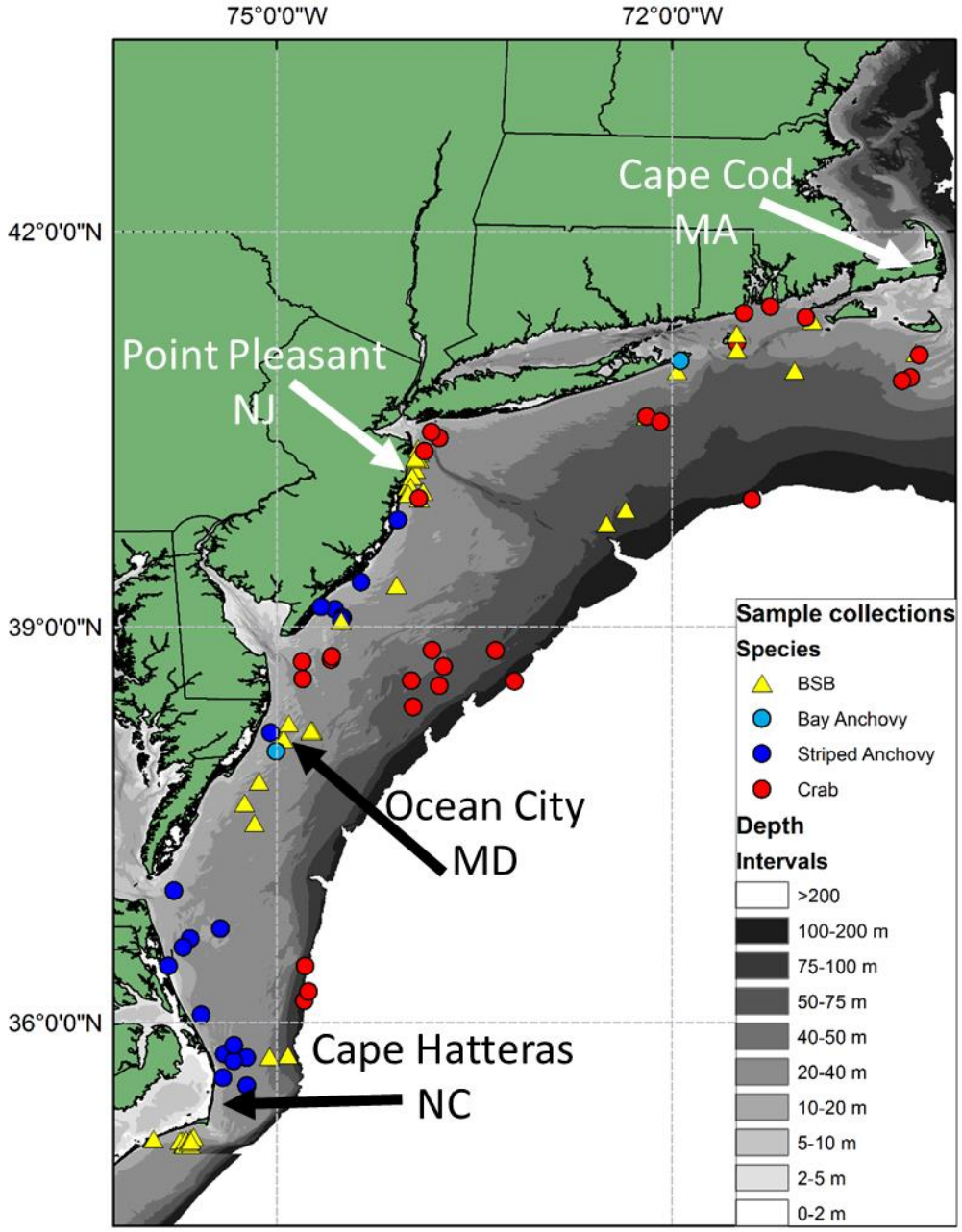

Figure 3.1. Map of sampling sites of *Centropristis striata* (black sea bass, BSB), *Anchoa mitchilli* (Bay Anchovy), *A. hepsetus* (Striped Anchovy), and *Cancer irroratus* (Crab) along the Middle Atlantic Bight in 2016 and 2017.

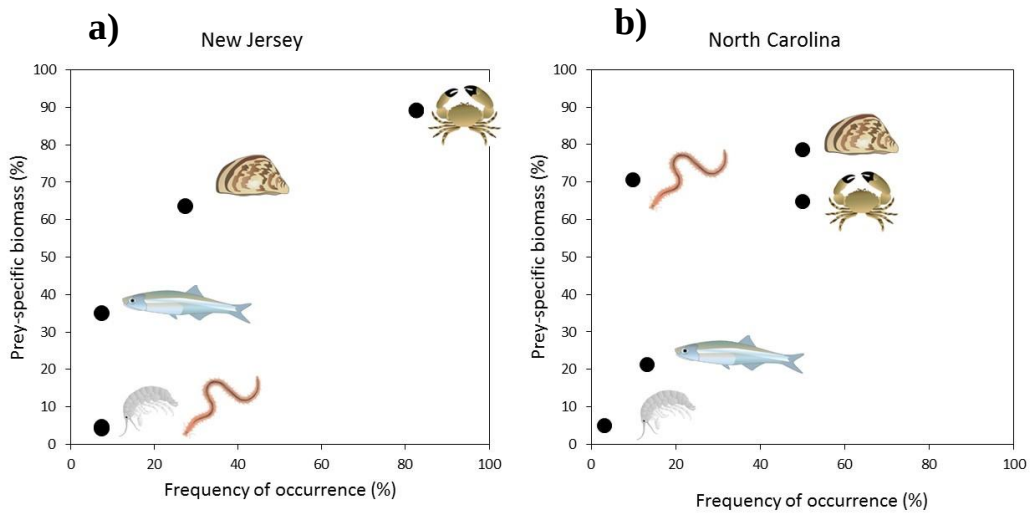

Figure 3.2. Feeding strategy plots for *Centropristis striata* at reefs of the Middle Atlantic Bight in summer (June-August) 2016. Data are presented from a subset of stomachs examined for a) New Jersey (n = 40) and b) North Carolina (n = 30) reef sites. Images from the Integration and Application Network, University of Maryland Center for Environmental Science (ian.umces.edu/imagelibrary/).

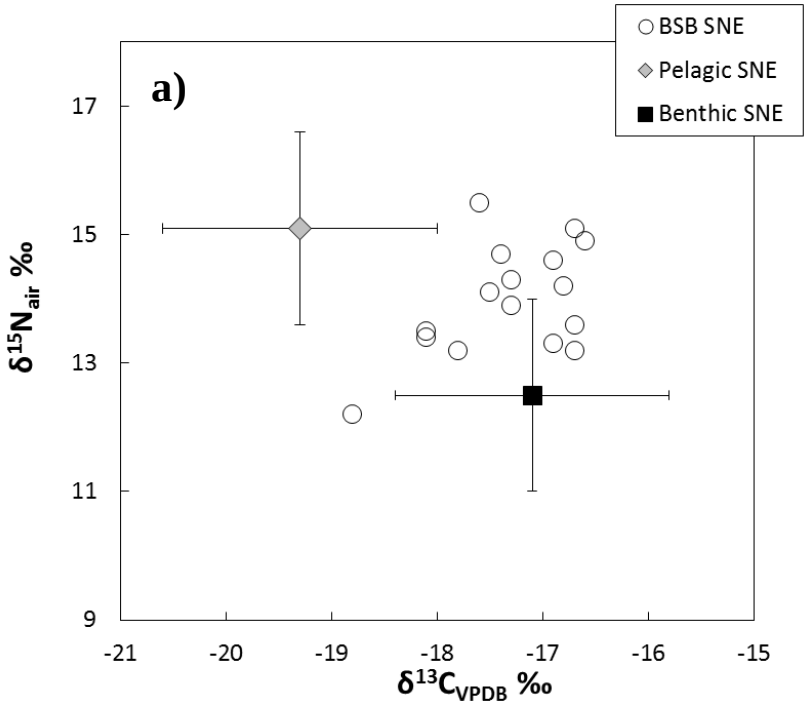
a)
BSB SNE
Pelagic SNE
Benthic SNE
17
15
13
11
9
-21
-20
-19
-18
-17
-16
-15
δ15Nair ‰
δ13CVPDB ‰

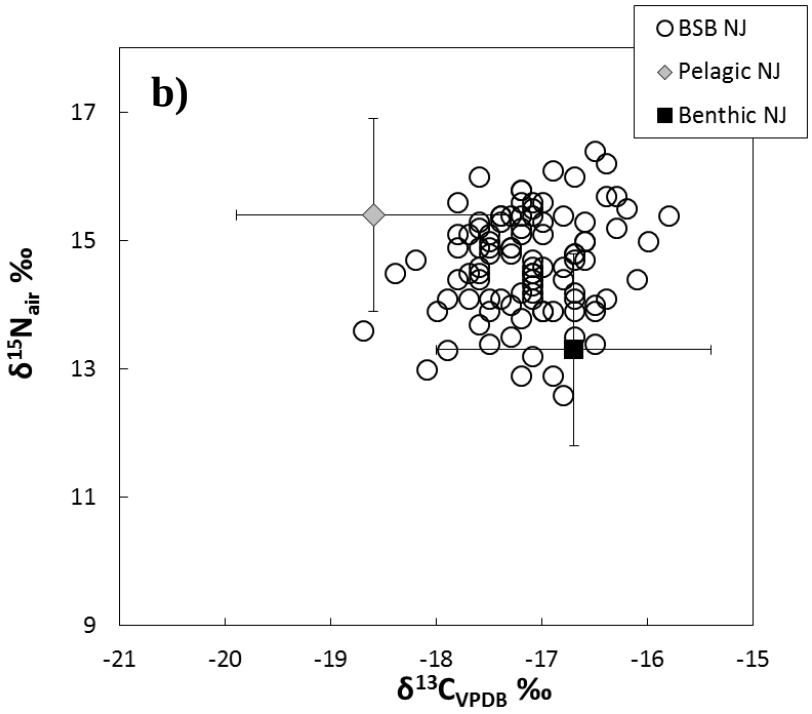
b)
BSB NJ
Pelagic NJ
Benthic NJ
17
15
13
11
9
-21
-20
-19
-18
-17
-16
-15
δ15Nair ‰
δ13CVPDB ‰

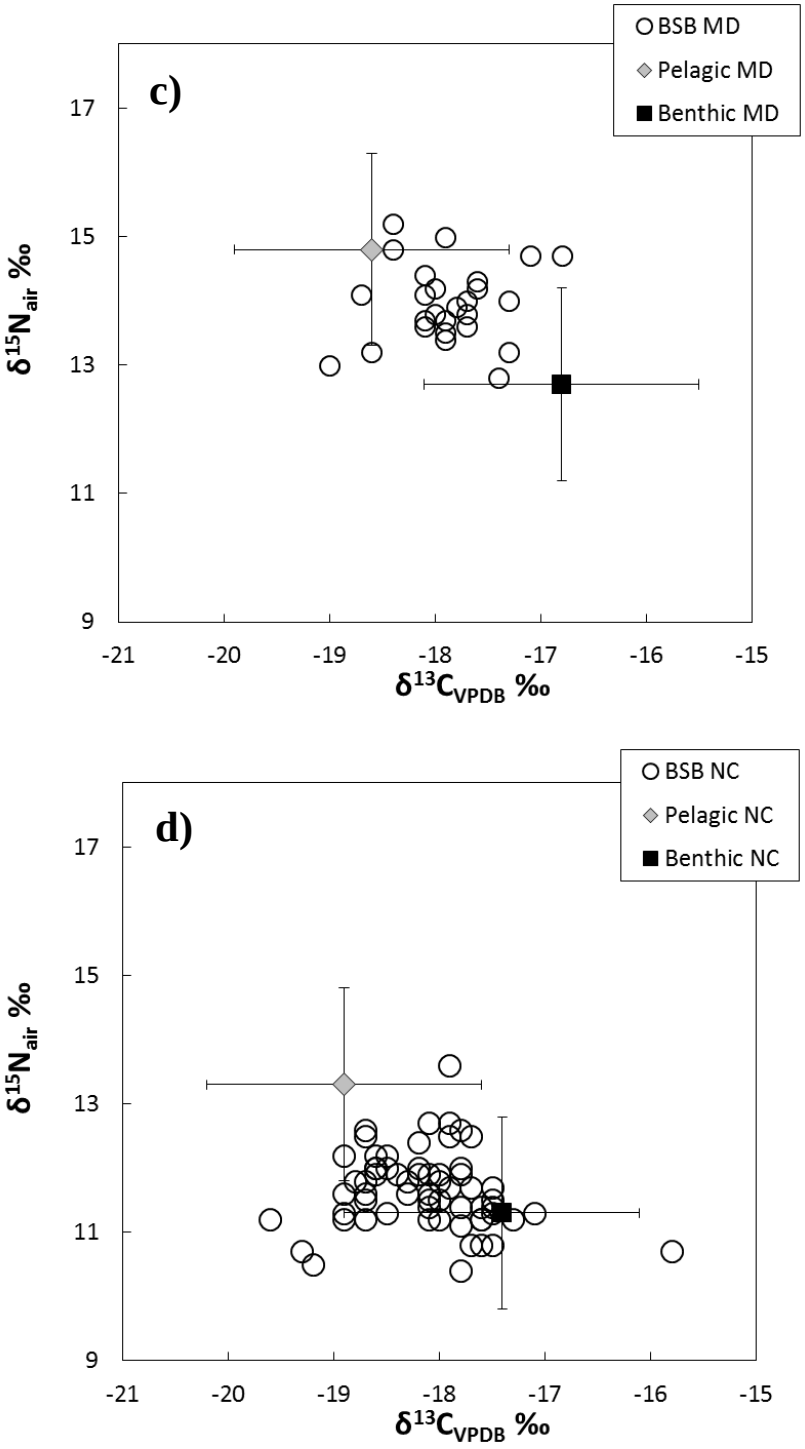

Figure 3.3. Stable isotope mixing model plots by region: a) Southern New England (SNE), b) New Jersey (NJ), c) Maryland (MD), and d) North Carolina (NC). Open circles are individual *Centropristis striata* (black sea bass, BSB) muscle tissue samples (mixtures) sampled in 2016. Shapes with error bars represent regional prey sample means increased by one level of a trophic enrichment factor [(TEF), 0.5‰ for δ^{13}C and 2.3‰ for δ^{15}N, from McCutchan et al. (2003)]. Error bars represent one

standard deviation of the TEF [±1.3‰ for $\delta^{13}C$ and ±1.5‰ for $\delta^{15}N$, from McCutchan et al. (2003)]. Combined pelagic anchovy samples are *Anchoa hepsetus* and *A. mitchilli*, and benthic rock crab samples are *Cancer irroratus* sampled in 2016 and 2017.

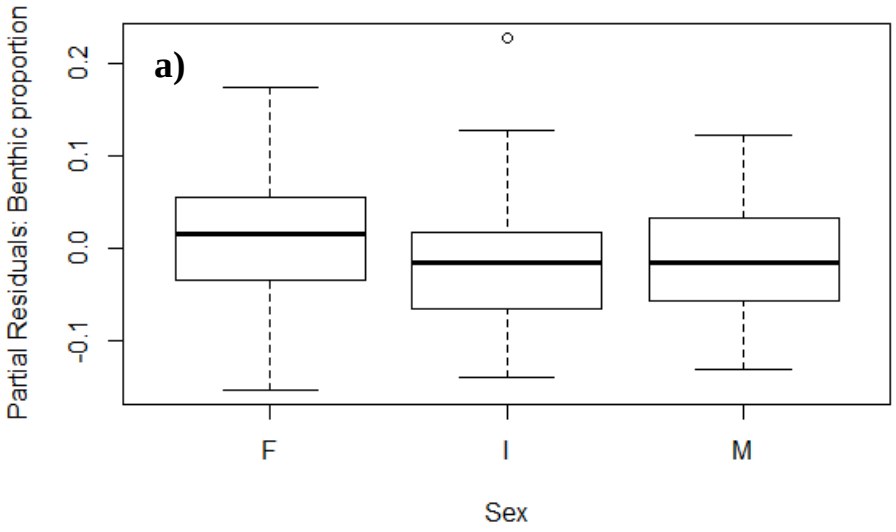
a)
Partial Residuals: Benthic proportion
0.2
0.1
0.0
-0.1
F
I
M
Sex

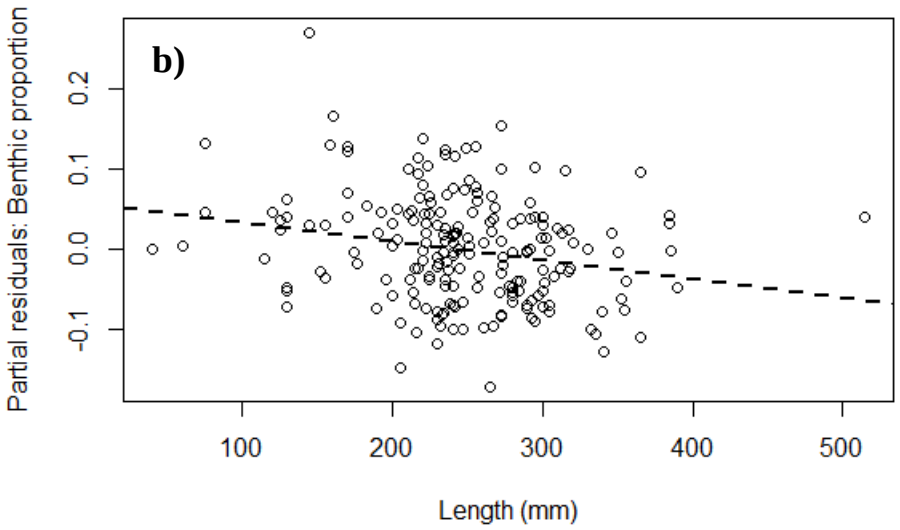
b)
Partial residuals: Benthic proportion
0.2
0.1
0.0
-0.1
100
200
300
400
500
Length (mm)

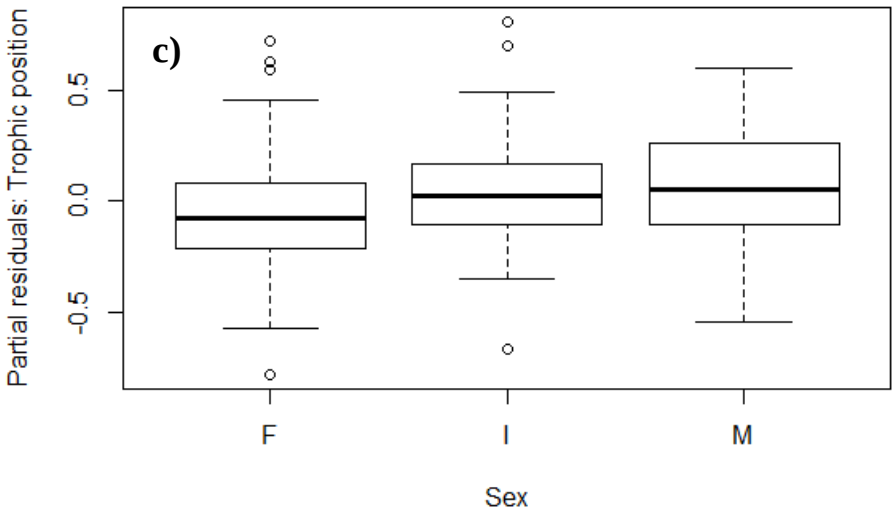
c)
Partial residuals: Trophic position
0.5
0.0
-0.5
F
I
M
Sex

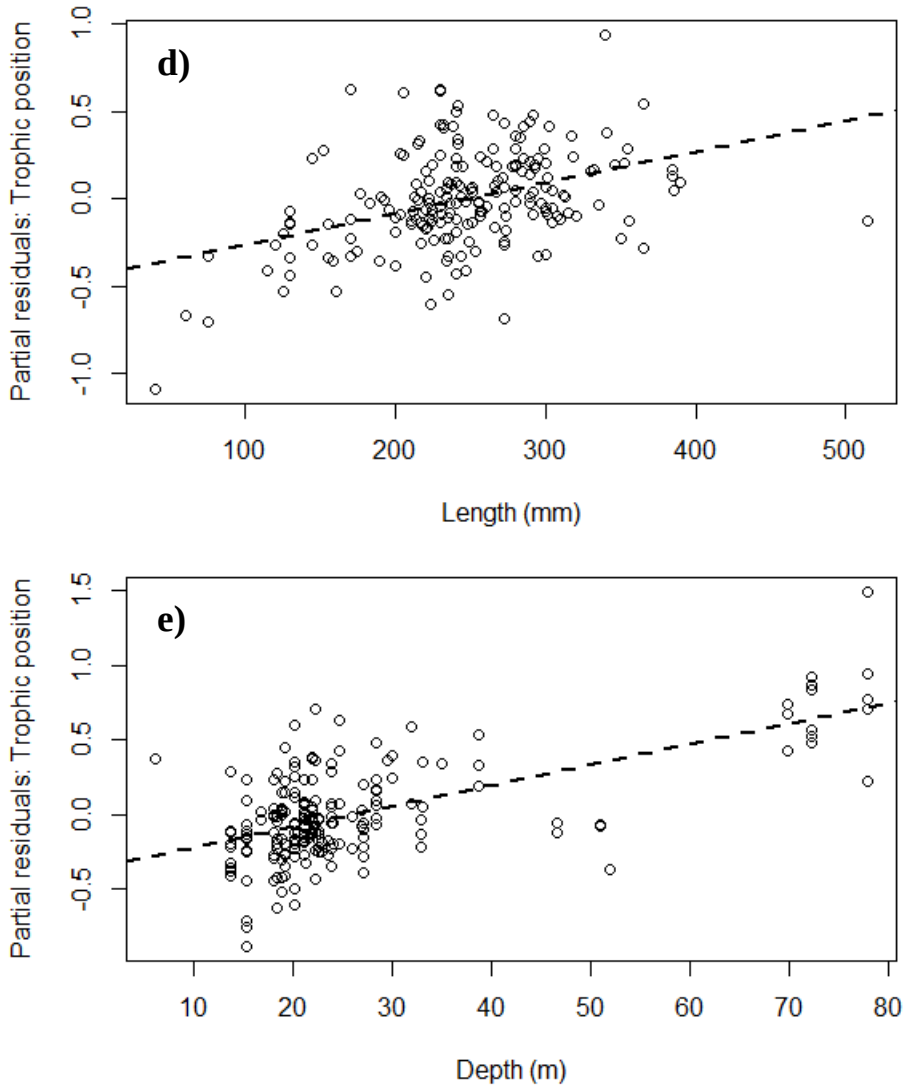

Figure 3.4. Generalized linear model results for benthic proportion of diet (BP) and trophic position (TP) derived from isotope analysis of *Centropristis striata* muscle tissue. Significant variables for BP were a) Sex [female (F), Indeterminate (I), Male (M)] and b) Length. Significant variables for TP were d) Sex, d) Length, and e) Depth. For regional pairwise comparisons, see Table 3.1. For significance of each variable, see Table 3.6.

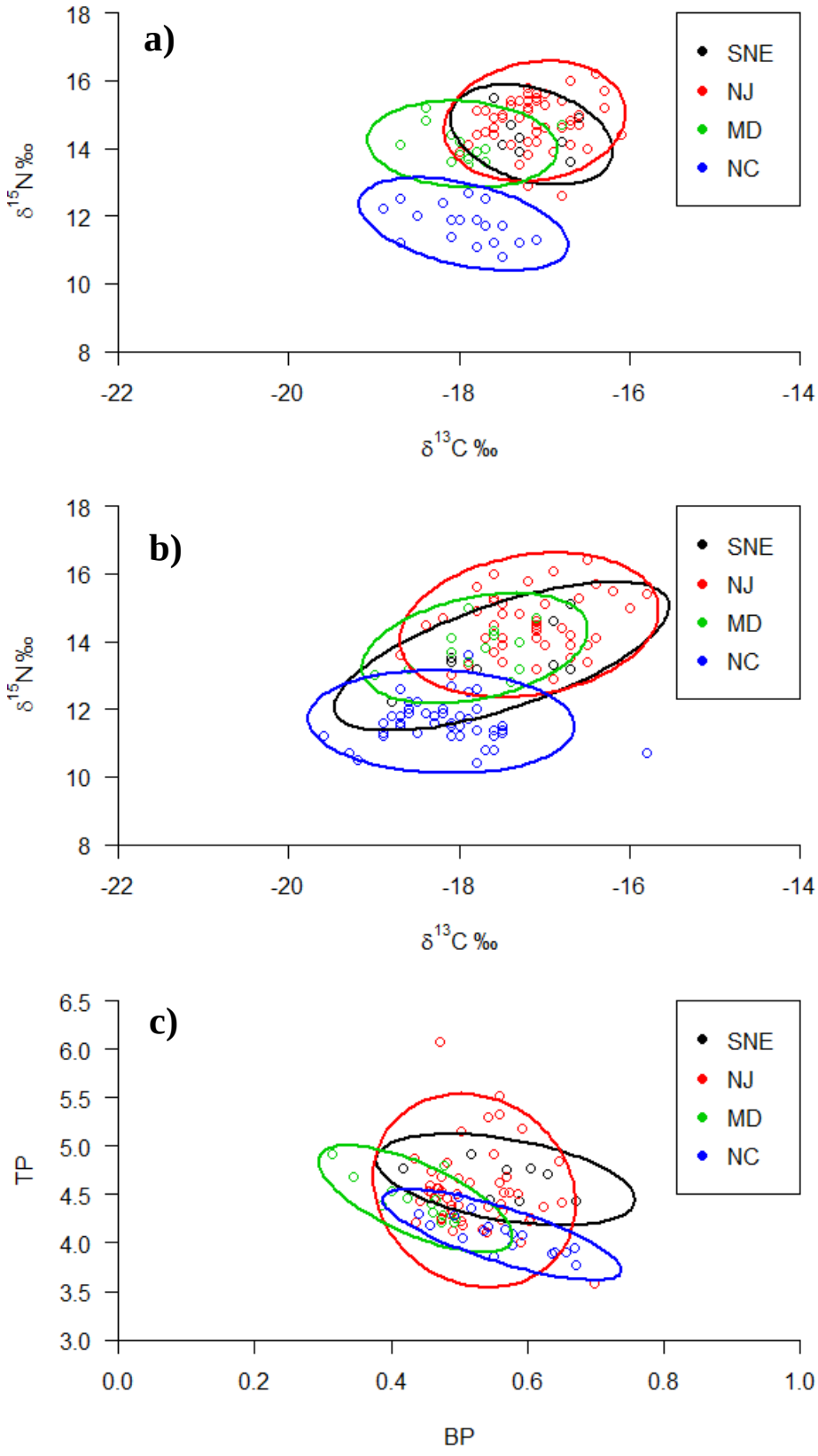
a)
b)
c)
SNE
NJ
MD
NC
δ15N‰
δ13C ‰
TP
BP
18
16
14
12
10
8
-22
-20
-18
-16
-14
6.5
6.0
5.5
5.0
4.5
4.0
3.5
3.0
0.0
0.2
0.4
0.6
0.8
1.0

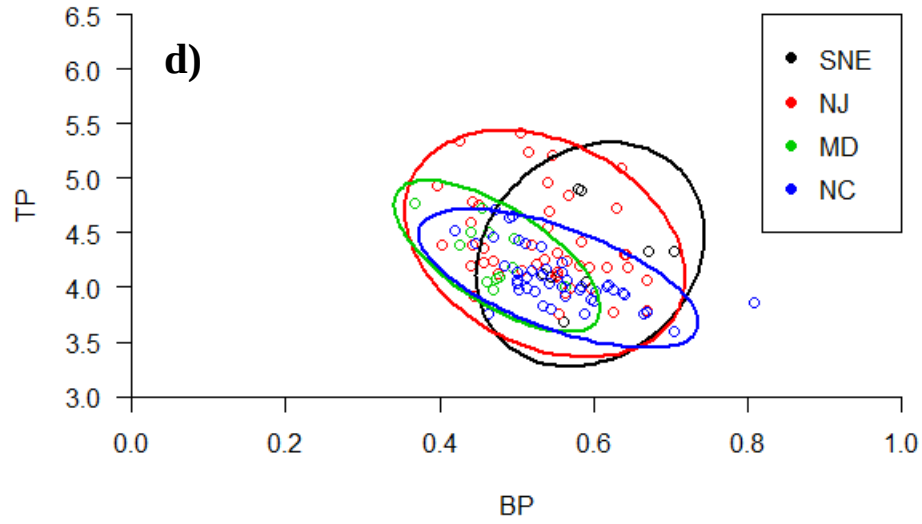
d)
SNE
NJ
MD
NC
TP
BP
6.5
6.0
5.5
5.0
4.5
4.0
3.5
3.0
0.0
0.2
0.4
0.6
0.8
1.0

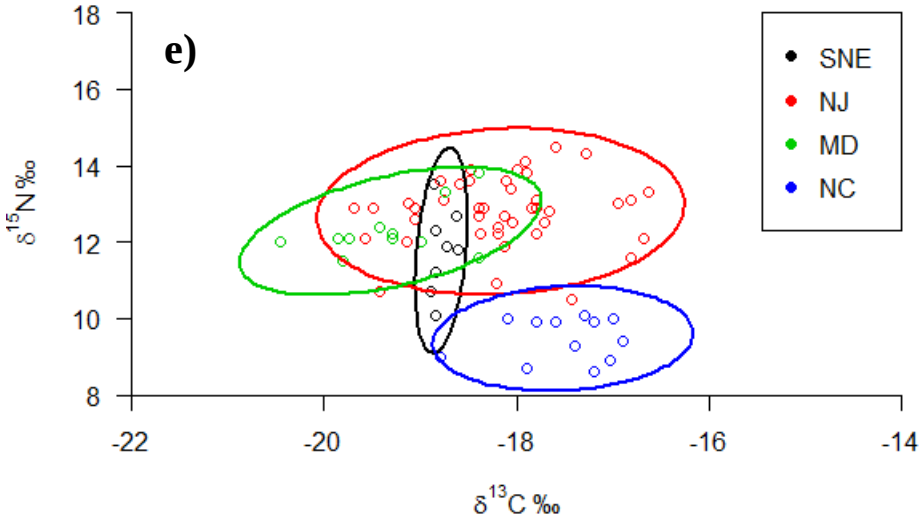
e)
SNE
NJ
MD
NC
δ15N‰
δ13C ‰
18
16
14
12
10
8
-22
-20
-18
-16
-14

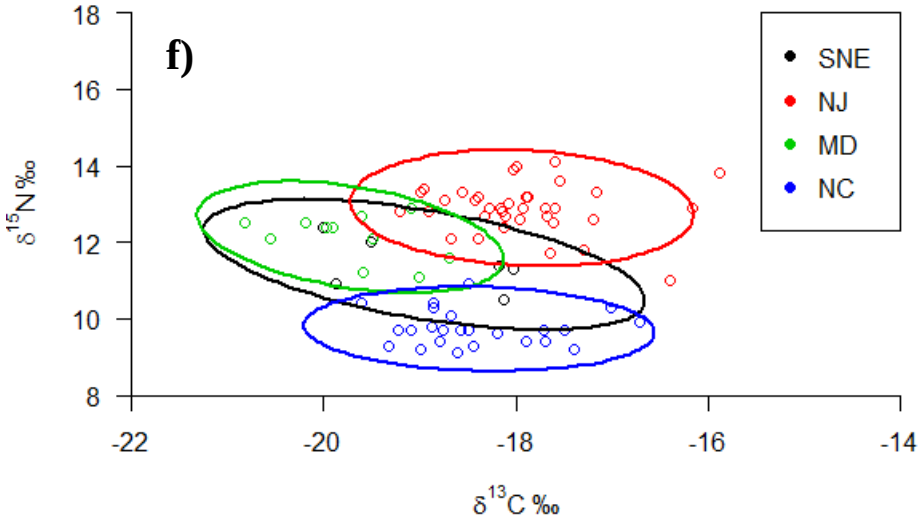
f)
SNE
NJ
MD
NC
δ15N‰
δ13C ‰
18
16
14
12
10
8
-22
-20
-18
-16
-14

Figure 3.5. SIBER ellipses for *Centropristis striata* in isotope space (i.e., isospace, $\delta^{13}C$ vs. $\delta^{15}N$) and in actual niche space [benthic proportion of diet (BP) vs. trophic position (TP)]. Plots are in the following order: a) muscle tissue: large size class (≥ 250 mm TL) in isospace, b) muscle tissue: small size class (< 250 mm TL) in isospace, c) muscle tissue: large size class in niche space, and d) muscle tissue: small size class in niche space, e) liver tissue: large size classes in isospace, and f) liver tissue: small size class in isospace.

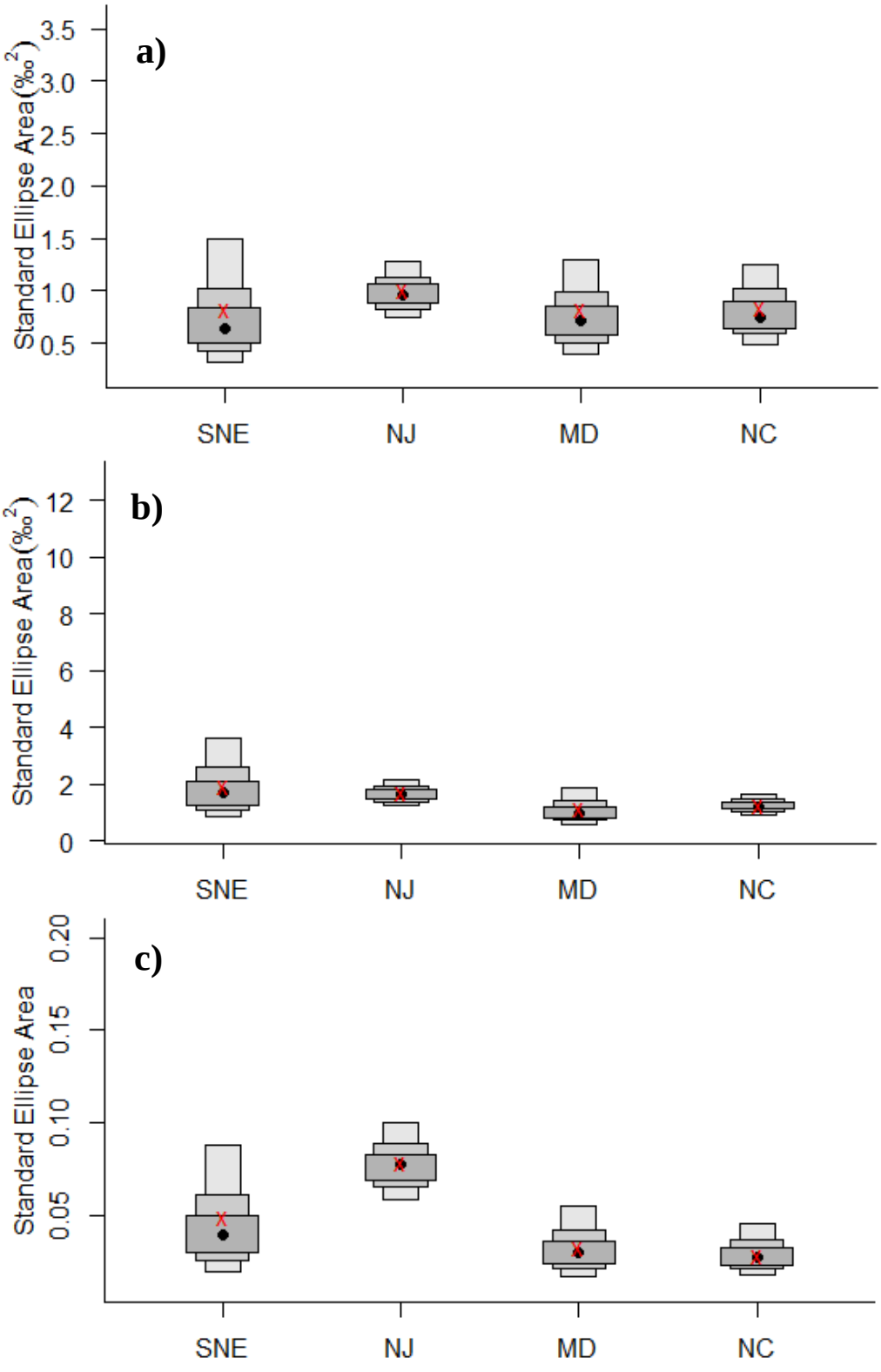
a)
Standard Ellipse Area(‰²)
3.5
3.0
2.5
2.0
1.5
1.0
0.5
SNE
NJ
MD
NC
b)
Standard Ellipse Area(‰²)
12
10
8
6
4
2
0
SNE
NJ
MD
NC
c)
Standard Ellipse Area
0.20
0.15
0.10
0.05
SNE
NJ
MD
NC

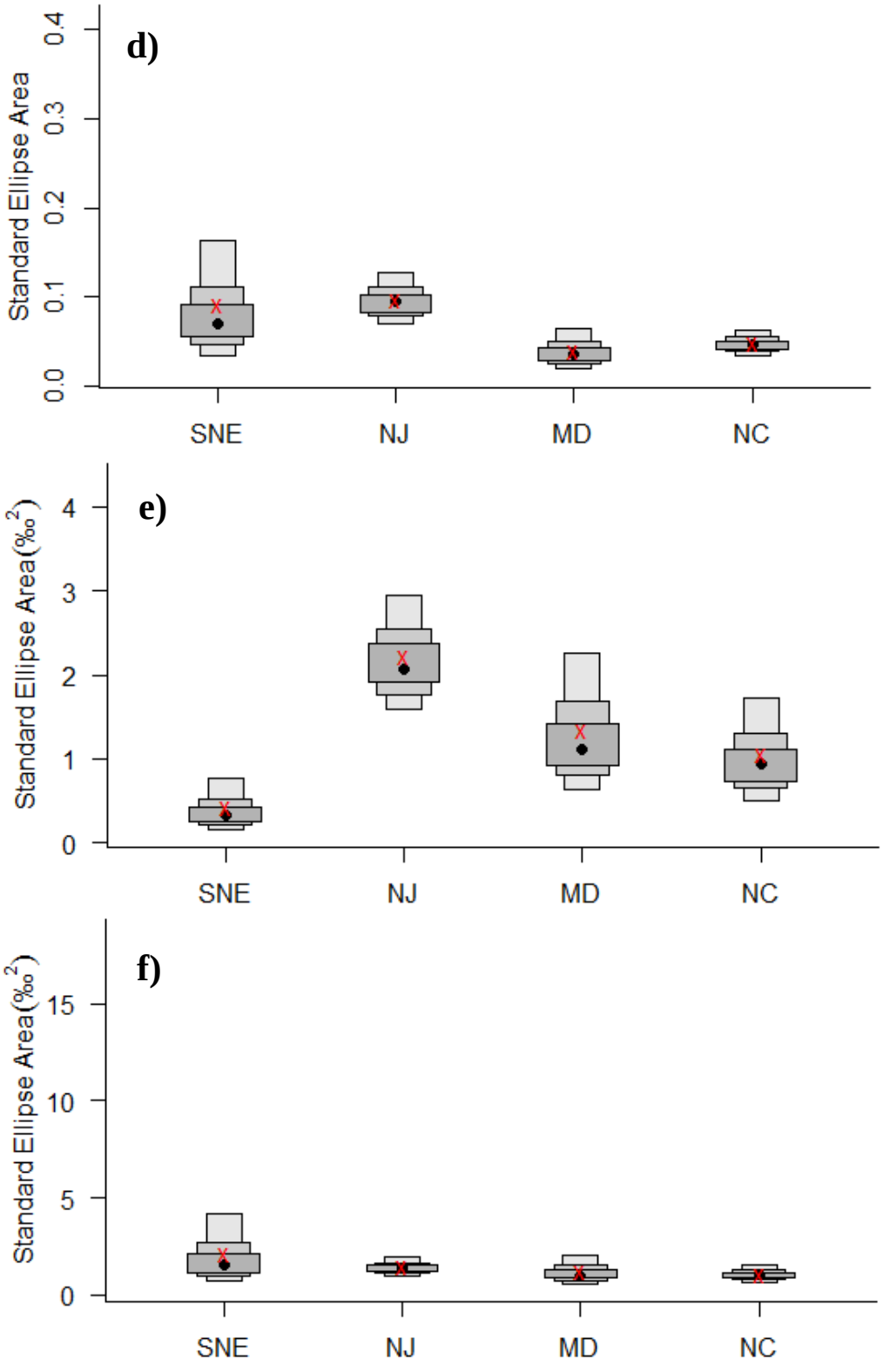
d)
Standard Ellipse Area
0.0
0.1
0.2
0.3
0.4
SNE
NJ
MD
NC
e)
Standard Ellipse Area(‰²)
0
1
2
3
4
SNE
NJ
MD
NC
f)
Standard Ellipse Area(‰²)
0
5
10
15
SNE
NJ
MD
NC

Figure 3.6. SIBER Bayesian Standard Ellipse Area density plots for *Centropristis striata*: a) muscle tissue: large size class in isospace, b) muscle tissue: small size class in isospace, c) muscle tissue: large size class in niche space, d) muscle tissue: small size class in niche space, e) liver tissue: large size class in isospace, and f) liver tissue: small size class in isospace. Boxes represent 50%, 75%, and 95% credible intervals. Red x's represent the Standard Ellipse Area corrected for small sample size (SEA_c) point estimates.

Full Bibliography

Able KW, Fahay MP (2010) Ecology of estuarine fishes: temperate waters of the Western North Atlantic. The Johns Hopkins University Press, Baltimore, MD

Akin S, Winemiller KO (2008) Body size and trophic position in a temperature estuarine food web. Acta Oecologica-International Journal of Ecology 33:144-153

Alam MS, Watanabe WO, Carroll PM, Rezek T (2009) Effects of dietary protein and lipid levels on growth performance and body composition of black sea bass *Centropristis striata* (Linnaeus 1758) during grow-out in a pilot-scale marine recirculating system. Aquaculture Research 40:442-449

Amundsen PA, Gabler HM, Staldvik FJ (1996) A new approach to graphical analysis of feeding strategy from stomach contents data - Modification of the Costello (1990) method. Journal of Fish Biology 48:607-614

Bacheler NM, Paramore LM, Buckel JA, Hightower JE (2009) Abiotic and biotic factors influence the habitat use of an estuarine fish. Marine Ecology Progress Series 377:263-277

Bentley CD, Watanabe WO, Rezek TC, Seaton PJ (2009) Preliminary investigations on the effects of dietary lipid on the spawning performance and egg quality of black sea bass *Centropristis striata* L. Aquaculture Research 40:1873-1883

Benton CB, Berlinsky DL (2006) Induced sex change in black sea bass. Journal of Fish Biology 69:1491-1503

Bowman RE, Stillwell CE, Michaels WL, Grosslein MD (2000) Food of Northwest Atlantic Fishes and Two Common Species of Squid. NOAA Technical

Memorandum NMFS-NE-155. National Oceanic and Atmospheric Administration: National Marine Fisheries Service, Woods Hole, Massachusetts

Byron CJ, Link JS (2010) Stability in the feeding ecology of four demersal fish predators in the US Northeast Shelf Large Marine Ecosystem. Marine Ecology Progress Series 406:239-250

Cabana G, Rasmussen JB (1994) Modelling food chain structure and contaminant bioaccumulation using stable nitrogen isotopes. Nature 372:255-257

Chapman DC, Beardsley RC (1989) On the origin of shelf water in the Middle Atlantic Bight. Journal of Physical Oceanography 19:384-391

Cowen RK, Hare JA, Fahay MP (1993) Beyond hydrography: can physical processes explain larval fish assemblages within the Middle Atlantic Bight? Bulletin of Marine Science 53:567-587

Cresson P, Ruitton S, Harmelin-Vivien M (2014) Artificial reefs do increase secondary biomass production: mechanisms evidenced by stable isotopes. Marine Ecology Progress Series 509:15-26

DeNiro MJ, Epstein S (1977) Mechanism of carbon isotope fractionation associated with lipid-synthesis. Science 197:261-263

Dobush GR, Ankney CD, Krementz DG (1985) The effect of apparatus, extraction time, and solvent type on lipid extractions of snow geese. Canadian Journal of Zoology-Revue Canadienne De Zoologie 63:1917-1920

Drohan AF, Manderson JP, Packer DB (2007) Essential fish habitat source document: black sea bass, *Centropristis striata*, life history and habitat characteristics. NOAA Technical Memorandum

Fagan K, Koops MA, Arts MT, Power M (2011) Assessing the utility of C:N ratios for predicting lipid content in fishes. Canadian Journal of Fisheries and Aquatic Sciences 68:374-385

Filippino KC, Mulholland MR, Bernhardt PW (2011) Nitrogen uptake and primary productivity rates in the Mid-Atlantic Bight (MAB). Estuarine, Coastal and Shelf Science 91:13-23

Flagg CN, Dunn M, Wang D-P, Rossby HT, Benway RL (2006) A study of the currents of the outer shelf and upper slope from a decade of shipboard ADCP observations in the Middle Atlantic Bight. Journal of Geophysical Research 111:C06003. doi:10.1029/2005JC003116

Focken U, Becker K (1998) Metabolic fractionation of stable carbon isotopes: implications of different proximate compositions for studies of the aquatic food webs using delta C-13 data. Oecologia 115:337-343

Fry B (2006) Stable Isotope Ecology. Springer, New York, NY

Garrison LP, Link JS (2000) Dietary guild of the fish community in the Northeast United States continental shelf ecosystem. Marine Ecology Progress Series 202:231-240

Giménez J, Marçalo A, Ramírez F, Verborgh P, Gauffier P, Esteban R, Nicolau L, González-Ortegón E, Baldó F, Vilas C, Vingada J, Forero MG, de Stephanis R (2017) Diet of bottlenose dolphins (*Tursiops truncatus*) from the Gulf of

Cadiz: Insights from stomach content and stable isotope analyses. PLoS ONE 12(9):e0184673. doi:10.1371/journal.pone.0184673

Glibert PM, Fullerton D, Burkholder JM, Cornwell JC, Kana TM (2011) Ecological stoichiometry, biogeochemical cycling, invasive species, and aquatic food webs: San Francisco estuary and comparative systems. Reviews in Fisheries Science 19:358-417

Gotelli NJ, Colwell RK (2001) Quantifying biodiversity: procedures and pitfalls in the measurement and comparison of species richness. Ecology Letters 4:379-391

Herzka SZ (2005) Assessing connectivity of estuarine fishes based on stable isotope ratio analysis. Estuarine, Coastal and Shelf Science 64:58-69

Hoffman JC, Sierszen ME, Cotter AM (2015) Fish tissue lipid-C:N relationships for correcting C-13 values and estimating lipid content in aquatic food-web studies. Rapid Communications in Mass Spectrometry 29:2069-2077

Honeycutt ME, McFarland VA, McCant DD (1995) Comparison of 3 lipid extraction methods for fish. Bulletin of Environmental Contamination and Toxicology 55:469-472

Hutchinson GE (1957) Concluding remarks: Cold Spring Harbor symposium. Quantitative Biology 22:415-427

Hyslop EJ (1980) Stomach contents analysis- a review of methods and their application. Journal of Fish Biology 17:411-429

Jackson AL (2016) SIAR-examples-and-queries/learning-resources/siber-comparing-populations.Rmd. Accessed August 31 2018.

https://github.com/AndrewLJackson/SIAR-examples-and-queries/blob/master/learning-resources/siber-comparing-populations.Rmd

Jackson AL, Inger R, Parnell AC, Bearhop S (2011) Comparing isotopic niche widths among and within communities: SIBER - Stable Isotope Bayesian Ellipses in R. Journal of Animal Ecology 80:595-602

Jennings S, Kaiser MJ, Reynolds JD (2001a) Marine Fisheries Ecology. Blackwell Science Ltd., Oxford, UK

Jennings S, Pinnegar JK, Polunin NVC, Boon TW (2001b) Weak cross-species relationships between body size and trophic level belie powerful size-based trophic structuring in fish communities. Journal of Animal Ecology 70:934-944

Kiljunen M, Grey J, Sinisalo T, Harrod C, Immonen H, Jones RI (2006) A revised model for lipid-normalizing δ^{13}C values from aquatic organisms, with implications for isotope mixing models. Journal of Applied Ecology 43:1213-1222

Lambert Y, Dutil JD (1997) Can simple condition indices be used to monitor and quantify seasonal changes in the energy reserves of cod (*Gadus morhua*)? Canadian Journal of Fisheries and Aquatic Sciences 54:104-112

Lentz SJ (2008) Observations and a model of the mean circulation over the Middle Atlantic Bight continental shelf. Journal of Physical Oceanography 38:1203-1221

Link JS (2002) Ecological considerations in fisheries management: when does it matter? Fisheries 27:10-17

Lloret J, Planes S (2003) Condition, feeding and reproductive potential of white seabream *Diplodus sargus* as indicators of habitat quality and the effect of reserve protection in the northwestern Mediterranean. Marine Ecology Progress Series 248:197-208

Love JW, Chase PD (2007) Marine fish diversity and composition in the Mid-Atlantic and South Atlantic Bights. Southeastern Naturalist 6:705-714

MacNeil MA, Drouillard KG, Fisk AT (2006) Variable uptake and elimination of stable nitrogen isotopes between tissues in fish. Canadian Journal of Fisheries and Aquatic Sciences 63:345-353

Malek AJ, Collie JS, Taylor DL (2016) Trophic structure of a coastal fish community determined with diet and stable isotope analyses. Journal of Fish Biology 89:1513-1536

Manirakiza P, Covaci A, Schepens P (2001) Comparative study on total lipid determination using Soxhlet, Roese-Gottlieb, Bligh & Dyer, and modified Bligh & Dyer extraction methods. Journal of Food Composition and Analysis 14:93-100

McCartney MA, Burton ML, Lima TG (2013) Mitochondrial DNA differentiation between populations of black sea bass (*Centropristis striata*) across Cape Hatteras, North Carolina (USA). Journal of Biogeography 40:1386-1398

McConnaughey T (1978) Ecosystems naturally labeled with carbon-13: applications to the study of consumer food webs. M.S., University of Alaska, Fairbanks

McConnaughey T, McRoy CP (1979) Food-web structure and the fractionation of carbon isotopes in the Bering Sea. Marine Biology 53:257-262

McCutchan JH, Lewis WM, Kendall C, McGrath CC (2003) Variation in trophic shift for stable isotope ratios of carbon, nitrogen, and sulfur. Oikos 102:378-390

Mercer LP (1989) Species profile: life histories and environmental requirements of coastal fishes and invertebrates (south Atlantic): black sea bass. Book 82(11). U.S. Fish and Wildlife Service Biological Report

Miller AS, Shepherd GR, Fratantoni (2016) Offshore habitat preference of overwintering juvenile and adult black sea bass, *Centropristis striata*, and the relationship to year-class success. PLoS ONE 11(1): e0147627. doi:10.1371/journal.pone.0147627

Minagawa M, Wada E (1984) Stepwise enrichment of N-15 along food-chains - further evidence and the relation between delta-N-15 and animal age. Geochimica Et Cosmochimica Acta 48:1135-1140

Moore JW, Semmens BX (2008) Incorporating uncertainty and prior information into stable isotope mixing models. Ecology Letters 11:470-480

Moser J, Shepherd GR (2009) Seasonal distribution and movement of black sea bass (*Centropristis striata*) in the Northwest Atlantic as determined from a mark-recapture experiment. Journal of Northwest Atlantic Fishery Science 40:17-28

Musick JA, Mercer LP (1977) Seasonal distribution of black sea bass, *Centropristis striata*, in the Mid-Atlantic Bight with comments on the ecology and fisheries of the species. Transactions of the American Fisheries Society 106:12-25

Nash RDM, Valencia AH, Geffen AJ (2006) The origin of Fulton's condition factor - Setting the record straight. Fisheries 31:236-238

Nelson J, Chanton J, Coleman F, Koenig C (2011) Patterns of stable carbon isotope turnover in gag, *Mycteroperca microlepis*, an economically important marine piscivore determined with a non-lethal surgical biopsy procedure. Environmental Biology of Fishes 90:243-252

Newsome SD, Martinez del Rio C, Bearhop S, Phillips DL (2007) A niche for isotopic ecology. Frontiers in Ecology and the Environment 5:429-436

Northeast Fisheries Science Center (2017) 62nd Northeast Regional Stock Assessment Workshop (6nd SAW) Assessment Summary Report. US Department of Commerce, Woods Hole, Massachusetts

Parnell AC, Inger R, Bearhop S, Jackson AL (2010) Source partitioning using stable isotopes: coping with too much variation. PLoS ONE 5(3): e9672. doi:10.1371/journal.pone.0009672

Parnell AC, Phillips DL, Bearhop S, Semmens BX, Ward EJ, Moore JW, Jackson AL, Grey J, Kelly DJ, Inger R (2013) Bayesian stable isotope mixing models. Environmetrics 24:387-399

Perga ME, Gerdeaux D (2005) 'Are fish what they eat' all year round? Oecologia 144:598-606

Phillips DL, Inger R, Bearhop S, Jackson AL, Moore JW, Parnell AC, Semmens BX, Ward EJ (2014) Best practices for use of stable isotope mixing models in food-web studies. Canadian Journal of Zoology 92:823-835

Pikitch EK, Santora C, Babcock EA, Bakun A, Bonfil R, Conover DO, Dayton P, Doukakis P, Fluharty D, Heneman B, Houde ED, Link J, Livingston PA,

Mangel M, McAllister MK, Pope J, Sainsbury KJ (2004) Ecosystem-based fishery management. Science 305:346-347

Pinnegar JK, Polunin NVC (1999) Differential fractionation of δ^{13}C and δ^{15}N among fish tissues: implications for the study of trophic interactions. Functional Ecology 13:225-231

Post DM (2002a) The long and short of food-chain length. Trends in Ecology & Evolution 17:269-277

Post DM (2002b) Using stable isotopes to estimate trophic position: models, methods, and assumptions. Ecology 83:703-718

Post DM, Layman CA, Arrington DA, Takimoto G, Quattrochi J, Montaña CG (2007) Getting to the fat of the matter: models, methods and assumptions for dealing with lipids in stable isotope analyses. Oecologia 152:179-189

Provost MM, Jensen OP, Berlinsky DL (2017) Influence of size, age, and spawning season on sex change in black sea bass. Marine and Coastal Fisheries 9:126-138

R Core Team (2016) R: A language and environment for statistical computing. R Foundation for Statistical Computing, Vienna, Austria

R Core Team (2018) R: A language and environment for statistical computing. R Foundation for Statistical Computing, Vienna, Austria

Roy EM, Quattro JM, Greig TW (2012) Genetic management of black sea bass: influence of biogeographic barriers on population structure. Marine and Coastal Fisheries 4:391-402

Savidge DK, Savidge WB (2014) Seasonal export of South Atlantic Bight and Mid-Atlantic Bight shelf waters at Cape Hatteras. Continental Shelf Research 74:50-59

Scharf FS, Juanes F, Rountree RA (2000) Predator size - prey size relationships of marine fish predators: interspecific variation and effects of ontogeny and body size on trophic-niche breadth. Marine Ecology Progress Series 208:229-248

Schloesser RW, Fabrizio MC (2017) Condition indices as surrogates of energy density and lipid content in juveniles of three fish species. Transactions of the American Fisheries Society 146:1058-1069

SEDAR (2018) SEDAR 56 - South Atlantic black seabass assessment report. Book SEDAR, North Charleston SC

Sedberry GR (1988) Food and feeding of black sea bass, *Centropristis striata*, in live bottom habitats in the South Atlantic Bight. The Journal of the Elisha Mitchell Scientific Society 104:35-50

Shepherd GR, Terceiro M (1994) The Summer Flounder, Scup, and Black Sea Bass Fishery of the Middle Atlantic Bight and Southern New England Waters. NOAA Technical Report NMFS. U.S. Department of Commerce, Seattle, Washington

Sheridan MA (1988) Lipid dynamics in fish: aspects of absorption, transportation, deposition, and mobilization. Comparative Biochemistry and Physiology 90B:679-690

Skinner MM, Martin AA, Moore BC (2016) Is lipid correction necessary in the stable isotope analysis of fish tissues? Rapid Communications in Mass Spectrometry 30:881-889

Steimle FW, Figley W (1996) The importance of artificial reef epifauna to black sea bass diets in the Middle Atlantic Bight. North American Journal of Fisheries Management 16:433-439

Steimle FW, Zetlin C (2000) Reef Habitats in the Middle Atlantic Bight: Abundance, Distribution, Associated Biological Communities, and Fishery Resource Use. Marine Fisheries Review 62:24-42

Sweeting CJ, Barry J, Barnes C, Polunin NVC, Jennings S (2007a) Effects of body size and environment on diet-tissue delta N-15 fractionation in fishes. Journal of Experimental Marine Biology and Ecology 340:1-10

Sweeting CJ, Barry JT, Polunin NVC, Jennings S (2007b) Effects of body size and environment on diet-tissue delta C-13 fractionation in fishes. Journal of Experimental Marine Biology and Ecology 352:165-176

Thomas CJ, Cahoon LB (1993) Stable isotope analyses differentiate between different trophic pathways supporting rocky-reef fishes. Marine Ecology Progress Series 95:19-24

Tocher DR (2003) Metabolism and functions of lipids and fatty acids in teleost fish. Reviews in Fisheries Science 11:107-184

Vander Zanden MJ, Cabana G, Rasmussen JB (1997) Comparing trophic position of freshwater fish calculated using stable nitrogen isotope ratios (δ^{15}N) and

literature dietary data. Canadian Journal of Fisheries and Aquatic Sciences 54:1142-1158

Wagenmakers EJ, Farrell S (2004) AIC model selection using Akaike weights. Psychonomic Bulletin & Review 11:192-196

Ward CL, McCann KS (2017) A mechanistic theory for aquatic food chain length. Nature Communications 8. doi: 10.1038/s41467-017-02157-0

Wood SN (2006) Generalized Additive Models: An Introduction with R. Chapman and Hall/CRC, Boca Raton, FL

Woodland RJ, Rodriguez MA, Magnan P, Glemet H, Cabana G (2012) Incorporating temporally dynamic baselines in isotopic mixing models. Ecology 93:131-144

Woodland RJ, Secor DH (2011) Differences in juvenile trophic niche for two coastal fish species that use marine and estuarine nursery habitats. Marine Ecology Progress Series 439:241-U290

Woodland RJ, Secor DH (2013) Benthic-pelagic coupling in a temperate inner continental shelf fish assemblage. Limnology and Oceanography 58:966-976

Wuenschel MJ, Jugovich AR, Hare JA (2006) Estimating the energy density of fish: The importance of ontogeny. Transactions of the American Fisheries Society 135:379-385

Wuenschel MJ, McBride RS, Fitzhugh GR (2013) Relations between total gonad energy and physiological measures of condition in the period leading up to spawning: Results of a laboratory experiment on black sea bass (*Centropristis striata*). Fisheries Research 138:110-119

Wuenschel MJ, Shepherd GR, McBride RS, Jorgensen R, Oliveira K, Robillard E, Dayton J (2011) Sex and maturity of black sea bass collected in Massachusetts and Rhode Island waters; preliminary results based on macroscopic staging of gonads with a comparison to survey data. 53rd SAW Assessment Report. National Oceanic and Atmospheric Administration, National Marine Fisheries Service, Northeast Fisheries Science Center, Woods Hole, Massachusetts

Zudaire I, Murua H, Grande M, Pernet F, Bodin N (2014) Accumulation and mobilization of lipids in relation to reproduction of yellowfin tuna (*Thunnus albacares*) in the Western Indian Ocean. Fisheries Research 160:50-59